REFERENCE ONLY

UNIVERSITY OF LONDON THESIS

Degree PhD Year 2006 Name of Author ALAM.T

UCL THESES DECLARATION FORM

Readers of UCL theses are required to abide by the rules set out below and to sign the undertaking which follows:

This is a theses accepted for a Higher Degree of the University of London. It is an unpublished typescript and the copyright is held by the author. All persons consulting this theses must read and abide by the Copyright Declaration below.

Copyright Declaration
I recognise that the copyright of this theses rests with the author and that no quotation from it or information derived from it may be published without the prior written consent of the author.

The amount that may be photocopied is limited to
5% or one chapter, whichever is the greater

This theses is for **reference only** and may not be removed from the Library. It must be signed for and returned to the Issue Desk or Stores Desk **before 6.45 p.m (or 4.00pm on a Saturday). Failure to return theses on time may result in suspension of library privileges.**

Readers are responsible for all theses issued to them and must sign below on receiving and upon returning them.

Author:	Tahirah Alam
Title:	Changes in Gene Expression During Human ...
Date:	2006

Your full name:	SUSAN CLIFFORD
Home address:	
Email:	
Tel:	
Barcode no.:	

Your status: *(please tick)*

- ☑ UCL staff
- ☐ UCL student
- ☐ Non UCL Borrower
- ☐ Non UCL Reference
- ☐ Visitor

I agree to abide by the regulations set out above.

Issued: *Sign here*		Date: 17/10/06
Returned: *Sign here*		Date: 17/10/86
Issued: *Sign here*		Date:
Returned: *Sign here*		Date:
Issued: *Sign here*		Date:
Returned: *Sign here*		Date:

Changes in Gene Expression During Human Prostate Epithelial Cell Differentiation

A thesis submitted to the University of London
for the degree of Ph.D. in the Faculty of Clinical Sciences

2006

Tahirah Alam

Institute of Urology

University College London

ProQuest LLC
789 East Eisenhower Parkway
P.O. Box 1346
Ann Arbor, MI 48106-1346

ABSTRACT

The prostate is the most common site of disease in the human male. An understanding of its normal growth and development is required in order to elucidate the underlying mechanisms of prostatic diseases, namely benign prostatic hyperplasia (BPH) and prostate carcinoma. The prostate epithelium consists of three distinct cells types: basal, luminal and neuroendocrine cells. Several authors have postulated that there is a putative stem cell population in the prostate epithelium that gives rise to all three of these cell types. The stem cells are thought to reside in the basal cell layer and upon cell division give rise to an intermediate, transit amplifying (TA) cell. TA cells undergo rapid proliferation before undergoing terminal differentiation into a luminal or neuroendocrine cell. Despite accumulating evidence for the existence of prostatic stem cells, the regulation of cell growth and differentiation in the normal and diseased prostate is poorly understood.

The aims of this research project are to identify genes that are involved in the regulation of growth and differentiation in the normal human prostate. As a model for investigating epithelial cell differentiation, a conditionally immortalised prostate epithelial cell line was employed. BPH cells were conditionally immortalised using a SV40 construct containing the large T antigen to give rise to the prostate epithelial cell line PrE2.8 (Daly-Burns *et al* , in preparation). These cells exhibit a basal phenotype at the permissive temperature of 33°C and are highly proliferative. When switched to 39°C, growth of the PrE2.8 cells is inhibited and they begin to differentiate. Using the differential display technique and microarray analysis, changes in gene expression between a proliferative and a non-proliferative phenotype were investigated. The protein expression of genes of interest were then confirmed in prostate tissue using immunohistochemistry. These genes may represent early markers of prostate epithelial cell differentiation and may also play a role in the progression of BPH and prostate cancer.

TABLE OF CONTENTS

TABLE OF FIGURES

TABLE OF TABLES

DECLARATION

No portion of the work referred to in this thesis has been submitted in support of an application for another degree or qualification at this or any other university or institute of learning.

ACKNOWLEDGEMENTS

There are many people who put time, effort and love into this piece of work (either directly or indirectly) and my warm thanks go to all of you:

First and foremost, I would like to express my gratitude and thanks to my supervisors Professor John Masters and Dr David Hudson for the opportunity to work in this exciting area of prostate cancer research, visit some great laboratories and attend some of the best conferences in the field. Thank you for your belief in me and for all your support.

To Alan Mackay, for his immense help in teaching me the method of differential display and his constructive criticism. To Professor Mike O'Hare for his assistance in the generation of the PrE2.8 cell line and to Bernadette Daly-Burns for all her hard work and effort into the characterization of the PrE2.8 cell line. To Shamit Soneji for assisting me with the microarray analysis.

To all my friends and colleagues in the laboratory for their friendship and support (you made me smile, laugh and kept me going!). In particular, Rena Meimaridou, no one could ask for a greater friend than you. Thank you for all the good times we had (those were the days!) and for helping me through the tough times. To Vero Blanc, what can I say, apart from, "you crazy girl – don't ever change!" To Istvan Lazcko, it was nice to have someone to share the joys and pains of immunohistochemistry, staining section, after section, after section! Bernadette Daly-Burns, for your friendship and help in the lab, and to Theo Theodossiou, for making me laugh and for telling some great stories! Also to Roger Tatoud for sharing all your knowledge and wisdom of the world!

To my friends outside the lab, in particular, Kay Moorcroft and Dany Maneely. Thanks guys for all your support and encouragement, and most of all for putting up with me; I know it wasn't easy!

To Francis, I owe you a debt of gratitude. Without your unfailing support and encouragement, this thesis would not have been possible. Thank you for distracting me, helping me, and loving me. Life with you is a greater gift than I could ever have dreamt of!

I am immensely grateful to my family, in particular, Yasmin and Nadeem, thank you so much for all your help, support and advice throughout my PhD. I am forever grateful to you both.

Last but not least, I would like to thank my parents for their constant support and encouragement to pursue my studies and career further. I would not have made it without you. This PhD thesis is dedicated to you.

1 INTRODUCTION

The prostate gland is an organ associated with the genitourinary system and is the most common site of pathological disease in the human male. This pathology is most commonly manifested as either of two distinct conditions: benign prostatic hypertrophy (BPH) or adenocarcinoma. Both give rise to a significant level of morbidity and adenocarcinoma is the 2nd most common cause of mortality amongst males in the developed world (Parkin et al., 1999). Despite the prevalence and incidence of this disease, only in recent years has there developed a level of interest, similar to that which has been traditionally focused on breast and colorectal carcinomas, in understanding the underlying mechanisms in the development of this disease.

From its embryonic development until the age of approximately 35 years, the prostate is generally considered to be free from abnormalities. However, from this point onwards an age-associated increase in abnormalities occurs. This is commonly manifested as the non-malignant overgrowth known as BPH. BPH occurs in the transition zone and results in a progressive constriction of the urethra. Unless treated, either by using drugs or by the procedure known as transurethral resection of the prostate, this gives rise to a progressive difficulty to urinate and ultimately to kidney failure.

Carcinoma of the prostate is a multi-focal entity and by the age of 50 years, some 30% of males will have latent forms of this disease present. By the age of 85 years, almost 100% will. In a smaller proportion of individuals, latent carcinoma of the prostate will become clinically invasive disease. The challenge is to identify those individuals most susceptible to developing this life-threatening condition. In order to achieve this, a better understanding of the underlying molecular events involved in the progression of normal prostate cells to a malignant phenotype is required. Such an understanding may facilitate earlier treatment of the disease with better prognostic outcomes or the development of prevention strategies.

1.1 The Anatomy of the Prostate

In the young adult male, the normal prostate is 20ml ±6 in size and weighs approximately 10-15 g. The organ is composed of both fibromuscular and glandular components and lies beneath the bladder surrounding the urethra (Figure 1-1). The anatomy of the human prostate was the subject of debate for many years since its first detailed description in 1912 (Lowsley, 1912). The anatomy and morphology of the prostate has since been studied in detail by several investigators. Of these, the work of McNeal (McNeal, 1980; McNeal, 1981a; McNeal, 1981b; McNeal, 1984; McNeal, 1988) (McNeal, 1968, 1978, 1980, 1981, 1983, 1988) is the most widely accepted. McNeal's model of the prostate is based on dissections and embryological considerations of hundreds of autopsy prostates of all ages. He identified for the first time, the existence of histological heterogeneity in the glandular tissue of the prostate. It was proposed that the prostate is made up of four different regions, or zones, which are tightly fused together. Each zone makes contact with a specific portion of the prostatic urethra, which is used as the primary anatomical reference point in McNeal's model. As the urethra passes through the prostate, it is divided into a proximal (from the bladder neck to the verumontanum) and distal segment (from the verumontanum to the external sphincter), forming a 35° angle at the verumontanum (Figure 1-2). The verumontanum lies entirely in the distal segment. Ejaculatory ducts drain into the urethra at this point. A cylindrical sphincter of smooth muscle, known as the preprostatic sphincter, surrounds the urethra from the upper end of the verumontanum, proximally to the bladder neck. Together with the internal sphincter located at the bladder neck, the preprostatic sphincter helps prevent retrograde ejaculation.

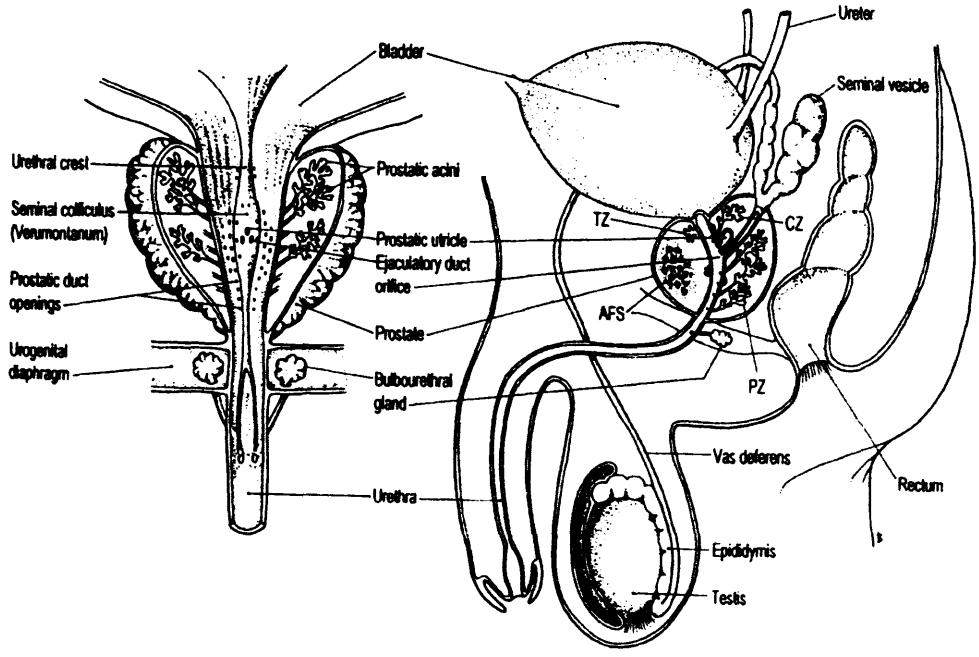

Figure 1-1: Anatomical position of the prostate: frontal and sagittal sections.

Central zone (CZ), peripheral zone (PZ), transition zone (TZ) and anterior fibromuscular stroma (AFS). From Timms (1997).

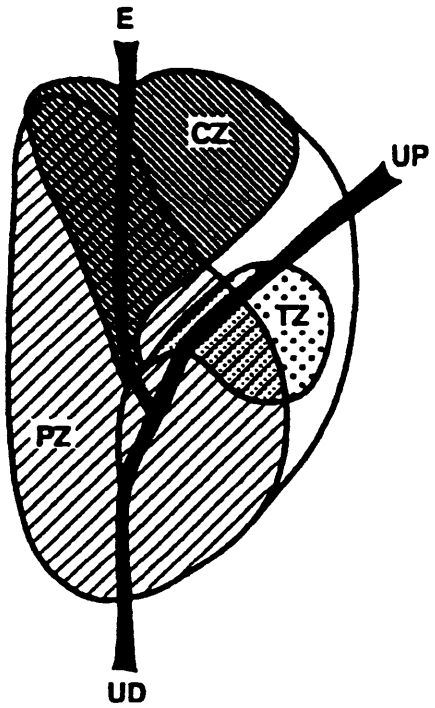

Figure 1-2: Sagittal diagram of the human prostate.
The figure illustrates the distal urethra (UD), proximal urethra (UP) and ejaculatory duct (E) in relation to the zones of the prostate: CZ, central zone; PZ, peripheral zone and TZ, transition zone. From McNeal, 1988.

McNeal (1988) described the four zones of the prostate in detail (Figure 1-3). Three glandular regions were described, each of which drains into a specific segment of the urethra. The central zone comprises approximately 25% of the normal human prostate gland. It contacts the urethra only at the upper end of the verumontanum and surrounds the ejaculatory ducts along their entire course through the prostate. Histologically, the central zone is identified by the presence of relatively large, round acini with irregular contours. These acini are lined by cuboidal and columnar epithelium, the cells of which have a granular cytoplasm and large, pale nuclei packed irregularly at different levels from the basement membrane. The smooth muscle stroma of the central zone is dense and compact. The ducts of the central zone open into the urethra at the verumontanum on either side of the ejaculatory ducts. The histological features of the central zone resemble those of the seminal vesicle suggesting that they are of the same

wolffian duct origin. This was confirmed more recently in studies carried out by Laczko *et al* , (2005); the histology and immunohistochemistry of the zones of the prostate were compared with the seminal vesicles. Using a panel of lectins and antibodies, immunohistochemistry was carried out on normal prostate sections from nine organ donors. The study revealed identical staining patterns in the seminal vesicle and central zone, with significant differences from the peripheral zone. In addition, over 70% of epithelial cells in the seminal vesicle stained positive for lactoferrin, compared with 31.2% of cells in the central zone and 2.1% in the peripheral zone. Prostate nuclear antigen (PNA) staining was present in luminal cells in all zones but there was distinctive basal staining in the peripheral zone alone (Laczko et al., 2005). These observations lend further support to the theory that the central zone and seminal vesicle share a common embryological origin from the Wolffian duct.

The peripheral zone in the normal adult human prostate gland comprises approximately 70% of the total glandular tissue. It surrounds the central zone and extends around the posterolateral peripheral aspects of the gland from its apex to its base. The histological appearance of this region is characterised by small, round acini with smooth walls, which are lined by tall columnar secretory epithelial cells. In contrast to the epithelium of the central zone, the peripheral zone epithelial cells have a clear cytoplasm, with basally located small, dark nuclei. The muscle fibres of the stroma in the peripheral zone are arranged in a more random manner and have a looser texture than the stroma of the central zone. The ducts of the peripheral zone drain into the distal urethra on either side of the verumontanum

The transition zone comprises around 5% of the normal prostate and is composed of two bilaterally symmetrical lobules found on the two sides of the prostatic urethra. The ducts of the region empty bilaterally into the urethra at the base of the verumontanum. Histologically, the acini of the transition zone are identical to those of the peripheral zone. However, the surrounding stroma of this transition region is more dense and compact and is similar to that of the central zone.

The anterior fibromuscular stroma, which comprises approximately one third of the prostatic volume, covers the entire anterior surface of the prostate. The stroma lacks any glandular elements, and surrounds the urethra proximally at the

bladder neck. It is composed of smooth and striated muscle, elastin and collagen fibroblasts. The function of the prostatic stroma may be to enhance the emptying of the prostatic secretions into the urethra at the time of ejaculation.

The histological differences of the zones of the prostate suggest biological or functional differences between the regions. For example, it has been reported that pepsinogen II, a major proteolytic enzyme of the seminal fluid, is produced by cells in the central zone, rather than those of the peripheral zone (Reese et al., 1986). The zonal anatomy of the prostate is also of clinical significance in terms of the development of benign prostatic hyperplasia (BPH) and prostate cancer. The majority of BPH arises within the transition zone; malignancies may also arise in this region, although this is rare. In contrast, the majority of cancers, around 70%, originate within the peripheral zone. In contrast, only about 1-5% of cancers arise in the central zone. The differences in incidence of prostatic disease observed between the zones may be related to their cell kinetics. In studies using normal prostate sections from nine organ donors, it was reported that the proportion of Ki-67-positive epithelial cells was 50% lower in the central zone and seminal vesicles compared with the peripheral and transition zones (Laczko et al., 2005). The proportion of apoptotic cells between the zones also differed, with approximately 2% of epithelial cells in the transition and peripheral zones being apoptotic compared with 1% in the central zone. The increase in cell turnover in the peripheral and transition zones may therefore play a role in the susceptibility of these zones to prostate cancer and BPH.

There is a rich blood supply entering the prostate with its arterial supply arising from the inferior vesical artery which divides into two main branches as it approaches the gland. The arteries extend throughout the prostate distributing a blood supply to the glandular and stromal elements of the organ. The prostate also receives sympathetic and parasympathetic nerve fibres. Parasympathetic nerves end at the acini on cholinergic receptors and promote secretion; sympathetic nerves end on alpha2 receptors on blood vessels and on alpha1 receptors on muscle fibres causing contraction of the smooth muscle.

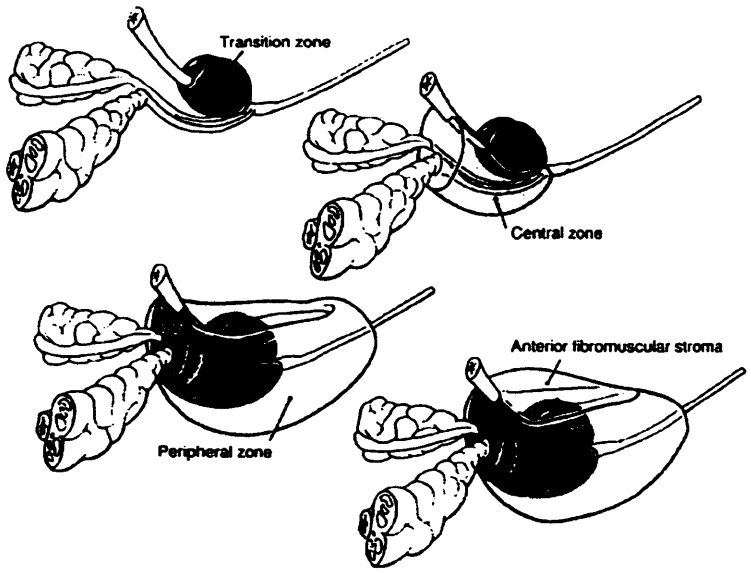

Figure 1-3: The diagram shows the zonal anatomy of the prostate as described by McNeal, 1978.

1.2 Embryology and Development of the Prostate

Embryogenesis of both the male and female gonads are initially identical, a stage known as the indifferent stage where the gonads are morphologically undifferentiated. During this stage of development, the Wolffian and Müllerian ducts and their openings into the urogenital sinus (UGS) develop as precursors of the inner genital organs. Male embryonic development is initiated by genes located on the Y chromosome, which influence the medullary sex cords of the embryonic gonad to differentiate into secretory Sertoli cells. From the seventh week onwards, the Sertoli cells secrete anti-Müllerian hormone or Müllerian-Inhibiting Substance (MIS), a glycoprotein which causes involution of the Müllerian ducts, the female sexual organ precursors, and switches differentiation down the male pathway. MIS also stimulates the production of testosterone by the Leydig cells of the embryonic testis from around the eighth to ninth week of gestation and induces the first stage of testicular descent.

Under the influence of testosterone, the Wolffian ducts differentiate into the epididymis, vas deferens, seminal vesicles and ejaculatory ducts. Penile, scrotal and prostatic development requires the presence of a third hormone, dihydrotestosterone (DHT), a metabolite of testosterone. During the third foetal

month, mesenchymal tissue associated with the UGS responds to DHT produced from foetal testosterone, through the action of the enzyme 5α-reductase, and induces outgrowths of the adjacent urothelium of the UGS to form the prostate. At about the tenth week of gestation, the budding of prostatic glandular epithelium from the UGS occurs in response to binding of DHT to androgen receptors which are localized in the mesenchyme (Sinowatz et al., 1977) Sinowatz *et al* , 1994). These outgrowths begin as solid epithelial buds that arise on the posterior side of the UGS on both sides of the verumontanum and invade the mesenchyme to form the prostate. Initially, five epithelia ducts form in a paired manner, and it is during this stage of development that ductal lumina appear and definitive basal and luminal cells are distinguishable. The top pairs of buds form the inner zone of the prostate and appear to be of mesodermal origin, while the lower buds form the outer zone of the prostate and appear to be of endodermal origin.

By around the 15th week of gestation, the prostate is composed of approximately 70 ducts surrounded by stromal components that arise from the mesenchyme. Secretory epithelial cells are functional at this stage and produce prostate-specific antigen (PSA); well-differentiated basal and NE cells are also present (Aumuller et al., 1990). In distal regions of the prostate however, the cells of solid epithelial ducts remain undifferentiated. By the 16th week of gestation, the undifferentiated mesenchymal cells take on the differentiated phenotype of stroma which consists of both smooth muscle cells and fibroblasts.

Maturation of the gland continues during embryonic development when testosterone levels are high (Bentvelsen et al., 1995). However, at birth, the gland enters a quiescent state of growth and this arrangement persists until puberty when there is an increase in prostate weight and size due to a further rise in testosterone levels. The epithelium differentiates fully into basal, secretory luminal and NE cells in all parts of the gland, as well as an increase in the diameter of the lumen of the ducts. The luminal cells also express androgen receptors (AR) and begin to secrete PSA and prostatic acid phosphatase (PAP). During development of the prostate, there is a close reciprocal interaction between the stromal and epithelial tissue components that remains important for normal growth and maintenance of the gland throughout life (Cunha, 1994).

1.3 Prostate Epithelium

The adult human prostatic epithelium is composed of three distinct epithelial cell types: basal cells, luminal cells (Figure 1-4A) and neuroendocrine (NE) cells (Figure 1-4B). These three cell types are found irrespective of the region of the prostate gland. They can be distinguished morphologically, as well as on the basis of specific phenotypic features.

The most common cell type in the epithelium of the prostate is the secretory luminal cell and these represent more than 75% of the total epithelial cell population (Bonkhoff et al., 1994a). The luminal cells are highly differentiated, tall and columnar in shape and are connected to each other by cell adhesion mediated attachments such as desmosomes and tight junctions. The nucleus lies at the base of the cell below a clear zone of abundant golgi apparatus, and the upper cellular cytoplasmic area is rich in secretory granules and enzymes. Luminal cells require continuous exposure to androgens for their maintenance and survival (Aumuller et al., 1983). They contribute a variety of products to the seminal fluid such as PSA, PAP and other enzymes such as leucine amino peptidase (Aumuller et al., 1983). They can also be distinguished by expression of the androgen receptor and keratins 8 and 18. These epithelial cells circle the periphery of the acinus and luminal secretions drain into the ducts that connect to the urethra. Due to their terminally differentiated phenotype, luminal cells have a finite life span at the end of which they are removed through the process of programmed cell death.

Secretory luminal cells are separated from the basement membrane and stroma by a layer of basal cells. These cells are undifferentiated, flattened or cuboidal in shape and lie parallel to the basement membrane. They have slender, cigar-shaped, dark nuclei and little cytoplasm which is more dense than that of luminal cells (McNeal, 1988). They stain positive for the high molecular weight keratins 5 and 14 (Isaacs, 1984) as well as Bcl-2 (McDonnell et al., 1992). They lack expression of the major prostatic secretory proteins, such as PSA and PAP. Low levels of androgen receptor have been observed in these cells also (Bonkhoff and Remberger, 1993). Basal cells are thought to serve a proliferative role as demonstrated by experiments carried out by Bonkhoff and Remberger (1996) in which three well-characterised proliferating agents, Ki-67, proliferating cell nuclear antigen (PCNA) and MIB-1, were investigated in normal and benign

prostate tissue. Seventy percent of positive staining was found in cells of a basal phenotype. Taking into account the ratio of basal to luminal cells (1:3) in the normal prostate gland, the proliferative activity in the basal cell layer exceeds that of the luminal cells by a factor of up to ten (Bonkhoff and Remberger, 1996; Hudson et al., 2001). Compared with luminal cells, basal cells are less vulnerable to apoptosis induced by androgen withdrawal (English et al., 1987). This is probably due to the presence of Bcl-2 in basal cells, which inhibits apoptosis (Lu et al., 1995). Additional studies have shown that isolated basal cells are capable of generating luminal cells in both monolayer and 3-dimensional cultures (Hudson et al., 2001; Liu et al., 1999; Robinson et al., 1998). And so, although their specific role in prostate biology is not fully known, basal cells are now widely accepted as the precursors of secretory luminal cells (Robinson et al., 1998).

Early ultra-structural studies identified a third cell type co-localised in the basal cell compartment. This cell is rich in electron-dense, round granules of different sizes (Biagini et al., 1982). It is now clear that these cells are prostate NE cells. The human prostate contains the largest number of NE cells of any genitourinary organ (di Sant'Agnese, 1992). Morphologically, two types of NE cells can be identified in the prostate: open, flask-shaped cells with long slender extensions towards the glandular lumen, and closed cells with dendritic luminal extensions, but often displaying horizontal or oblique processes (di Sant'Agnese, 1992). Differences in the distribution of NE cells between the zones of the prostate have recently been reported (Laczko et al., 2005). The frequency of NE cells in the central zone was reported to be approximately 50% lower than in the transition and peripheral zones.

NE cells are known to produce a number of neuropeptides such as chromogranin A, serotonin, neuron-specific enolase (NSE), calcitonin, thyroid-stimulating hormone-like peptide, gastrin-releasing peptide and somatostatin (di Sant'Agnese, 1992); (Wu et al., 1996). The exact functions of these substances in the prostate is not clearly understood, but they are thought to induce a variety of intracellular events including changes in ion flux and depolarisation, activation of calcium release, from intracellular stores and activation of ATP formation (Xue et al., 1998b). There is now a growing consensus that prostate NE cells may play a fundamental role in the regulation of normal growth and gland development (Abrahamsson, 1996). Prostate NE cells may contain neurosecretory granules of

more than one type, and the distribution of different NE cells may indicate their various biological functions. Recently, reports have revealed that receptors for some NE products are present in prostate NE cells. For example, Wu *et al* , (1996) identified the presence and location of calcitonin receptor mRNA in the normal prostate using RT-PCR and *in situ* hybridisation. These experiments demonstrated that the luminal, exocrine cells were positive for the calcitonin receptor, and that some calcitonin receptor expressing cells also had a calcitonin secreting function. This suggests that the neuropeptides produced by the prostatic NE cells may also act in an autocrine/paracrine fashion.

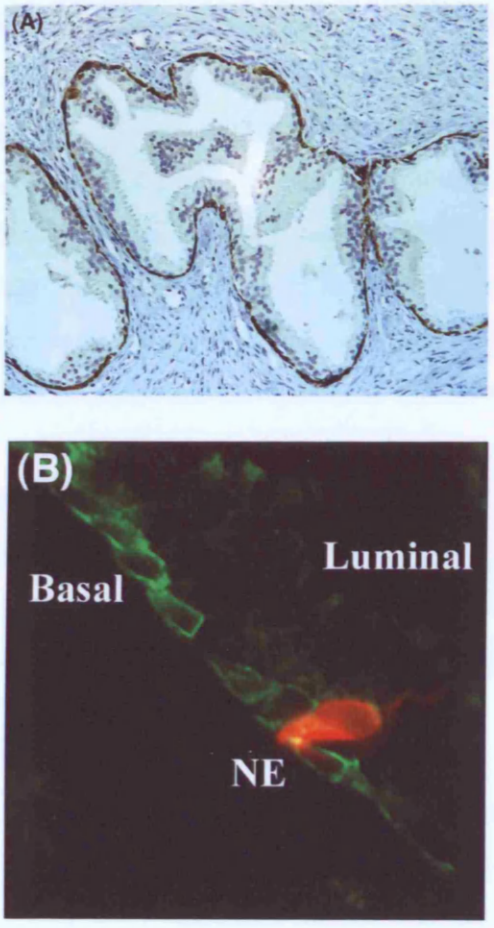

Figure 1-4: Cross sections of adult human prostate glands showing different epithelial cell types.

(A) Brown staining (DAB labelling) indicates basal cells stained for keratin 5 while luminal cells are negative. (B) Immunofluorescent staining in which basal cells are detected by positive staining for keratin 14 (FITC, green) and the neuroendocrine (NE) cell is stained for Chromogranin A (TRITC, red).

1.4 Stem Cell Self Renewal and Differentiation

Tissue stem cells (SC) form the cellular basis for organ homeostasis and repair. In the adult, SCs are responsible for the generation and maintenance of terminally differentiated cell populations in tissues that undergo continuous turnover. The prevailing view is that SCs are slow-cycling cells with the capacity for unlimited or prolonged self-renewal and that they can produce at least one type of differentiated progenitor cell (Till and Mc, 1961). A SC division can either give rise to two daughter SCs via a 'symmetrical division' leading to an increase in SC number, or it may undergo asymmetric division producing one identical daughter and another cell that is committed to differentiate (Till and Mc, 1961). The committed daughter cell then enters a transient state of rapid proliferation giving rise to transiently amplifying (progenitor) cells that are able to undergo a limited number of cell divisions before finally undergoing terminal differentiation (Figure 1-5) (Potten et al., 1979). SCs are believed to reside in most organs of the body and in most tissues. They form a minority subgroup, usually fewer than 1-2% of the total cell population of the tissue. Because relatively undifferentiated, in most tissues they are unable to carry out the specialist functions their progeny are designed to.

Several theories have been proposed to explain the methods of lineage determination: extrinsic (through growth factors, stroma or external influences), intrinsic (for example, nuclear factors) or a combination of both. The external, or extrinsic, signals that control stem cell fate collectively make up its microenvironment, or 'niche' (Quesenberry and Becker, 1998). A niche is a subset of tissue cells and extracellular substrates, which, *in vivo*, favours the existence of the SC in the undifferentiated state and controls its self-renewal and progeny production. Interaction with other cell types and the components of the extracelluar matrix are believed to influence the survival and development of cells committed to terminal differentiation. In addition, several signalling pathways are known to be important in regulation of SC self-renewal and cell fate determination and these include the Notch (Lowell et al., 2000), Sonic hedgehog (Shh) (Kim et al., 2003) and Wnt signalling pathways (Lako et al., 2001).

Differentiation pathways have been studied in many adult organs and a number of markers and regulatory pathways of SC self-renewal and

differentiation have been identified. There remains, however, a clear need for further markers to distinguish stem from transit cells as well as the identification of potential cascades of gene expression that specify particular differentiation pathways. This is in order to understand how these pathways are disrupted during disease. Towards this end, considerable progress has been made in understanding the lineage pathways of many adult tissues such as the skin, intestine and most extensively, the hematopoietic system (Baum et al., 1992; Spangrude et al., 1988).

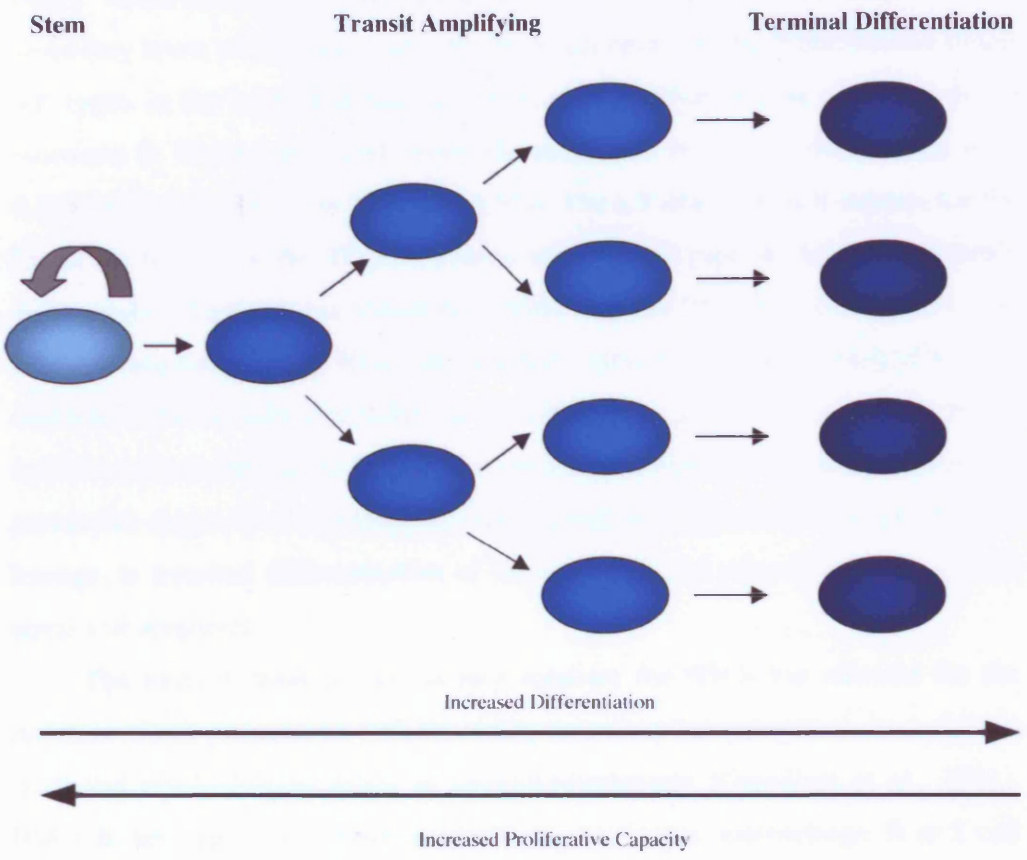

Figure 1-5: Schematic representation of a stem cell differentiation hierarchy.

1.4.1 Haematopoiesis

Blood cells can be classified into two main types: lymphoid cells (T, B, and natural killer cells) and myeloid cells (granulocytes, monocytes, erythrocytes and

megakaryocytes). All blood cells have a limited lifespan: several hours for granulocytes, several weeks for red blood cells and up to several years for memory T cells. Therefore, vast numbers of blood cells must be continually generated in order to keep up with this extremely high rate of cell turnover. It has been established that all blood cells are derived from a small population of pluripotent cells called haematopoietic SCs (HSCs) that are located in the bone marrow (BM). The first evidence for HSCs came from experiments in mice in which BM cells from healthy mice were found to generate myeloerythroid colonies in the spleens of hosts that had been lethally irradiated (Till and Mc, 1961). These clonogenic cells gave rise to cells that could be transferred to secondary hosts where they were able to reconstitute all the differentiated blood cell types in the host (Siminovitch et al., 1963). More recent experiments by Morrison & Weissman (1994) have identified two classes of HSCs: long term (LT-HSCs) and short term (ST-HSCs) SCs. The LT-HSC cell self-renews for the life of the host while the ST-HSC retains self-renewal capacity for approximately eight weeks (Morrison and Weissman, 1994). In adult life, HSCs constitute a very small compartment in the BM with estimates varying from less than 0.05% to as much as 0.5% of cells (Gunsilius et al., 2001). The generation of mature blood cells from these pluripotent HSCs involves a highly regulated progression through successive stages from intermediate cells, which are committed to a specific cell lineage, to terminal differentiation of lineage-restricted progenitor cells, growth arrest and apoptosis.

The identification of cell surface markers for HSCs has allowed for the isolation of cell populations with the ability to restore haematopoiesis in recipients receiving myeloablative doses of chemoradiotherapy (Gunsilius et al., 2001). HSCs do not express any markers of either granulocyte, macrophage, B or T cell lineages but have the phenotype $Lin^{-/low}/Thy\text{-}1^{low}/c\text{-}kit^{high}/Sca\text{-}1^{+}$ in the mouse (Morrison et al., 1995) and $Lin^{-}/Thy\text{-}1^{+}/CD34^{+}/CD38^{-/low}$ in humans. The CD34 cell surface antigen is able to identify a cell population that contains HSCs as well as lineage-committed haematopoietic cells. In humans, 1-4% of the marrow cells express the CD34 antigen compared with 0.1-0.2% in peripheral blood and 0.8-1.2% in umbilical cord blood. This $CD34^{+}$ fraction contains the stem cells as well as lineage-committed progenitor cells. Another surface antigen which defines haematopoietic stem and progenitor cells is CD133. This antigen is selectively

expressed on CD34-bright haematopoietic stem and progenitor cells derived from human foetal liver, BM and blood (Yin et al., 1997). HSCs isolated on the basis of these cell surface markers are used in the treatment of a number of blood diseases such as leukemias, myelodysplastic syndromes, severe aplastic and sickle cell anaemias and beta-thalassemia, to restore the patients hematopoietic system.

1.4.2 Epidermis

The mammalian epidermis provides a barrier to protect the body from dehydration, injury and infection. As the first line of defense against various physical traumas of the environment, including exposure to mutagenic ultraviolet radiation, the skin is continually being renewed throughout life and therefore exhibits a high rate of cell turnover. This cell renewal process is accelerated in response to injuries such as burn or wounding. The rate of cell turnover in the human is estimated at about 60 days and around 7 days in mice (Potten, 1981).

The skin consists of an outer layer known as the epidermis, a stratified squamous epithelium, and an inner layer known as the dermis. The epidermis and dermis are separated by a basement membrane. The epidermis is composed almost entirely of epithelial cells known as keratinocytes. The layer of keratinocytes directly contacting the basement membrane is termed the basal layer. The basal cells are relatively undifferentiated, proliferative cells consisting of a network of keratin intermediate filaments (IF). They are also believed to be the progeny of SCs, which are thought to reside in the basal layer (Potten, 1981). As the population of basal cells increases through cell division, some cells detach from the basement membrane and begin to move towards the skin surface. As these cells leave the basal layer they increase in strength through the synthesis of new sets of keratin filaments linked to tightly adhesive desmosomes. As these differentiating, transit amplifying cells near the outer surface of the skin, they produce proteins, which organise into bilayers through cross-linking to form the cornified envelope. Terminally differentiated cells that reach the skin surface are enucleated, flattened squames that are subsequently sloughed and are continuously replaced by new cells differentiating and moving up towards the surface from the basal layer [Potten, 1981 #5343].

Although SCs have been identified in the basal layer of the epidermis, it is now believed that the upper portion of the hair follicle known as the bulge,

constitutes the SC compartment (Oshima et al., 2001). Oshima and colleagues demonstrated that when the bulge from a normal mouse follicle was surgically replaced with bulge tissue from a mouse ubiquitously expressing *lacZ*, the chimeric follicles produced *lacZ*-positive cells contributing to all the differentiation lineages of the hair follicle and also produced progeny that differentiated into sebocytes of the sebaceous gland and the epidermis. It has therefore been suggested that bulge SCs migrate downwards from the bulge to the base of the hair follicle where their progeny give rise to the outer root sheath inner root sheath and hair shaft. In addition, bulge cells may also migrate upwards to populate the basal layer of the epidermis and the sebaceous gland.

Molecular markers that differentiate epidermal SCs from transit amplifying cells are essential to further the understanding of lineage pathways of cellular maturation. The most useful cell surface markers of human epidermal SCs are the B1 integrins, receptors that bind extracellular matrix proteins. All basal keratinocytes express B1 integrin, however, cells thought to be SCs within the basal layer, express two to three fold higher levels of the protein. In addition, it has been shown that as cells leave the basal layer, they down-regulate its expression. B1 integrin can therefore be used to enrich for SCs in the epidermis (Hertle et al., 1995). Other proteins have been identified as markers of epidermal SCs such as keratin 19 (Michel et al., 1996), keratin 15 (Lyle et al., 1998) and p63, a homologue of the p53 tumour suppressor gene (Pellegrini et al., 2001). Although these markers provide additional information about epidermal SCs and differentiation pathways, they are of limited use in isolating particular cell populations, as they are intracellular proteins.

1.4.3 Intestine

The mammalian intestinal mucosa is a rapidly proliferating tissue and provides an additional model for the study of proliferative hierarchies, regulation of cell division and differentiation. The tissue is lined by a simple columnar epithelium, which is continually being replaced as cells are shed into the gut lumen. The epithelium is folded to form a number of invaginations, or crypts that are embedded in the connective tissue; each crypt is composed of around 250 simple epithelial columnar cells. In the small intestine, several crypts surround the base of finger-like luminal projections called villi. Epithelial cells produced in the

lower part of the crypt migrate up the crypt onto an adjacent villus where they perform their differentiated absorptive function before being shed, into the lumen.

It is widely accepted that SCs are located near or at the base of each crypt and are responsible for maintaining tissue homeostasis in the intestine. Estimates of SC number vary widely from 0.4-0.6% of the crypt cells, with the smallest value implying that a single SC is located in each crypt. As in other regenerative tissue models such as the epidermis, SCs in the intestine are thought to give rise to intermediate, transiently proliferating committed progenitors. These progenitor cells migrate up the crypt towards the surface and subsequently differentiate into either the absorptive brush border enterocytes, mucus-secreting goblet cells, or the peptide hormone secreting enteroendocrine cells of the villi. Differentiated cells eventually die and are shed from the villi into the lumen of the gut approximately 5-7 days after the onset of cell division. Additionally, a number of progenitor cells migrate down to the base of the crypt to become the fourth cell type, the Paneth cells. These cells synthesize and secrete antimicrobial peptides, digestive enzymes and growth factors and are eventually cleared from the crypt by phagocytosis (Cheng and Leblond, 1974). It has also been suggested that the intermediate progenitor cells are of two types: short lived cells that give rise to one or two cell types and long lived progenitors that give rise to all epithelial cell types (Bjerknes and Cheng, 1999). However, the search for markers differentiating stem from intermediate progenitor cells is ongoing.

Evidence for the existence of SCs within the intestinal epithelium came from radiation experiments where following radiation-induced cell death, surviving proliferative cells were able to form a regenerative crypt containing all cell lineages. (enterocytes, goblet cells, Paneth cells and endocrine cells) (Cheng and Leblond, 1974). In addition, subcutaneous injection of single cells from rat colonic adenocarcinoma into mice can give rise to tumours containing all cell lineages (Cox and Pierce, 1982). However, unlike the epidermis and hematopoietic system, molecular markers of intestinal SCs have not yet been identified and they are instead defined by their characteristics. Recently however, Musashi-1 (Msi-1) has been identified as a putative marker of intestinal stem and early lineage progenitor cells. The Msi-1 gene is also thought to be involved in the early asymmetric divisions that generate differentiated cells from neural SCs or

progenitor cells since it was found to be expressed by neural SCs but was down regulated in the differentiated progeny (Kaneko et al., 2000).

1.4.4 Mammary Gland

In humans the epithelium of the mammary gland consists of a network of ducts that branch and invade the mammary fat pads. The ducts are made up of a basal layer of myoepithelial cells that express keratins 5 and 14, and a luminal layer of specialised epithelial cells expressing keratins 8, 18 and 19. It has been suggested that the breast epithelium houses a population of cells with properties resembling those of SCs and it is these cells that maintain tissue homeostasis (Daniel and Young, 1971). The search for breast SCs has gained potential in recent years and there have been many further studies investigating the isolation and characterisation of the putative mammary SC.

The adult mammary gland is a dynamic organ that undergoes significant changes in morphology during developmental periods such as pregnancy and lactation. During puberty, ductal outgrowth rapidly increases under hormonal stimulation resulting in side branching. Full development of mammary epithelium occurs only during pregnancy and lactation, when numerous lobulo-acinar structures containing the milk-secreting alveolar cells are formed through extensive proliferation, followed by terminal differentiation. Cessation of lactation following weaning is accompanied by massive apoptosis and tissue remodelling, and the gland returns to a structure resembling that before pregnancy. This cycle of pregnancy-associated proliferation, differentiation, apoptosis and remodelling can occur many times during the reproductive lifespan of mammals, suggesting the presence of a cell population with high proliferative potential and differentiation ability, a description that fits the definition of stem or progenitor cells (Dontu et al., 2003b).

While mammary SCs have not as yet been isolated and characterised, there is strong evidence for their existence. Studies in mice and rats demonstrated that an entire mammary gland could be generated from fragments, or even single cells, of breast epithelium. Removal of the endogenous mammary epithelium from a mammary fat pad created a cleared pad that was used as a site of transplantation. Cells from normal mammary epithelium were able to grow and fill the empty fat pad. Serial transplantation of epithelial fragments regenerated the entire functional

gland reaching growth senescense after several generations. Furthermore, any portion of the normal mammary parenchyma was able to regenerate a complete mammary gland, over several transplant generations, suggesting the existence of cells capable of reproducing new mammary epithelium through several rounds of self renewal (Daniel and Young, 1971).

Recently, ultrastructural studies of mouse mammary epithelial explants, from various stages of development, revealed the existence of a population of pale or light staining cells and it was only these cells that entered mitosis when the mammary explants were cultured. These pale cells were undifferentiated but were able to differentiate towards secretory cells in vitro. Two forms of undifferentiated pale cells were recognised: small light cells (SLC) and undifferentiated large light cells (ULLC). The SLC were found to have a basal location and did not touch the lumen. They contained few organelles and showed little evidence of specialised function (Smith and Chepko, 2001). By contrast, ULLC made contact with the basement membrane and the lumen. The cytoplasm contained some mitochondria, sparse endoplasmic reticulum and an inactive Golgi complex. Both SLC and ULLC displayed condensed mitotic chromosomes suggesting an ability to replicate. During pregnancy, the rapidly proliferating mammary epithelium revealed a number of partially differentiated ULLC, or differentiating large light cells (DLLC). It was suggested that the DLLC represented the transit amplifying epithelial cells committed to differentiation to a secretory cell type. Furthermore, mitotic chromosomes were not observed in differentiated cells suggesting a state of terminal differentiation. Based on these observations, a hypothetical pathway of differentiation in the human mammary gland was suggested whereby the pale-staining or light cells are situated between the luminal and myoepithelial cell layers and give rise to all cells types of the mammary gland (Smith and Boulanger, 2003).

The isolation of mammary SCs has been hindered by the lack of suitable systems that maintain these cells in culture in an undifferentiated state, and by the lack of defined SC markers. Dontu *et al* (2003) studied human mammary epithelial cells isolated from reduction mammoplasties cultured on a non-adhesive substratum. The vast majority of cells underwent apoptosis. However, a small number of cells were able to survive and proliferate and form multicellular spheroids, which were highly enriched in undifferentiated cells. Single cells from

the spheroids were able to generate multilineage colonies when cultured in the presence of serum on a collagen substratum, and gave rise to myoepithelial, ductal epithelial and alveolar epithelial cells (Dontu et al., 2003a). Several attempts to isolate mammary SCs have been made through the utilisation of cell surface markers and several candidate SC markers have thus been reported. For example, it was suggested that cells situated in an intermediate position between the myoepithelial and basal layers, the putative SCs, that do not contact the lumen, would not express apical membrane-specific sialomcin MUC-1 but would express the luminal epithelial-specific antigen (ESA). It was subsequently demonstrated that these ESA+/MUC-1- cells were able to produce both luminal and myoepithelial cell types in vitro, whereas ESA+/MUC-1+ cells were restricted in their ability to differentiate into multiple lineages (Gudjonsson et al., 2002). Similarly, studies with mouse mammary epithelial cells isolated based on their cell surface expression of Sca-1, showed that these cells were able to reconstitute the mammary glands of host mice cleared of endogenous tissue; transplantation of Sca-1 negative cells resulted in poor ductal outgrowths. Sca-1 is a GPI-anchored membrane protein expressed by murine bone marrow and muscle SCs and has therefore been suggested to be a potential marker of mammary stem/progenitor cells (Welm et al., 2002).

It has been postulated that the side population (SP) is a universal phenotype of SCs and these cells are characterised by their differential uptake of Hoechst dye. Using flow cytometric analysis, SP populations of SCs have been identified in haematopoietic and muscle cells (Goodell et al., 1996; Zhou et al., 2001). Recently, Alvi *et al* (2003) identified the presence of a SP of SCs within the human and mouse mammary glands. The mammary SP cells comprised of an undifferentiated subpopulation of cells that in vivo, generated ductal and lobular structures which contained both myoepithelial and luminal epithelial cell types. Freshly isolated SP cells expressed low levels of differentiated markers for luminal (K19) and myopeithelial cell types (K14). Oestrogen receptor was also detected in SP cells, suggesting they have the capacity to respond to the proliferative effects of oestrogen (Alvi et al., 2003). In addition, expression of the telomerase catalytic subunit was detected in mammary SP cells compared with non-SP cells; telomerase has been associated with SC compartments in other tissues (Kolquist et al., 1998). Furthermore, the mammary SP cells expressed the

haematopoietic SC marker Sca-1. The search for further markers of mammary SCs, and thus a better understanding of the differentiation pathway in this organ, is ongoing.

1.5 Models of Differentiation Lineages in the Human Prostate

All models of prostate epithelial cell differentiation and cell lineage are based on a stem cell theory and several models of epithelial cell differentiation in the human prostate have been postulated by a number of authors (Bonkhoff, 1996; Collins et al., 2001; English et al., 1987; Hudson et al., 2000; Isaacs and Coffey, 1989; Wang et al., 2001) in which a pluripotent stem cell located within the basal cell layer is postulated to give rise to the terminally differentiated secretory luminal cells and NE cells.

1.5.1 Evidence for prostate stem cells from *in vivo* studies

There is accumulating evidence derived from experiments carried out in the rat supporting the prostate stem cell hypothesis (English et al., 1987; Evans and Chandler, 1987; Kyprianou and Isaacs, 1988). The majority of adult prostatic epithelial cells are androgen dependent for growth and survival. For example, castration of the male rat via androgen ablation, leads to involution of the prostate with a loss of approximately 80-90% of total epithelial cells through apoptosis (Kyprianou and Isaacs, 1988). The remaining prostate tissue remains androgen responsive since the subsequent administration of exogenous androgens to the castrate rat results in the induction of cell proliferation and regeneration of the prostate to its original adult size and morphology (English et al., 1987). This process of involution and subsequent androgen-induced regeneration of the prostate can be repeated numerous times (English et al., 1987) supporting the existence of a stem cell population in the adult prostate that is androgen independent for survival but remains androgen responsive, and is responsible for generation of all epithelial cell lineages of the prostatic epithelium.

Verhagen *et al* (1988) also observed a decline in thickness of the epithelial layer of the acini which was seen upon androgen ablation, and which seemed to be caused mainly by a reduction of the luminal cell compartment. A very thin luminal layer was left and the basal cell compartment seemed to be mostly

unaffected, as was determined by keratin expression patterns. The residual luminal layer consisted of cells with morphological luminal characteristics but displayed a keratin expression pattern of both basal and luminal cell types. Testosterone administration to 14-day castrated rats caused rapid regeneration of the prostate resulting in restoration of the normal morphology of the luminal cell layer and the epithelium regaining its normal thickness (Verhagen et al., 1988).

Castration-related changes have also been reported for the expression of telomerase. The enzyme telomerase is responsible for maintaining the length of telomeres at the ends of eukaryotic chromosomes. Adult somatic cells do not contain functional telomerase. Thus with each complete cell division, a cell's telomeric length is shortened by about 50-100 bp (de Lange, 1994). When cells attain a critically short telomere length, they reach the Hayflick limit of cell replication and undergo senescence. However, there are certain cell types that do not appear to undergo this phenomenon. These are the germ-line cells, some stem cells and many malignant tumour cells. These cells differ from somatic cells in that they express functional telomerase and thus display an immortal phenotype, i.e. unlimited replicative potential (Kim et al., 1994; Lansdorp, 1995; Wright et al., 1996). Telomerase is undetectable in the normal adult prostate gland of the rat. However, following castration, the residual prostate gland expresses high levels of telomerase. Activity of the enzyme disappears again following testosterone-induced regeneration of the prostate. This suggests that stem cells are rare in the normal prostate. Also, since their survival is androgen-independent, the number of stem cells in the prostate may be increased as a result of castration, allowing telomerase detection (Meeker et al., 1996). This may be due to an increase in stem cell numbers but is most likely to be due to the loss of differentiated hormone dependent cells, leading to an increase in the relative proportion of cells being stem cells.

Studies using tissue recombination models, such as those of Kinbara *et al* (1996), also support the existence of stem cells within the prostate. Segments of adult rat prostate from the dorsal, lateral type 1 and lateral type 2 prostatic ducts, were removed and combined with mesenchyme from embryonic urogenital sinus, neonatal seminal vesicle or neonatal bulbourethral gland. The tissue recombinants were grafted under the renal capsule of syngeneic male hosts. The mesenchyme induced abundant epithelial cell growth, new ductal branching morphogenesis and

changes in prostate lobe identity that depended on the type of mesenchyme inducer. This result indicates that the adult prostate contains cells with a high proliferative capacity and the potential for multiple differentiation pathways, properties akin to those of stem cells (Kinbara et al., 1996). Adult urinary bladder epithelium has also been induced by urogenital sinus mesenchyme to undergo prostatic development, resulting in prostatic ductal morphogenesis, secretory cytodifferentiation, expression of epithelial AR, prostate-specific secretory proteins and androgen dependence for growth (Cunha et al., 1983; Cunha et al., 1980).

1.5.2 Evidence for prostate stem cells from *in vitro* cell culture studies

In cell culture, the ability of single cells to develop colonies is associated with stem cell and transit amplifying cell properties. Primary cultures of prostate epithelial cells have been studied for their colony-forming ability (Peehl and Stamey, 1986; Peehl et al., 1988) and it has been shown that at low plating densities (100 cells per 5 cm Petri dish), approximately 5% of adult prostate epithelial cells, cloned directly from biopsies and primary cultures, formed colonies, some of which were very large. These findings were extended to further characterize the putative stem cell-like properties of primary adult prostate epithelial cells (Hudson et al., 2000). The majority of primary epithelial cells (cloned directly from biopsies of benign prostatic hyperplasia) formed small irregular shaped colonies containing up to 8,500 cells. When stained for cytokeratin markers, the majority of cells in these colonies were positive for both K14 and K8, with few cells expressing only K14 or K8, indicating both undifferentiated and differentiated cells within these colony types. A small population of epithelial cells (approximately 0.5% of the cells plated) formed very large more tightly packed colonies containing between 8,000 and 40,000 cells. These colonies were mainly composed of K14-positive cells with little or no luminal cell-specific K8 expression. It was suggested that these larger colonies were founded by stem cells. Since one property of stem cells is the ability regenerate the different cell types of the tissue in which they reside. The ability of these epithelial cells to regenerate prostate epithelium was determined. When these colonies were grown in matrigel, three-dimensional spherical structures with

side branching formed which when sectioned and stained revealed a well-organised basal layer with one or more luminal layers surrounding a lumen partly filled by single cells. The outer layer of basal cells were positive for K5, K14 and CD44, where as the luminal cells expressed K8 as well as K17, K19 and weak K14; androgen receptor was expressed by cells within the lumen (Hudson et al., 2000).

The findings of Hudson *et al* (2000) were further extended to provide additional evidence for the existence of stem cells in the adult prostate by Collins and colleagues, (2001). By pre-selecting CD44-positive cells, basal epithelial cells were isolated and assessed for stem cell properties. Epidermal stem cells are known to express higher levels of integrins $\alpha 2\beta 1$ and $\alpha 3\beta 1$ than transit amplifying cells and also rapidly adhere to type I collagen in culture. Prostate epithelial cells were shown to share these properties of epidermal stem cells with 3% of the total basal population adhering to type I collagen within 5 minutes. These rapidly adherent cells were also alpha2-integrin bright suggesting that these cells represented the prostate stem cells. By grafting this integrin-bright cell population together with human stromal cells, into athymic male mice, their ability to regenerate the different cell types of the prostate was investigated. Indeed following 42 days of growth, a fully formed epithelium was observed with variable gland formation. The epithelium consisted of a layer of flattened cuboidal cells expressing basal cell specific markers K5 and K14. Columnar cells found facing the lumen were positive for PAP, PSA and AR. These findings lend further support to the hypothesis that a stem cell population located within the basal cell layer of the prostate is the progenitor of the luminal cell population.

Bonkhoff *et al* (1994) demonstrated through immunohistochemical experiments that not only basal and luminal, but also NE cells may be linked in a precursor-progeny relationship. In the normal and hyperplastic prostate, the co-expression of basal cell-specific cytokeratins and PSA in a sub-population of basal cells was observed, indicating the existence of epithelial cell types with both basal and luminal features. Tissue sections of hyperplastic prostate revealed a small number of cells expressing both the NE cell marker chromogranin A and PSA. Furthermore, co-expression of chromogranin A and basal cell-specific cytokeratins were focally observed in some NE cells in the hyperplastic and

normal prostate. Bonkhoff thus proposed (from this and basal proliferation studies and basal cell AR expts) that luminal cells originate from androgen-responsive basal cells via intermediate cell types (Bonkhoff et al., 1994a).

As in other adult tissues of the body where the existence of stem cells has been established, such as in the skin, gastrointestinal tract and haematopoietic system, the differentiation of stem cells in the prostate is also most likely a hierarchical process characterised by the presence of intermediate, transiently amplifying, progenitor cell types. Several authors have documented the existence of such intermediate cells, that co-express basal and luminal cell markers, in the human prostate, as candidates for a transit amplifying population, suggesting a hierarchical pathway of differentiation (Bonkhoff et al., 1994a; Nagle et al., 1991; Peehl et al., 1996; Robinson et al., 1998; Sherwood et al., 1990; van Leenders et al., 2000; Verhagen et al., 1988; Verhagen et al., 1992; Xue et al., 1998a). For example, the AR and PSA are found exclusively within the luminal population. However, it has been documented that a small number of basal cells in the normal and hyperplastic prostate also express nuclear AR and PSA, indicating differentiation intermediate between the basal and luminal cell types (Bonkhoff and Remberger, 1993; Bonkhoff et al., 1994b). These subsets of basal cells are suggested to be potentially androgen responsive and consequently, to be the precursors of the luminal secretory cells (Figure 1-6), with the differentiation pathway from basal to luminal cell types being an androgen-induced process (Bonkhoff and Remberger, 1996).

The simultaneous detection of numerous keratins in a single cell, has allowed the features of intermediate cells to be better characterised leading to further models of differentiation in the adult prostate. Van Leenders *et al* (2000) identified a subset of cells in the basal cell layer that expressed low levels of K18 together with K5 and K14 (K5++/K14++/K18+). It was proposed that this subset of cells represented the stem cells of the human prostate epithelium. These cells gradually lose expression of K14 leading to an intermediate basal cell type expressing K5 and K18 (K5++/K18+). By proliferation and translocation, a second intermediate cell type arises in the luminal layer (K5+/K18++). Terminal differentiation of the intermediate/transiently proliferating cells results in fully differentiated luminal cells (K18++) and NE cells (Figure 1-7) (van Leenders et al., 2000; van Leenders and Schalken, 2001).

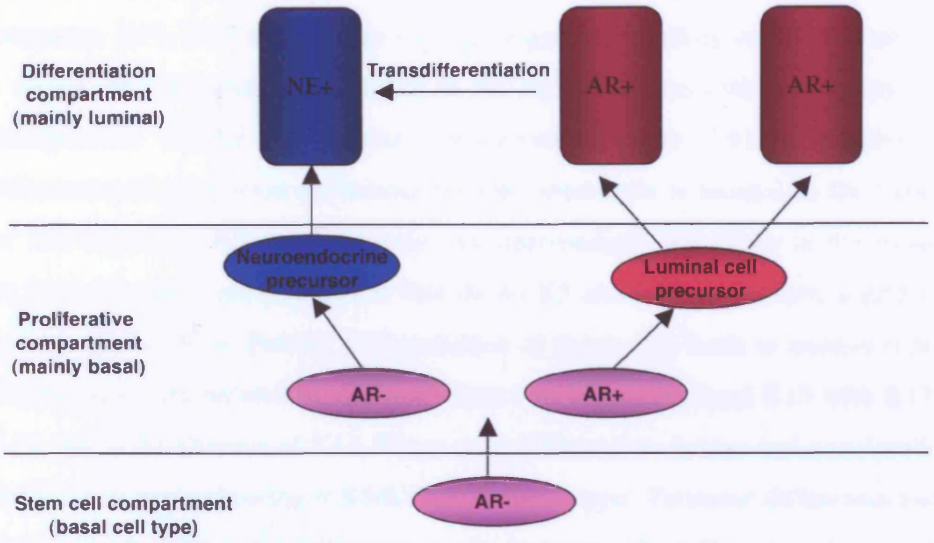

Figure 1-6: Diagramatic representation of the model of prostate epithelial cell differentiation as described by Bonkhoff & Remberger (1996).

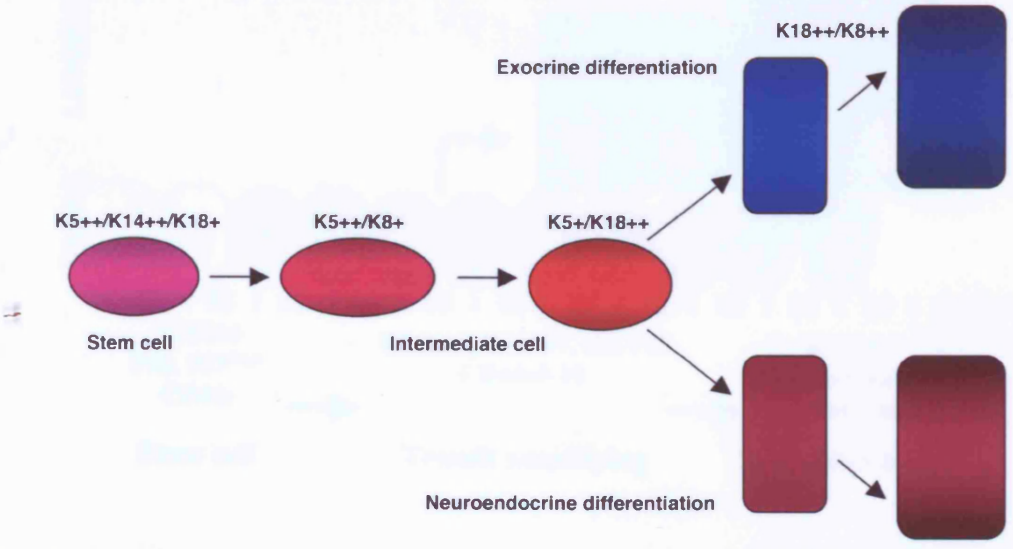

Figure 1-7: Diagramatic representation of the model of prostate epithelial cell differentiation as described by Van Leenders *et al* (2000).

By broadening the range of cytokeratins, Hudson *et al* (2001) proposed that cells with an intermediate basal and luminal phenotype expressed the additional cytokeratins K15, K17 and K19 to varying degrees depending on their location and degree of differentiation leading to the following theoretical pathway of differentiation within the prostate epithelium (Figure 1-8): a relatively undifferentiated population containing prostate stem cells is located in the basal layer and expresses K5 and K14 only. An intermediate cell arises in the basal layer from this stem cell population that shows K5 and K14 expression, together with K15, K17 or K19. Further differentiation of these cells leads to another type of intermediate cell located in the basal layer that express K5 and K15 with K17 or K19, but in the absence of K14. These cells differentiate further and translocate to the luminal layer showing a K8/K18/K19 phenotype. Terminal differentiation of these intermediate cell populations results in terminally differentiated luminal and NE cells (Hudson et al., 2001).

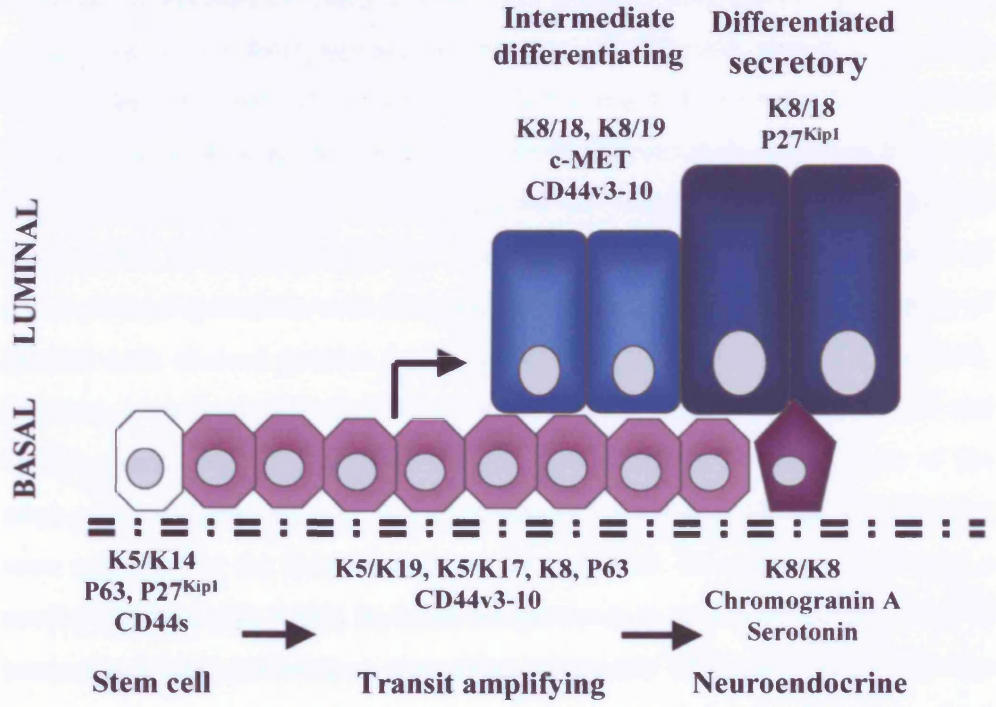

Figure 1-8: Diagramatic representation of the model of prostate epithelial cell differentiation as described by Hudson *et al* , 2001.

An alternative model of differentiation lineage in the human prostate has recently been proposed based on studies of foetal prostate (Wang et al., 2001). The adult prostate originates from the embryonic urogenital sinus epithelium (UGE). Immunohistochemical staining of human, mouse and rat UGE, prior to the growth of prostatic buds, which appear at week ten of gestation in the human foetus (and at days 17 and 19 in the rat and mouse respectively), revealed uniform expression of luminal cell markers K8 and K18 as well as basal cell markers K14 and p63. In addition, expression of K19, a proposed marker of an intermediate (or transit amplifying) cell type, and expression of GSTpi was also observed in the UGE at this stage of development. As prostatic buds appear, solid cords and canalised ducts develop; solid epithelial cords and early development of prostatic ducts revealed a similar differentiation marker profile to that seen in the embryonic UGE. However, as the canalised ducts develop further, a defined lumen appears in which two epithelial cell layers can be distinguished. Immunohistochemical staining of these cells revealed three distinct epithelial cell populations in all three species: a subgroup of cells that appear to be fully differentiated luminal cells expressing only K8 and K18; partially differentiated luminal cells expressing the luminal cell-specific K8 and K18, as well as K 19 and GSTpi; a third cell population expressing the full range of basal and luminal cell markers (K8, K18, K5, K14, p63, K19 and GSTpi). The adult prostate consists of a well-defined epithelium with clear basal and luminal cell layers. The majority of luminal cells showed positive immunohistochemical staining for K8 and K18, however, a small number of cells within the luminal layer also revealed K19 and GSTpi staining but were negative for K5, K14 and p63. The basal layer of the adult prostate contained cells that expressed K5, K14, p63, GSTpi and K19 but were negative for the luminal markers K8 and K18. Interestingly, however, a small fraction of cells within the basal compartment co-expressed the full range of luminal and basal cell markers resembling embryonic UGE cells. This UGE-like cell population represented approximately 0.6% of basal cells. Based on these observations, Wang *et al* (2001) proposed that this sub-group of cells, expressing the full complement of basal and luminal cell markers, represent the stem cells of the adult prostate. Through loss of expression of K5, K14, K19 and GSTpi, these

stem cells give rise to fully differentiated luminal cells and conversely loss of K8 and K18, the stem cells also give rise to basal cells (Figure 1-9).

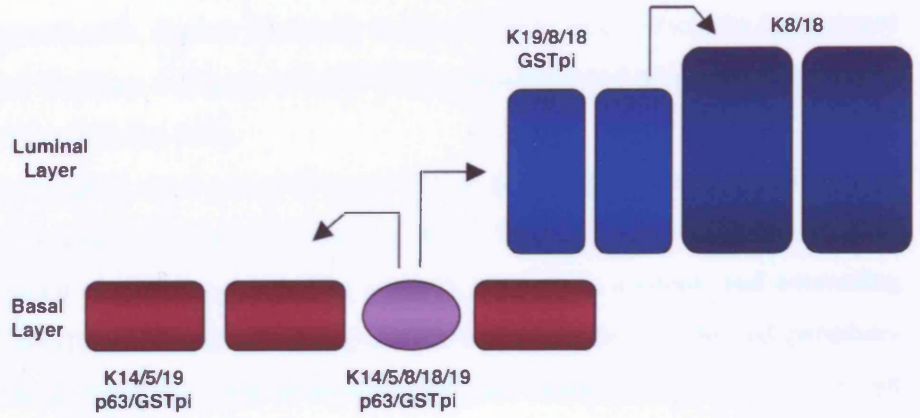

Figure 1-9: Diagramatic representation of the model of prostate epithelial differentiation as described by Wang *et al* , 2001.

1.6 Markers of Differentiation

Advances in our understanding of normal and aberrant prostate epithelial development will require the identification of lineage-specific markers. To date, the most commonly used markers of epithelial cell differentiation are the keratins. Additional proteins are also emerging as differentiation markers (e.g. p21), however there remains the need for markers of more specific stages of the epithelial differentiation process in order to elucidate the underlying mechanisms of disease.

1.6.1 Keratins

The ability of eukaryotic cells to adopt a variety of shapes and to carry out coordinated and directed movements depends on a complex network of protein filaments that extends throughout the cytoplasm, known as the cytoskeleton. All eukaryotic cells contain a cytoskeleton composed of three types of structurally dynamic proteins that reorganise continuously as the cell changes shape, divides and differentiates. These are the actin microfilaments, the microtubules and the intermediate filaments (IF). The intermediate filaments are rope-like fibres able to polymerise into 8-12nm thick filaments (between the diameter sizes of actin and tubulin) and are expressed in nearly all cells of the body. Actin and tubulin are

important for cell shape, movement and cell division whereas IFs have a role in cell and tissue strength. The IF proteins are very diverse and show cell type specific expression. The major types of IFs are vimentin filaments in mesenchymal cells, desmin filaments in muscle cells, neurofilaments in neuronal cells, glial fibrillary acidic protein (GFAP) in glial cells and astrocytes and keratin filaments in epithelial cells.

The keratins are a group of proteins that play a crucial role as scaffolding filaments within epithelial cells (Fuchs, 1988). They exist as a complex array in cells forming an elaborate, cage-like network around the nucleus, and emanating cables (tonofilament bundles) throughout the cell which impact the cell periphery at specialised junctions, such as desmosomes and hemidesmosomes. The keratin proteins constitute the major component of the cytoskeleton in epithelial cells providing structure and mechanical support to the cells and their nuclei (Fuchs and Cleveland, 1998). These filaments are also highly dynamic structures continuously exchanging protein throughout their length in response to different phases of the cell cycle, cell movement and epithelial cell differentiation (Steinert and Bale, 1993).

The keratin proteins are alpha helical polypeptides that have a central 310-amino acid alpha-helical rod domain that is interrupted by three short non-helical linker segments (Hanukoglu and Fuchs, 1982). The rod domain consists of four alpha-helical units designated 1A, 1B 2A and 2B and the linker segments are known as L1, L12 and L2. The end domains are divided into subdomains based on homologous (H), variable (V) and end (E) sequences. E1, V1 and, in type II only, H1, make up the non-helical head domains and V2, E2, and in type II only, H2, comprise the non-helical tail domain (McLean and Lane, 1995) (Figure 1-10).

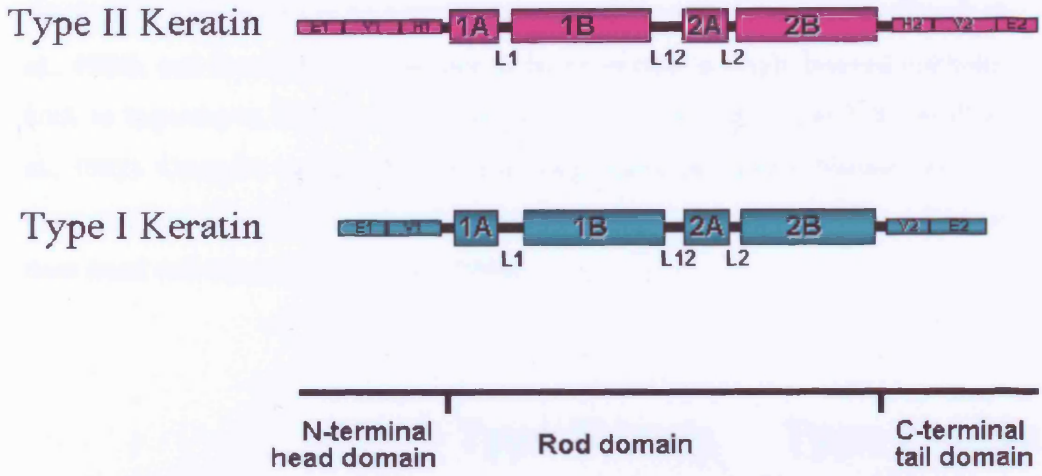

Figure 1-10: Schematic diagram representing the secondary structure of type I and type II keratins.

(Adapted from McLean and Lane, 1995).

The keratins are a large multigene family encoding over thirty different proteins (Lane and Alexander, 1990; Steinert and Bale, 1993) and are expressed in epithelial cells. They have been subdivided into two groups (Type I and Type II) according to their physio-chemical characteristics such as isoelectric point (pI, as determined by 2D electrophoresis), molecular weight, amino acid sequence homology and studies involving reactivity towards monoclonal antibodies AE1 and AE3 recognising acidic and basic proteins respectively (Galvin et al., 1989). Type I cytokeratins are small (Mr 44-65 KDa), acidic (pI:4-6) and comprise of cytokeratins K9-K20. Type II represents the large (Mr 50-70 Kda) neutral/basic (pI:6-9) keratins K1-K8 (Lane and Alexander, 1990). Epithelial cells of different tissues will express a defined pair of a type I, acidic, and a type II, basic/neutral keratin, which is characteristic for that particular epithelium. These pairs of type II and type I keratins are expressed differentially in most epithelial cells at various stages of development and differentiation (Fuchs and Green, 1980; Wu et al., 1982). The type of keratin synthesised and the stage of cell differentiation are so tightly linked that this has lead to the keratins being widely used markers of various stages of epithelial cell differentiation, e.g. progenitor and differentiating cells express different sets of keratins. Figure 1-11 is a summary of specific keratin pair expression in different epithelial tissues. K8 (type II) and K18 (type I)

are the first keratin pair to be expressed during embryonic development (Bosch et al., 1988), and in adults they continue to be expressed in single layered epithelia such as hepatocyte, kidney, which may also express K7, K19 and K20 (Moll et al., 1982). Complex epithelia of trachea, lung, mammary gland, bladder and the prostate gland also express K8 and K18 (Zehner, 1991) as well as K5 and K14 in their basal cell layers (Purkis et al., 1990).

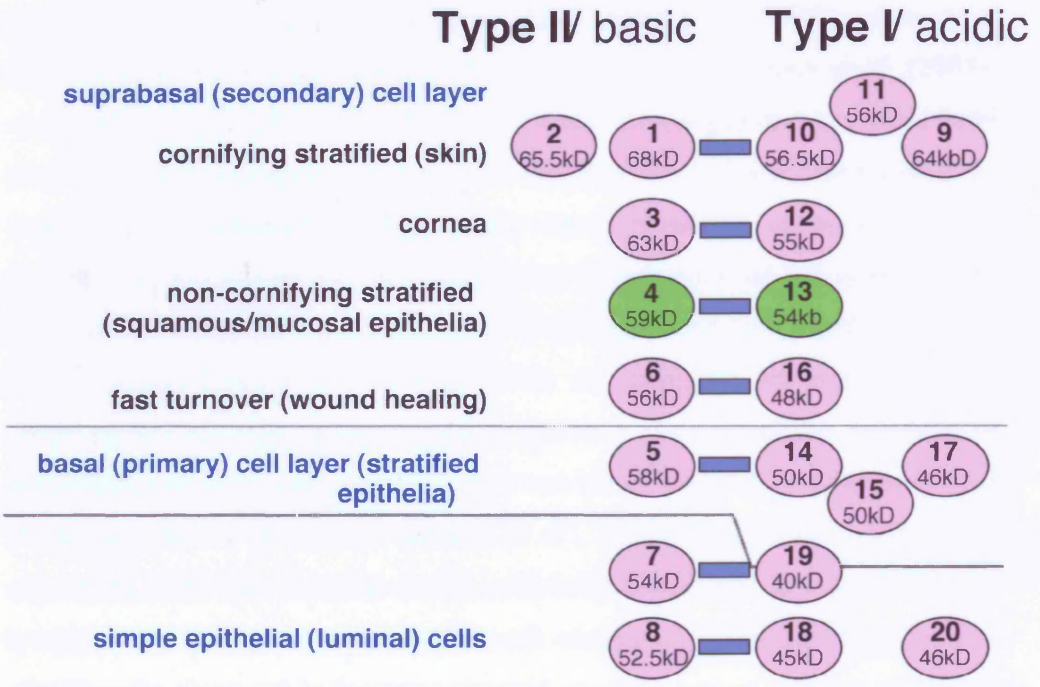

Figure 1-11: Summary of the pairwise expression of keratins in different epithelial types.

Molecular weights are given underneath each keratin in kilodaltons (kDa) (Adapted from Lane and Alexander, 1990).

1.7 Cellular Composition and Differentiation in Prostate Cancer

Prostate carcinoma is predominantly composed of cells with a luminal phenotype (i.e. staining positive for K8, K18, PSA), and dispersed amongst these cancer cells are cells of a neuroendocrine phenotype. Loss of the basal layer in neoplastic foci is a hallmark of the disease; reactivity of the 34βE12 antibody (anti-K1, 5, 10 14)

has therefore been used to distinguish between atypical benign lesions to determine whether adenocarcinoma might be present. As a consequence of these observations, it is thus generally believed that prostate cancer arises from luminal cells.

However, during the last decade, a number of researchers have found expression of high molecular weight keratins in prostate tumours. Expression of K5 has been reported in primary prostate carcinomas (Verhagen et al., 1992) and reactivity with the antibody 34βE12 has been encountered in up to 54% of prostate cancer metastases (Googe et al., 1997; Yang et al., 1999b). A more in depth analyses of cellular markers, carried out by van Leenders *et al* (2001), examined the expression of keratins 5, 14, 18 and chromogranin A in tissues from prostate cancer metastases, and also investigated the cellular composition of regressed and hormone-refractory prostate cancer. Phenotypic characterisation of prostate cancer cell lines was also carried out. Three epithelial cell types present in prostate carcinoma were identified: the predominant cell population were phenotypically luminal cells (K18-positive); an additional cell population was characterised by expression of Chromogranin A, indicating the presence of neuroendocrine cells; and a third cell type was identified by the expression of K5 in the absence of K14 (Van lenders *et al* , 2001). Interestingly, keratin 5-expressing cells were found in tumour cell emboli localised in vessels close to lymph nodes. Furthermore, the median cell number of K5-expressing cells was significantly increased in hormone-escaped prostate cancer samples compared with androgen-dependent prostate cancer. Androgen deprivation did not affect expression of K18. Keratin 14 expression was not observed in the prostate cancer specimens analysed. Ch A expression was also observed in prostate cancer metastases, however its expression did not differ significantly between regressed and hormone-escaped prostate cancer.

As prostate cancer is considered a monoclonal expansion of a transformed epithelial cell type, its heterogeneous cellular composition requires further investigation and understanding. Because of the different phenotypical characteristics of cells found in adenocarcinoma of the prostate, there is some debate regarding exactly which cell type gives rise to prostate cancer. Likely candidates include the stem cell, the intermediate transiently proliferating cell and

the terminally differentiated luminal cell. The presence of distinct epithelial cell types suggests that one cell type is very possibly the progenitor of the other two cell populations. Consequently, it has been proposed that malignant transformation in the prostate may arise from a neoplastic intermediate amplifying cell population, that retains the ability to differentiate into more committed cells. These finally undergo terminal differentiation into K18-expressing luminal cells (Isaacs and Coffey, 1989).

With regards to cells expressing low levels of keratin 5, others have postulated that early intermediate cells express K5 whilst more committed late intermediate cells lose K5 expression, and that it is from these, late, more committed cells that prostate cancer is derived (van Leenders *et al* , 2001). In support of this hypothesis, studies carried out by Verhagen *et al* (1992), demonstrated that K5 expression was more often observed in well-differentiated primary prostate carcinomas (Gleason sum 2-4), whilst K5 was completely absent from tumours with the worst grade of differentiation, Gleason sum 8-10. It was thus postulated that the degree of differentiation of the initially transformed cell type influences the growth pattern of prostate tumours (Verhagen *et al* , 1992).

Irrespective of the molecular pathway leading to cells phenotypically resembling intermediate cells, analysis of this specific cell population might contribute to a better understanding of androgen-independent prostate cancer progression (van Leenders *et al* , 2001).

1.8 *In Vitro* Prostate Epithelial Cell Models

Cellular proliferation, lineage-specific differentiation, migration and apoptosis are highly coordinated processes that occur within tissues or *in vitro* cell systems in a sequential and spatially organised manner. However, deregulation of one or more of these coordinated processes in the human prostate may lead to aberrant proliferation and differentiation; these are characteristics of two of the most common prostatic diseases, BPH and prostate carcinoma. The underlying factors that regulate these processes remain to be fully understood. Therefore elucidating such underlying mechanisms involved in normal prostate epithelial cellular homeostasis is imperative towards then understanding the pathogenesis of these diseases and their subsequent treatment. To date, such research has been

somewhat hindered by a lack of suitable in vitro models for the study of normal prostate epithelial cell differentiation.

1.8.1 Immortalised human prostatic epithelial cell lines

A number of non-tumourigenic immortalised human prostate cell lines have been established. These cell lines have been derived by transfection with different viral immortalising genes of DNA viruses, SV40 (Cussenot et al., 1991; Iype et al., 1998; Kaighn, 1980; Kaighn et al., 1989; Webber et al., 1996b), Human Papilloma Virus-16 (HPV-16) (Bright et al., 1997; Lechner et al., 1978; Schwab et al., 2000) or HPV-18 (Bello et al., 1997; Weijerman et al., 1994). Cells immortalised by SV40 include the PNT1 cell line (Cussenot et al., 1991) and pRNS-1-1 (Lee *et al* , 1994). The PWR-1E cell line was derived by transfection with the adenovirus 12-simian virus 40 hybrid virus (AD12-SV40) (Webber et al., 1996a). Cells immortalised by human Papillomavirus include the PZ-HPV-7 cell line (Weijerman et al., 1994) and the RWPE-1 cell line (Bello et al., 1997). None of the above cell lines form tumours in nude mice. However, only the PWR-1E and RWPE-1 cell lines have been reported to express both the androgen receptor (AR) and prostate-specific antigen (PSA) (Bello et al., 1997; Webber et al., 1996a). Although such cell lines are useful for the study of the progression from a normal to malignant phenotype, they represent a differentiated state and cannot be manipulated to mimic stages of normal prostate epithelial cell differentiation.

Amongst the best characterised and studied prostatic carcinoma cell lines are DU145 derived from a metastatic central nervous system lesion (Stone *et al* , 1977) and PC3 which was derived from a bone metastasis (Kaighn et al., 1978). Both these cell lines are androgen insensitive and independent and do not secrete PSA. Another widely used prostate cancer cell line is LNCaP which was derived from a lymph node metastasis (Horoszewicz et al., 1980). This cell line expresses AR and responds to androgens that stimulate their growth. In addition, the cell line expresses prostatic acid phosphatase (PAP) and PSA.

Other prostatic carcinoma cell lines that have been established include TSU-Pr1 (Iizumi et al., 1987), PPC-1 (Brothman et al., 1989), JCA-1 (Muraki et al., 1990) ND-1 (Narayan and Dahiya, 1992), ALVA-31 (Loop et al., 1993), ALVA-41 (Nakhla and Rosner, 1994), LAPC-4 (Klein *et al* , 1997) and PC-346C (Romija *et al* , 1995). With the exception of LNCaP, most of the prostate cancer

cell lines available to date are of limited value as *in vitro* models of prostate cancer since many prostate-specific characteristics, such as AR and PSA expression, are lost. Thus there is a further need for more, well characterised prostate cell lines.

1.8.2 SV40 immortalisation of human cells

Many cell lines have been derived through immortalization using the SV40 genome. The SV40 genome is a covalently closed, circular, double stranded DNA. This viral genome is divided into early and late regions dependent on when in the infection cycle these genes are transcribed. The early region of the SV40 genome encodes two nonstructural proteins, the large T antigen (T-ag) and the small t antigen. The late region genes encode for viral coat proteins (Bryan and Reddel, 1994). Of the early genes, the large T-ag is required for immortalisation of human cells. It is an essential replication protein that initiates viral DNA synthesis and also stimulates host cells to enter S phase and undergo DNA synthesis. Because of this ability to override cell cycle control, it represents the major transforming protein of SV40.

Normal human fibroblasts or epithelial cells transfected with the SV40 genome have an extended lifespan of 20-30 population doublings compared with untransfected cells (Ide et al., 1984). They then enter a period known as crisis, which may last from weeks to months. During this period, cell numbers become static before gradually declining. There are also gross karyotypic abnormalities and apparently failed mitosis (Sack, 1981). Occasionally however, a cell may escape crisis and acquire the ability to multiply without limit, i.e. become immortal (Wright et al., 1989). The frequency of human cell immortalisation obtained using this method is around 1 per 10^7 cells.

Temperature-sensitive mutants of the A gene encoding the T-ag of SV40 (tsA mutants) have been constructed (Tegtmeyer, 1975) and used to conditionally immortalise cells. Cells immortalised using tsA mutants exhibit temperature-dependent growth. They are able to proliferate at the permissive temperature of 33°C since the T-ag remains active. However, at the non-permissive temperature of 39°C, the T-ag is conformationally inactivated and the cells are no longer driven to replicate, thus allowing the cells to differentiate (Jat and Sharp, 1989). This method has been used to conditionally immortalise several cell types

including embryonic fibroblasts and mammary epithelial cells (Kim et al., 1998; Radna et al., 1989; Small et al., 1982; Stamps et al., 1994).

The mechanism of T-ag-induced immortalisation has been deduced. The T-ag of SV40 forms complexes with the tumour suppressor proteins p53 and pRb and abolishes their normal functions in cell growth control. The cell cycle control of pRb depends upon its phosphorylation state, with under-phosphorylation of pRb preventing cells from entering S phase (Goodrich et al., 1991). T-ag binds preferentially to under-phosphorylated pRb (Ludlow et al., 1989), suggesting that this is one such mechanism by which T-ag confers immortality. The T-ag also binds to the p53 tumour suppressor gene. Wild-type p53 senses DNA damage and either causes the cell to pause in late G_1-phase for DNA repair or directs the cell through the apoptotic pathway if repair is not possible (Levine, 1997) T-ag binding sequesters p53 and allows cells to enter the S phase. The tsA58 mutant of T-ag, fails to bind p53 at the non-permissive temperature and binds pRb with lower affinity.

Transgenic mice have also been generated (Weis *et al* , 1983) that harbour the SV40 strain tsA58 early region coding sequences. These genes are under the control of the mouse major histocompatability complex H-2K^b class I promoter which is active in almost all tissues of the body. Furthermore, the promoter can be induced to higher levels of expression in all cells by interferons (IFNs) (Wallach et al., 1982). Cells derived from such transgenic mice proliferate continuously when cultured at the permissive temperature (33°C) in the presence of IFN-γ. When cells are grown at the non-permissive temperature (39°C) and without IFN-γ they stop dividing and exhibit the capacity to differentiate. This method has been utilised to generate a variety of conditionally immortal cell lines including skin fibroblasts as well as thymus epithelial cells (Jat et al., 1991). It is considered that this manner of generating immortalised cell lines is superior in that the crisis period is omitted in comparison to the aforementioned *in vitro* methods of viral-induced immortalisation. This method has also been very useful in developing cell lines from cells that have previously proved very difficult to establish in culture such as normal intestinal epithelial cells (Whitehead et al., 1993).

1.8.3 The PrE2.8 cell line as a model for the study of human prostatic epithelial differentiation

Although many of the prostate cell lines described above provide useful tools for identifying genes that may play a role in carcinogenesis, many of these immortalisations have produced cell lines that have either a secretory luminal (Cussenot et al., 1991; Iype et al., 1998; Kaighn, 1980; Kaighn et al., 1989; Webber et al., 1996b), or a non-secretory intermediate luminal phenotype (Hayward et al., 1995). Thus, cell lines suitable for studying normal prostate epithelial cell differentiation are limited in terms of translation to the real situation. An appropriate model would prove an invaluable asset towards elucidating the control mechanisms of epithelial cell differentiation and hence towards understanding diseases such as BPH and prostate adenocarcinoma. Therefore, an immortalised cell line, PrE2.8 (Daly-Burns *et al* , in preparation), that maintained characteristics of proliferative prostate cells, while also being capable of undergoing differentiation and growth arrest, was used in this study as a means of identifying genes involved in the regulation of normal prostate epithelial cell growth and differentiation.

The PrE2.8 cell line was derived from BPH tissue and immortalised by transfection of epithelial cells with a temperature-sensitive SV40 Large T construct (Jat and Sharp, 1989); Daly-Burns *et al* , in preparation). This allows the cells to proliferate at a permissive temperature of 33°C. However, when incubated at the non-permissive temperature of 39°C, the Large T antigen is inactivated, the cells cease to proliferate (Figure 1-12 (b)) and undergo genotypic and phenotypic changes consistent with prostate epithelial cell differentiation. PrE2.8 cells grow as small, tightly packed colonies at 33°C and exhibit a homogenous cobblestone appearance; the mean diameter of cells at this growth temperature is 40μm. At the non-permissive temperature of 39°C, PrE2.8 cells become less tightly packed and increase in size to a mean diameter of 52μm (Figure 1-12 (a)). Also, at 39°C, the cells become vacuolated and some are shed from the medium. The epithelial origin of the cells has been confirmed by positive staining for K14, K17 and K8. The keratins were also used to examine the morphological changes related to differentiation in the PrE2.8 model. The basal cell marker K14 was down-regulated at the non-permissive temperature, as determined by FACS analysis. In addition, expression of K8, a marker of differentiated luminal cells, was increased

from occasional staining at 33°C to over half of all cells grown at 39°C expressing the protein (Figure 1-12 (a)). These staining patterns are consistent with the fact that in the prostate, as well as in other epithelial tissues, K14 is expressed by basal cells whereas K8 is a marker of differentiated luminal cells. Furthermore, K19 and K17, also expressed by more differentiated epithelial cells, were undetected in PrE2.8 cells at 33°C but were expressed by a small number of cells grown at 39°C.

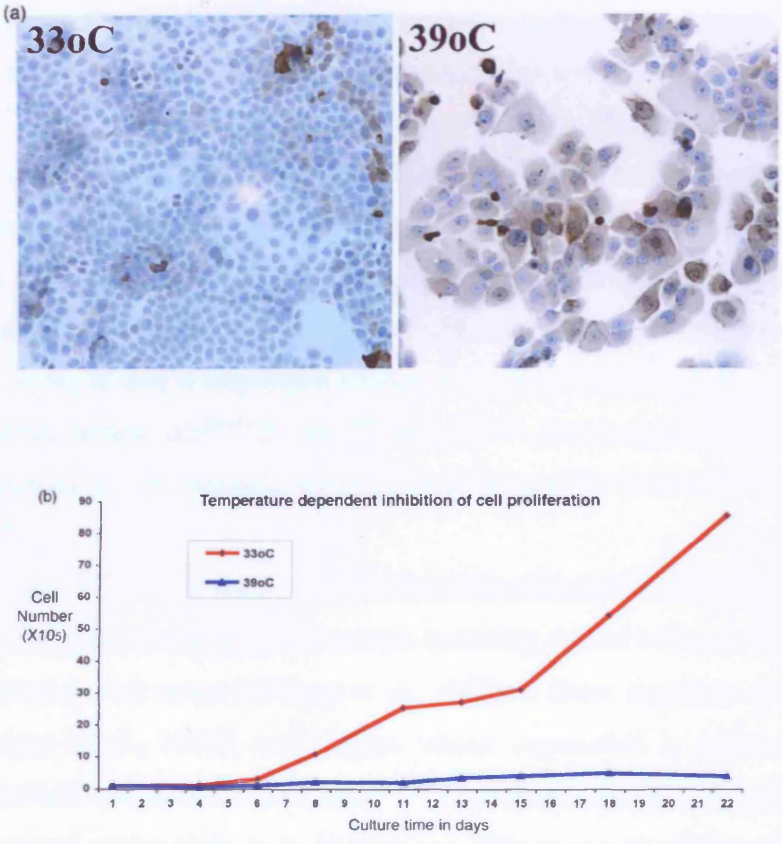

Figure 1-12: Growth characteristics of the PrE2.8 cell line.

(a) shows the growth and marker expression of PrE2.8 cells. Images show cultures of PrE2.8 cells incubated at permissive (33°C) and non-permissive (39°C) growth temperatures. At 33°C, the cells are small, densely packed and show occasional K8 (brown) expression. An altered cell morphology is observed at 39°C with an increase in cell size as well as a vacuolated appearance. This is accompanied by an increase in K8 expression levels. (b) shows growth curves for PrE2.8 cells incubated at 33°C (red) and 39°C (blue). At the permissive temperature, exponential cell proliferation is observed over time, whereas at 39°C, little or no cell proliferation is observed.

In addition to the keratins, other markers of differentiating cells were also examined. For example, expression of $p21^{Waf1/Cip1}$, a gene involved in cell cycle control and differentiation, was undetectable at 33°C but expression levels rose in a time-related fashion in the presence of a subsequent increase in growth temperature. Cellular factors that determine whether cells continue to proliferate or cease dividing and differentiate appear to function during the first gap phase (G_1) of the cell cycle. Progression through the G_1-phase and initiation of DNA synthesis (S phase) during the mammalian cell division cycle are cooperatively regulated by several classes of cyclin-dependent kinases (CDKs) whose activities are in turn constrained by CDK inhibitors (CDKIs). There are two classes of CKIs based on their structure and CDK targets. The first class is known as the INK4 proteins due to their ability to specifically inhibit the catalytic subunits of CDK4 and CDK6; these include the proteins $p16^{INK4a}$, $p15^{INK4b}$, $p18^{INK4c}$ and $p19^{INK4d}$. The second class of CKIs belong to the Cip/Kip family, which inhibit the activity of cyclin D-, E- and A-dependent kinases that are involved in G_1-S transition. These proteins include $p21^{Waf1/Cip1}$, $p27^{Kip1}$ and $p57^{Kip2}$, which share significant sequence homology in their amino-terminal portions that enable them to bind to cyclins and CDKs.

$p21^{Waf1/Cip1}$ was the first cyclin-dependent kinase CDKI to be identified and was found to have multiple functions including that of being a mediator of p53-induced growth arrest (el-Deiry et al., 1993), a direct regulator of CDK activity (Harper et al., 1993), and a gene whose expression is induced at cellular senescence (Noda et al., 1994). $p21^{Waf1/Cip1}$ interacts directly with cyclins through a conserved region close to its N-terminus. This region also has a separate CDK2 binding site. The unique carboxy-terminal domain of $p21^{Waf1/Cip1}$ associates with proliferating cell nuclear antigen (PCNA) and can inhibit DNA replication directly, without affecting DNA repair (Li et al., 1994b). CDK inhibition by $p21^{Waf1/Cip1}$ results in dephosphorylation of the retinoblastoma protein (pRb) and the inhibition of E2F transcription factors that regulate many genes involved in DNA replication and cell cycle progression (Nevins, 1998).

Besides the functions of $p21^{Waf1/Cip1}$ in cell cycle control, it also plays a role in differentiation. Differentiating cells exhibit a prolonged G_1-phase of the cell cycle and inhibition of G_1-S transition (Clegg et al., 1987). Expression of

$p21^{Waf1/Cip1}$ is increased in a variety of differentiating cells (Steinman et al., 1994). In the skin as well as the intestinal epithelium, expression of $p21^{Waf1/Cip1}$ is induced in postmitotic cells immediately adjacent to the proliferative compartment, but is decreased in cells further along the differentiation pathway (el-Deiry et al., 1995; Gartel et al., 1996; Ponten et al., 1995). A similar down modulation of $p21^{Waf1/Cip1}$ expression occurs in cultured epidermal cells at late stages of differentiation (Di Cunto et al., 1998) suggesting that $p21^{Waf1/Cip1}$ is necessary for the early stages of the differentiation process in these cell types. In retinoic acid-induced differentiation of acute promyelocytic leukaemia cells, $p21^{Waf1/Cip1}$ has also been shown to play a necessary function, which is unlinked to its effects on the cell cycle (Casini and Pelicci, 1999). However in this case, unlike the keratinocyte and epithelial systems, $p21^{Waf1/Cip1}$ appears to play a positive promoting role in differentiation. Thus, the emerging consensus is that $p21^{Waf1/Cip1}$ can play an important regulatory function in differentiation, which is not directly linked to its effects on the cell cycle, and which can be either negative or positive depending on cell type and on specific stages of differentiation. The increase in expression of $p21^{Waf1/Cip1}$ in the PrE2.8 model at 39°C therefore further supports a differentiating phenotype of the cells at this temperature.

The expression of prostate stem cell antigen (PSCA) was also observed in the PrE2.8 cells. PSCA, a prostate-specific cell surface antigen, was originally reported to be restricted to a subset of basal cells, and due to its homology to stem cell antigen 2 (SCA-2), it was hypothesised that PSCA may play a role in stem/progenitor cell functions such as self renewal or proliferation (Reiter et al., 1998). More recent studies (Chau *et al* , 2002) however, have indicated that PSCA is more likely a marker of an intermediate sub-population of epithelial cells in transition from a basal to a terminally differentiated luminal phenotype. This is supported by the observation that PSCA-positive primary prostate epithelial cells show a more differentiated morphology and phenotype than PSCA-negative cells. In addition, cells positive for PSCA expressed basal cell markers such as K5, K14 and CD44, but also the luminal cell marker K18; however, expression of p63, a putative stem cell marker, was lost. Also, the PSCA-expressing cells localised above the monolayer and expressed PSA and AR transcripts, but not PSA or AR protein, indicating early differentiation of this subpopulation. In line with this study, expression of PSCA in the PrE2.8 cell line was very low or undetectable at

33°C, whereas at the non-permissive temperature, PSCA expression was strongly detected.

Taken together, the genotypic and phenotypic changes observed in the PrE2.8 cell line, when the cells are switched from a permissive to a non-permissive temperature, are consistent with the Hudson *et al* (2001) epithelial differentiation pathway model. At 33°C, the PrE2.8 cells exist as small, tightly packed, highly proliferative colonies and express the basal cell marker K14. When switched to 39°C, the cells cease proliferating, exhibit a larger morphology and become vacuolated. In addition, expression of K14 is down-regulated, accompanied by up-regulation of cell differentiation-associated markers, including K8/17/19, $p21^{Waf1/Cip1}$ and PSCA. The cells do not however express PSA or AR, markers of terminally differentiated prostate epithelial cells. It is proposed therefore, that the PrE2.8 cell line represents prostate epithelial cells undergoing early stages of differentiation, representative of an intermediate transit-amplifying population (Daly-burns *et al* , in preparation). The absence of PSA and AR may also be due to the lack of specific signalling factors required for the expression of these genes. For example, some authors have speculated that the presence of stromal cells (Liu et al., 1997) or testosterone (Peehl et al., 1988) is required for PSA/AR expression in primary prostate epithelial cells in culture. Furthermore, Hudson *et al* (2000) performed studies in which primary epithelial cell cultures were grown in Matrigel in the presence of Mibolerone and stromal cell-conditioned medium. These conditions resulted in the formation of spheroid cellular structures consisting of an outer basal cell layer surrounding a luminal layer and lumen containing AR-expressing cells. Similarly, the PrE2.8 cells also formed small spherical structures with detectable levels of AR transcript, when grown in Matrigel in the presence of stromal cells and Mibolerone, however AR protein was not detected. Thus, full differentiation, including PSA expression was not observed in the PrE2.8 model, suggesting that additional factors may be required for terminal differentiation to occur (Daly-Burns *et al* , in preparation). Nevertheless, the PrE2.8 cell system represents a viable model for the study of the early changes in gene expression occurring during the process of prostate epithelial cell differentiation.

The PrE2.8 cell line was therefore used in this research project as a model system in which to identify genes that may be involved in the process of normal

prostate epithelial cell differentiation. Although many authors have proposed putative models of the normal differentiation pathway in the prostate epithelium, the underlying mechanisms controlling this process remain poorly defined. There also remains a lack of informative markers representing the distinct cell types residing in the prostate epithelium, i.e. stem, basal, "intermediate" and luminal cells. The use of *in vitro* models, such as the PrE2.8 cell line, provide invaluable tools for identifying such markers and gaining a global genetic insight into the molecular mechanisms controlling prostate epithelial cell growth and differentiation. The aim of this research was to identify genes involved in the process of normal epithelial cell differentiation using the PrE2.8 cell line as a model system. Therefore, a research strategy was followed in order to discover genes involved in this pathway. The technique of differential display was used to ascertain differences in gene expression between a proliferative and differentiating phenotype in the PrE2.8 cell line. A more global approach was then implemented, through the use of microarray analysis, to provide additional insights into the genetic events that may be involved in the differentiation of prostate epithelial cells. This approach led to the identification of a number of putative markers of prostate epithelial cell differentiation. An explanation at the molecular level to the biological basis of cellular homeostasis in the prostate, and moreover, the clinical heterogeneity observed in prostatic diseases is critical to their appropriate therapy. Genes identified in this study may therefore provide diagnostic and prognostic markers, as well as markers for the targeted therapy of diseases such as BPH and prostate cancer.

2 MATERIALS AND METHODS

2.1 Standard Solutions and Media

DNA loading buffer (3x)	30mM EDTA, 30% sucrose, 0.1% bromophenol blue, 0.1% xylene cyanol FF, 1M Tris-HCl pH8.
20x SSC	3M NaCl, 300mM sodium citrate, pH7.0.
LB medium	10g Bacto-trytone (Oxoid), 5g Bacto-yeast (Oxoid), 5g NaCl dissolved in 1L dH_2O and autoclaved.
LB agar	LB media plus 1.5% Bacto agar (Oxoid).
LB-Amp	LB media containing 100µl/ml ampicillin.
0.5M EDTA	186.52g dissolved in 1L dH_2O, pH adjusted to 8.0 with conc. NaOH then autoclaved.
5M NaCl	292.2g in 1L dH_2O autoclaved.
3M Na-acetate	246.08g in 1L dH_2O, pH adjusted to 5.5 with glacial acetic acid.
20% SDS	50g dissolved in 250ml dH_2O, autoclaved.
1M Tris-HCl pH8.8	121.2g in 1L dH_2O, pH adjusted to 8.8 with conc. HCl, autoclaved.
X-gal solution	0.2% X-gal (from 2% stock in DMF), 1mM $MgCl_2$, 150mM NaCl, 3.3mM $K_4Fe(CN)_6.3H_2O$, 3.3mM $K_3Fe(CN)_6$, 60mM Na_2HPO_4, 40mM NaH_2PO_4. Filtered through a 0.2µm pore filter.
0.1% DEPC sdH_20	5ml DEPC (Sigma) in 5L dH_2O stirred at r/t o/n and then autoclaved.
Ampicillin (100mg/ml)	2.5g dissolved in 25ml sdH_2O, aliquoted into 5ml bijous and stored at -20°C for long term storage.
1M IPTG	1g dissolved in 4.2ml sdH_2O, stored as 1ml aliquots at -20°C.

50x TAE	242g/L Tris base, 57.1ml/L glacial acetic acid, 100ml/L 0.5M EDTA pH8.
RNase A (10mg/ml)	200mg RNase A in 200ml sdH_2O, heated to 100°C for 15 mins, cooled and stored as frozen 1 ml aliquots.
DAB solution	(Diaminobenzidine tetrahydrochloride). 25mg of DAB dissolved in 50ml Tris-HCl pH7.6, then 250µl 6% H_2O_2 added.
ABC solution (Dako)	To 5ml Tris-HCl pH7.6 was added 1 drop of reagent A (Avidin in PBS) and 1 drop of reagent B (biotinylated horseradish peroxidase), mixed well prepared 30 mins before use to allow formation of avidin-biotinylated horseradish complex. This is stable for 5 days at 4°C.
2.5% Trypsin	2.5g Trypsin dissolved in 1x PBS, pH7.0, filter sterilised and stored as 5ml aliquots at -70°C. When required for trypsinising cells the 2.5% solution was diluted 1:10 in sterile 1x PBS and stored as 5ml aliquots at -20°C.
GTC Stock solution.....	To 293 ml of deionised H_2O add, 250g guanadinium isothiocyanate, 17.6 ml 0.75 M sodium citrate pH 7, 26.4 ml 10% Sakosyl. Store the solution at 4°C. Before use, make up a 50 ml GTC solution by adding 360 µl β mercaptoethanol and 500 µl antifoam A.
3 M NaOAc.....	Dissolve 408.24 g sodium acetate-3H_2O in 800 ml H_2O. Adjust to pH 5.2 with glacial acetic acid. Adjust volume to 1 litre with deionised H_2O. Sterilise by autoclaving and store at room temperature.
Ethidium Bromide (EtBr).....	Prepare stock solution of 10 mg/ml by adding 1 g EtBr to 100 ml H_2O. Stir until the dye has completely dissolved. Store in the dark at room temperature. During electrophoresis add 0.5-1 µg per ml of agarose solution.

10% Ammonium persulphate..... Dissolve 1 g ammonium persulphate (APS) in 8ml H_2O. Adjust volume to 10 ml with H_2O. This solution is stable at 4°C for 2 weeks.

2.2 Oligonucleotide primers synthesised

Primer Name	Homology/Gene Name	Primer Sequence (5' – 3')	Annealing Temperature
A2.2 S	S100 calcium binding protein A8	ctttatcaccagaatgaggaactcc	60°C
A2.2 A	"	ggatgacctgaagaaattgctagag	
B9 S	BAC clone	gcatgtttcccaggctgatc	60°C
B9 A	"	cactcattggatcaatgttc	
B10 S	Newcastle disease virus inducible protein	caggcacacagtcactgaag	60°C
B10 A	"	catgagatgaatagagac	
C5.1 S	Cyclooxygenase 2	ggctgagggaacacaacagag	60°C
C5.1 A	"	caggatacagctccaacagcatc	
C5.2 S	Cytochrome c oxidase subunit II	aggcgacctgcgactccttg	60°C
C5.2 A	"	agacgatgggcatgaaactgtg	
C6 S	Human mitochondrial complete genome	gtcgcaggataccctctctc	55°C
C6 A	"	gagccccattgtgttgtgg	
C8.1 S	Arabidopsis thaliana DNA chromosome 3 clone	gaggaaataagtagcctttc	60°C
C8.1 A	"	gcacgatattgcagtcttgatc	
C8.2 S	PAC clone	gaggtttaatggactcacag	60°C
C8.2 A	"	cgatttgaacggtgggagat	
C9.2 S	Human mitochondrial complete genome	gaacaggctcctctagagg	55°C
C9.2 A	"	ggtgacactatgaatactc	
C9.3 S	"	agcggacgaagcgcgaag	60°C/65°C
C9.3 A	"	ggcatttgtggatgagcccag	
C14.1 S	S.pombe chromosome 3 cosmid	ggatacaactttgcaacttggc	60°C
C14.1 A	"	cttgaggaggaagaatgggttc	
C16 S	Small proline rich protein 1B	agcacattctttttggggg	60°C
C16 A	"	acactccagcaccagccc	
C18.1 S	Alpha tubulin	catgacatgctgcagggc	60°C
C18.1 A	"	aggaaggcgagttttcagagg	
D4 S	PAC clone	cgatatccgttcgagtcgcctag	60°C
D4 A	"	gatgagcctaagggtcatccg	
D7 S	Heat shock protein	agttcgcccatttctgcttcagg	60°C
D7 A	"	gaattcgattttggcacgggg	
E6 S	BAC clone	gtcgcaggataccctctctc	60°C
E6 A	"	gagccccattgtgttgtgg	
AP A2	Random 10mer	gaccacgtgc	40°C
AP A19	"	ttcgaccctg	40°C
AP B9	"	tgggggactc	40°C
AP B10	"	ctgctgggac	40°C
AP C5	"	gatgaccgcc	40°C
AP C6	"	gaacggactc	40°C

AP C8	"	tggaccggtg	40°C
AP C9	"	tggaccggtg	40°C
AP C14	"	tgcgtgcttg	40°C
AP C16	"	cacactccag	40°C
AP C18	"	tgagtgggtg	40°C
AP D4	"	tctggtgagg	40°C
AP D7	"	Ttggcacggg	40°C
AP E6	"	ttggcacggg	40°C
AP E7	"	aagacccctc	40°C

2.3 Tissue Culture

As a cellular model of differentiation, a conditionally immortalised prostate epithelial cell line, PrE2.8, was used (Daly-Burns *et al* , in preparation). Briefly, prostate tissue was obtained from a patient undergoing transurethral resection of the prostate as treatment for BPH. Prostate epithelial cells were isolated and conditionally immortalised with an SV40-construct containing a temperature-sensitive Large-T antigen. At 33°C, the Large-T antigen is functionally active and the cells proliferate. However, at 39°C, the cells stop proliferating due to temperature-induced inactivation of the Large-T protein, and undergo morphological changes consistent with differentiation.

The PrE2.8 epithelial cell line was maintained in complete PrEGM medium (Clonetics). Cells were grown in 75cm^3 tissue culture flasks at either 33°C or 39°C in a humidified incubator containing a 5% CO_2 environment. Cells were grown at the permissive temperature of 33°C or they were grown at 33°C to ~50% confluency prior to being transferred to the non-permissive temperature of 39°C. Passage of cells was carried out by the addition of 3 ml of trypsin/versine to the flasks followed by incubation at 37°C for 5-10 minutes. Twenty ml of PrEGM medium was then added to the flasks and the cell suspension was transferred to a 50 ml centrifuge tube and centrifuged at 1200 rpm to pellet the cells. The supernatant was aspirated and the cells resuspended in 10 ml of PrEGM medium. One in ten dilutions were subsequently re-seeded into 75cm^3 flasks that had been pre-coated with collagen.

2.4 Primary Cell Culture

Prostate tissue chips freshly collected from a transurethral resection of the prostate (TURP) were washed three times in collection medium and transferred into a petri dish. Burnt areas of tissue and areas of clotted blood were trimmed using a scalpel and the tissue was weighed. It was then finely cut into less than $1mm^3$ pieces using a pair of scalpels. The minced tissue was transferred to a sterile universal and resuspended in 20 ml of PBS. Once the tissue had settled to the bottom of the tube, the PBS was aspirated in order to remove blood and debris. This process was repeated until the supernatant was clear. In order to separate the stroma from the acini, the tissue was resuspended in 200 IU/ml collagenase type 1A (Sigma) and digested at 37°C with gentle agitation on a R100 Rotatest shaker (Luckham Ltd) for 18-20 hours. The digested tissue was centrifuged at 800 rpm for 20 secs, the sedimented acini transferred to 20 ml PBS and the process repeated twice. A single cell suspension was produced from the acini by digestion of the pellet in 20 ml 0.25% trypsin/versene in buffered saline at 37°C for 20 mins with agitation. The digested acini were centrifuged at 1000 rpm for 5 mins, the trypsin aspirated and the pellet resuspended in 10 ml DMEM containing 10% fetal calf serum in order to inactivate the trypsin. The pellet was then resuspended in PrEGM medium (Clonetics) and cells plated onto collagen type 1 (Vitrogen 100) pre-coated Petri dishes at 1000 cells per 6 cm dish in the presence of a feeder layer of lethally irradiated NIH 3T3 cells. The feeder cells were used to help maintain clonal growth of the cells.

2.5 Isolation of Total RNA from Cultured Cells

Total RNA was extracted from primary cultures or from PrE2.8 cells grown at 33°C when the flasks were ~60-70% confluent, or from PrE2.8 cells 4, 7, 10 and 14 days after being transferred to 39°C. Culture medium was aspirated and the cells were washed with ice cold PBS. Cells were lysed directly in the culture flask by the addition of 4 ml of GTC solution and agitation of the flasks for approximately 5 minutes until the cell layer was completely dissolved. The cell lysates (approximately 4 ml) were then transferred to 15 ml centrifuge tubes to which was added a 1/10 volume of 2 M NaOAc pH 4 (400µl), an equal volume of

phenol pH 4 (4.4 ml) and 2/10 volume of chloroform (1.76 ml). The solutions were vortexed and placed on ice for 20 minutes. The samples were then centrifuged at 4°C for 20 minutes at maximum speed (4400 rpm) in a Sorval bench top centrifuge after which the upper aqueous layer was transferred to a fresh centrifuge tube with a sterile Pasteur pipette. An equal volume of isopropanol was added to each sample and the RNA was allowed to precipitate at 4°C for at least 30 minutes. Following the precipitation step, the samples were centrifuged at maximum speed (4400 rpm) at 4°C in a Sorval bench top centrifuge for 20 minutes. The supernatant was removed and the RNA pellet was resuspended in 60 µl of DEPC-treated H_2O and transferred to autoclaved, nuclease-free microcentrifuge tubes. Samples of RNA were stored at –80°C prior to use.

2.6 Differential Display

It is crucial that the total RNA used for mRNA Differential Display (DD) is free of DNA contamination. Total RNA (50-100 µg) was DNase-treated following isolation according to the manufacturers instructions to remove contaminating DNA using a MessageClean kit (Biogene/GenHunter):

2.6.1 DNase I Digestion

Reaction tubes for each sample were set up as follows:

Reagent	Amount
Total RNA	50 µl (50-100 µg)
10x reaction buffer	5.7 µl
DNAse I	1.0 µl
Total volume	56.7 µl

The samples were mixed well and incubated for 30 minutes at 37°C.

2.6.2 Phenol/$CHCl_3$ (3:1) Extraction

This step is essential to ensure the removal of protein contamination and DNase I from the RNA. Following DNase I digestion, 40 µl of Phenol/$CHCl_3$ was added to each reaction tube and vortexed for 30 seconds. The samples were then incubated on ice for 10 minutes and spun in an Eppendorf microfuge at maximum speed (13,000 rpm) for 5 minutes at 4°C. After centrifugation, the upper phase was transferred to a new reaction tube.

2.6.3 Ethanol Precipitation

To each reaction tube, 5 µl of 3 M NaOAc and 200 µl 100% ethanol was added and the samples were incubated at –80°C for 1 hour. The samples were then re-spun at maximum speed (13000 rpm) for 10 minutes at 4°C and the supernatant was discarded. The RNA pellet was re-dissolved in 25 µl DEPC-treated H_2O.

Total RNA was diluted by adding 5 µl RNA to 995 µl DEPC-treated H_2O and the amount of RNA in each sample quantified by reading the OD_{260} on a spectrophotometer (Beckman). The concentration of total RNA in each sample was calculated using the following formula:

RNA concentration = OD_{260} x dilution factor x constant

Constant = 40 µg/ml = 1 OD_{260}.

2.6.4 Reverse Transcription

Total RNA was reverse transcribed and first strand cDNA was synthesised using Superscript II (Stratagene) reverse transcriptase. For each RNA sample (obtained from 33°C-incubated cells at day 7 or 39°C at day 7) 1 µg of cleaned total RNA was reverse transcribed from each of three single base-anchored oligo dT primers ($T_{11}G$, $T_{11}A$, $T_{11}C$). The following components were added to sterile, nuclease-free microcentrifuge tubes for each sample:

Reagent	Amount
Total RNA	1-5 µg
Oligo dT primer ($T_{11}G$, $T_{11}A$ or $T_{11}C$)	1.0 µl
DEPC-treated sterile H_2O	To a final volume of 12 µl

The samples were then heated at 70°C for 10 minutes and quick chilled on ice, after which they were briefly centrifuged (approximately 2-3 secs) to collect the contents at the bottom of the reaction tubes. The following components were then added to each reaction tube:

Reagent	Volume
5x first strand buffer	4 µl
0.1 M DTT	2 µl
10 mM dNTP mix	1 µl

After gentle mixing, reaction tubes were incubated at 42°C for 2 minutes after which 1 µl of Superscript II was added to each reaction tube. The contents were

mixed by pipetting gently up and down and incubated at 42°C for 50 minutes. Reactions were then inactivated by heating at 70°C for 15 minutes. The three reverse transcription (RT) reactions with each of the anchor primers were mixed ($T_{11}M$ (mixed) = $T_{11}G$, $T_{11}A$ and $T_{11}C$) and diluted 5-fold for each sample. Reactions were stored at –20°C prior to use.

2.6.5 Differential Display PCR

Following reverse transcription, samples were subjected to DD PCR. Each mixed reverse transcription was amplified in a 10 µl PCR reaction with AmpliTaq polymerase (Perkin Elmer). These reaction tubes were set up as follows:

Reagent	Amount
RT mix	1 µl
10x buffer	1 µl
dNTP (25 µM)	0.8 µl
α-(^{35}S)dATP	0.2 µl
T11M primer (2 µM)	1 µl
Random primer (2 µM)	1 µl
AmpliTaq (5 units/µl)	0.2 µl
sd H_2O	4.8 µl
Total volume	10 µl

After gentle mixing, a drop of mineral oil was added to each reaction tube, in order to prevent evaporation, prior to being placed into the thermal cycler (Perkin Elmer). The following temperature cycles were used for amplification:

94°C/ 5 min ---> 94°C/ 30 sec ---> 40°C/ 2 min ---> 72°C/ 30 sec ---> 72°C/ 5 min

I <---------- 40 cycles ----------> I

2.6.6 Acrylamide Gel Electrophoresis

After completion of the differential display PCR reactions, PCR products were loaded onto acrylamide/urea sequencing gels and electrophoresis was carried out using Biorad gel electrophoresis apparatus. Firstly, the glass plates were cleaned with acetone and siliconized by covering with approximately 1ml of Sigmacote. The glass plates and spacers were then clipped together and the gel was poured between the plates. A 6% acrylamide/urea sequencing gel was made by adding 20 ml of Buffer to 80 ml of Sequal gel 6 monomer (National Diagnostics) and 0.8 ml of 10% ammonium persulphate. Gels were allowed to set overnight. Once set,

the gels were pre-run at 1600 V (50 mA, 60 W) to warm the gel to approximately 50°C. The PCR products (10 µl) were mixed with 3.3 µl of 3X sequencing loading buffer, denatured at 80°C for 2 minutes and 3 µl of product loaded onto the sequencing gel. The gels were then run at 1700 V for 3-4.5 hours in 1X TBE running buffer, blotted onto Whatman 3MM paper and dried in a gel dryer for approximately 1 hour at 80°C. The gels were exposed to X-Omat LS X-ray film (Kodak) for 1-5 days.

2.6.7 Isolation of Differentially Amplified PCR Products

Bands of interest were identified by overlaying the autoradiographs onto the dried gels in order to locate the DNA bands on the gel. The DNA was cut out and eluted from the gel as follows. Excised bands were placed into microcentrifuge tubes with 100 µl of dH_2O and incubated at 37°C overnight. The samples were then boiled for 10 minutes in a water bath and centrifuged at 13,000 rpm for 2 minutes. The supernatant was transferred to a fresh microcentrifuge tube and ethanol precipitation was carried out by adding to each tube 10 µl 3 M NaOAc (pH 5.2), 300 µl EtOH and 10 µl glycogen (10 mg/ml). Samples were left to precipitate at -20°C overnight after which they were centrifuged at 13,000 rpm for 20 minutes. The supernatant was discarded and the DNA pellet re-suspended in 10 µl dH_20.

Eluted DNA, representing the differentially expressed bands of interest, was then used as a template for re-amplification in a PCR reaction, using the same primer pairs used for DD PCR. Reactions were set up as follows:

Reagent	Amount
Eluted DNA	1 µl
10x buffer	1 µl
dNTP (2 µM)	0.8 µl
$T_{11}M$ primer (2 µM)	1 µl
Random primer (2 µM)	1 µl
AmpliTaq (5 units/ µl)	0.2 µl
sd H_2O	5 µl
Total volume	10 µl

After gentle mixing, a drop of mineral oil was added to the reaction tube, in order to prevent evaporation, and samples were placed into the thermal cycler (Perkin

Elmer). The temperature cycles were exactly as used in the differential display PCR (see section 2.6.5).

2.6.8 Agarose Gel Electrophoresis

Agarose gel electrophoresis separates and detects different sized fragments of DNA following PCR amplification. Re-amplified DNA excised from the acrylamide gels was separated and visualised using this method. The gel apparatus was set up according to the manufacturers instructions. 1.5 g of ultrapure agarose (BDH) was dissolved in 100 ml of 1X TAE by heating at full power for 2-3 minutes in a microwave. The mixture was cooled to approximately 50°C, 5 µl 10 mg/ml ethidium bromide (EtBr) was added and the contents were swirled gently to mix. The gel mix was then carefully poured into the assembled gel cassette with the comb(s) inserted and the gel was allowed to set at room temperature for 20-30 minutes. Combs and the ends of the gel casting tray were carefully removed before the system was immersed into a reservoir of 1X TAE buffer. DNA samples were mixed with sucrose loading buffer and 10 µl of sample were loaded. The gel apparatus was then connected to a power supply and the system was run at 100 V for ~30-45 minutes. After electrophoresis for the appropriate time, the DNA was visualised on a UV transilluminator and image captured using a gel documentation system (BioRad).

2.6.9 DNA Band Nomenclature

Individual bands representing potential gene candidates were named according to the name of the arbitrary primer used to amplify the gene sequences. If more than one band was isolated following amplification with the same primer pair, then nomenclature was sub-sectioned according to size (Section 2.2).

2.6.10 Cloning of DNA into Plasmid Vector

Re-amplified DNA products were purified and cloned into a pGEM T-Easy vector prior to sequencing. The pGEM-T Easy vector has been prepared by adding a 3′ terminal thymidine (3′-T overhangs) to both ends of the vector. These prevent recircularisation of the vector and also provide compatible overhangs for PCR products generated by thermostable polymerases such as AmpliTaq. These polymerases add a single deoxyadenosine, to the 3′–ends of amplified DNA fragments. The vector also contains T7 and SP6 RNA polymerase promoters

flanking a multiple cloning region within the α-peptide coding region of the enzyme β-galactosidase. Successful cloning of an insert into the vector interrupts the coding sequence of β-galactosidase and recombinant clones can thus be identified by the production of white colonies whereas vectors that do not contain an insert produce blue colonies. The cloning procedure was as follows:

2.6.10.1 PCR Product Purification

DNA re-amplified from excised bands was purified using a QIAquick PCR Purification Kit (QIAgen). DNA was purified according to the manufacturers instructions.

2.6.10.2 Ligation of Vector to Insert DNA

After the PCR products were purified they were ligated to the pGEM-T Easy vector (Promega) system. The following reactions were set up for each purified PCR product:

Reagent	Standard Reaction	Positive Control	Background Control
2x rapid ligation buffer	5 µl	5 µl	5 µl
Pgem-T Easy vector (50ng)	1 µl	1 µl	1 µl
PCR Product (Insert DNA)	3 µl	–	–
Control insert DNA	–	2 µl	–
T4 DNA Ligase (3 units/µl)	1 µl	1 µl	1 µl
sd H_2O to a final volume of	10 µl	10 µl	10 µl

The components were mixed by pipetting and incubated either for 1 hour at room temperature or at 4°C overnight. An aliquot of the ligation reaction mix was then taken to be transformed into competent host bacterial cells. The remaining ligation mix was stored at 4°C for future use.

2.6.10.3 Plasmid Transformation of *E.coli*

Frozen aliquots of competent *E.coli* cells (MAX Efficiency DH5α Competent Cells, Gibco Life Technologies), stored at –70°C, were thawed on ice for 15 minutes. 20 µl of cells were aliquoted into pre-chilled 1.5 ml microcentrifuge

tubes to which 1 µl of DNA from ligation reactions was added. The tubes were mixed gently by tapping and incubated on ice for 30 minutes. The cells were then heat shocked for 45 seconds in a 42°C water bath and immediately placed on ice for 2 minutes. 200 µl of room temperature LB medium was added to each reaction and the transformed cells were incubated at 37°C with shaking (225 rpm) for 1 hour. The transformation mixtures were then plated onto LB agar plates containing 100 µg/ml ampicillin, 15 µg/ml X-Gal and 15 µg/ml IPTG and incubated at 37°C overnight. The presence of an insert in the pGEM-T Easy vector was tested for by using blue/white selection. The white colonies represented correct colonies containing both insert and vector.

2.6.10.4 Confirmation of Correct Insert DNA by Colony PCR

In order to confirm that the white colonies chosen for further analysis did indeed contain the DNA insert of interest, 10 colonies from each sample were picked at random and placed into 100 µl of PBS/0.1% Tween in a microcentrifuge tube, boiled for 15 minutes and centrifuged for 2 minutes at 13,000 rpm. The DNA was then used as a template for amplification in a PCR reaction. Primers used for amplification were complementary to the T7 and SP6 promoter regions flanking the multiple cloning region. Reactions were set up as follows:

Reagent	Amount
Colony DNA	2 µl
10x buffer	2 µl
dNTP (2 mM)	1 µl
T7 primer (10 µM)	1 µl
SP6 primer (10 µM)	1 µl
AmpliTaq (5 Units/µl)	0.2 µl
sd H_2O	12.8 µl
Total volume	20 µl

The samples were mixed, overlayed with a drop of mineral oil and placed in the thermal cycler (Perkin Elmer). The temperature cycles used were as follows:

94°C/ 5 min ---> 94°C/ 30 sec ---> 55°C/ 1 min ---> 72°C/ 1.5 min ---> 72°C/ 5 min

| <---------- 30 cycles ----------> |

Following PCR amplification, DNA products were visualised on agarose gels as previously described.

2.6.10.5 Minipreparation of Plasmid DNA

This method was used to prepare a small amount of DNA from the transformations. Six individual colonies from each cloned cDNA, chosen following the colony PCR confirmations, were inoculated into 5 ml of LB medium containing 50-100 μg/ml ampicillin and grown overnight at 37°C with shaking at 225 rpm. The samples were centrifuged at full speed in a Sorval bench top centrifuge. The pellet was then used for preparation of DNA using the QIAprep Miniprep kit (Qiagen) according to the manufacturers instructions.

The pelleted bacterial cells were resuspended in 250 μl of Buffer P1 and transferred to a microcentrifuge tube to which was added 250 μl of Buffer P2. The tubes were gently inverted 4-6 times to mix the samples. Buffer N3 (350μl) was then added to each sample and the tubes were immediately inverted gently 4-6 times to mix. The samples were centrifuged at 13,000 rpm for 10 minutes. The supernatants were applied to a QIAprep column and centrifuged for 30-60 seconds and the flow-through discarded. The QIAprep spin column was then washed by adding 500 μl of Buffer PB, centrifuged for 30-60 seconds and the flow-through discarded. The QIAprep column was washed again by the addition of 750 μl of Buffer PE, centrifuging for 30-60 seconds and the flow-through discarded. An additional centrifugal step was carried out for 1 minute in order to remove any residual wash buffer. The QIAprep column was then placed into a 1.5 ml centrifuge tube and in order to elute the DNA, 50 μl of Buffer EB was added to the centre of each column, incubated at room temperature for 1 minute followed by a final centrifuge step for 1 minute. The DNA was stored at –20°C until ready for use.

2.6.10.6 Restriction Enzyme Digestion of DNA

For analysis of miniprep DNA, 8 μl of DNA was digested with 1 μl of *Eco*R1 restriction enzyme (Stratagene) in the presence of the appropriate reaction buffer supplied with the enzyme (1 μl of 10X Buffer) to give a final reaction volume of 10 μl. The mixture was incubated at 37°C for 1 hour or overnight to ensure 100% digestion. The reactions were then mixed with 6X sucrose loading buffer and analysed by electrophoresis on a 1% agarose gel.

2.6.11 DNA Sequencing

Sequencing of the miniprep DNA was carried out in order to identify the genes of interest selected from differential display analysis. DNA templates were sequenced using the dRhodamine Cycle Sequencing Kit (PE Applied Biosystems) on an ABI Prism automated sequencer (Perkin Elmer). The Terminator Ready Reaction Mix in the kit consisted of:

- A-Dye Terminator labelled with dichloro(R6G)
- C-Dye Terminator labelled with dichloro(TAMRA)
- G-Dye Terminator labelled with dichloro(R110)
- T-Dye Terminator labelled with dichloro(ROX)
- dNTPs (dATP, dCTP, dITP, dTTP)
- AmpliTaq DNA Polymerase, FS, with thermally stable pyrophosphatase
- $MgCl_2$
- Tris-HCl buffer, pH 9.0

Cycle sequencing reactions were set up, using both the T7 and SP6 primers for each sample, as follows:

Reagent	Amount
Terminator ready reaction mix	8 µl
PCR product	11 µl
Primer (T7 or SP6) (5 µM)	1 µl
Total volume	20 µl

Reactions were mixed well and overlaid with mineral oil prior to thermo-cycling. The thermo cycles used were as follows:

96°C/ 1 min ---> 96°C/ 30 sec ---> 50°C/ 15 sec ---> 60°C/ 4 min ---> 4°C

| <---------- 25 cycles ----------> |

The cycle sequencing PCR products were then purified by the addition of 80 µl H_20, 100 µl $CHCl_3$ and 100 µl PCIA to each reaction tube which was then centrifuged for 10 minutes at 13,000 rpm. The top layer was transferred to a fresh microfuge tube and to this was added 10 µl 3M NaOAc pH5.2 and 300 µl EtOH. The samples were then allowed to precipitate at –20°C overnight. Following precipitation, the samples were centrifuged for 10 minutes and the supernatant

discarded. Finally the DNA pellet was allowed to air dry, mixed with 3X sequencing loading buffer and loaded onto an ABI Prism automated sequencer.

2.6.12 Identification of Gene Sequences

Three sequencing reactions from three separate clones were carried out for each gene of interest. In order to identify the genes, the three sequences obtained for each gene were compared with the Genbank/EMBL non-redundant nucleotide (nr) and expressed sequence tag (EST) databases with the BLAST algorithm (blastn) available via the world wide web at the NCBI.

2.6.13 Confirmation of Differential Gene Expression by RT-PCR

Semi-quantitative RT-PCR was used as a screen to verify expression of candidate genes identified by differential display. 5 μg of total RNA was reverse transcribed from an oligo- $(dT)_{12-18}$ primer essentially as previously described. Total RNA was extracted from the PrE2.8 cell line from cells that had been incubated at 33°C or 39°C after 4, 7, 10 and 14 days of growth. The resulting reactions were diluted 5-fold in DEPC-treated H_2O and 2 μl used as a template for amplification with primers designed within the DD PCR cloned sequences. Primers were designed to be between 18-22 bases in length, G/C clamped at the 3' end, G/C rich (~50%), unique to that sequence (BLAST) and to have a T_m of >60°C. PCR was performed in a 50 μl reaction volume as follows:

Reagent	Amuont
RT reaction	2 μl
10x buffer	5 μl
dNTP (10 mM)	1 μl
Sense primer (10 μM)	1 μl
Antisense primer (10 μM)	1 μl
AmpliTaq (5 units/μl)	0.5 μl
sd H_2O	39.5 μl
Total volume	50 μl

The reactions were mixed and a drop of mineral oil was added to each tube. The temperature cycles used were:

94°C/ 5 min ---> 94°C/ 30 sec ---> 55-65°C/ 1 min ---> 72°C/ 1.5 min ---> 72°C/ 5 min

| <---------- 25-35 cycles ----------> |

Control amplifications were performed with GAPDH-specific primers. After completion of the PCR reactions, 10 µl of each PCR product was mixed with 6X loading buffer and resolved on 1.5% agarose gels after different cycle numbers. Ten µl of a 50 µl reaction were removed from RT-PCR amplifications after different numbers of PCR cycles with each of the specified primer pairs and analysed by agarose gel electrophoresis as previously described in section 2.6.8.

2.7 Immunocytochemistry

2.7.1 Preparation of prostate tissue sections and cultured cells for immunohistochemistry and Immunocytochemistry

Cells were grown, as described in section 2.4, on $2cm^2$ glass cover slips and washed three times with PBS. They were fixed in either 1 ml cold methanol/acetone (1:1) solution or formaldehyde at 4°C for 10 mins and stored in PBS at 4°C until required. Paraffin-embedded prostate tissue sections were incubated at 60°C for 20 mins and deparaffinated in the following solutions: Xylene 3 mins - x2; 100% EtOH 1 min – x2; 70% EtOH 1 min. The sections were rinsed in dH_2O before antigen retrieval. Antigen unmasking solution (Vector) was prepared by adding 15 ml of the solution to 1,600 ml of dH_2O. This was heated in a microwave to 100°C after which the tissue sections were added and the solution heated on full power for a further 30 mins. The solution was allowed to cool to room temperature and the tissues were washed in PBS for 5 mins. A wax pen (Dako) was used to draw around the edges of the tissues in order to prevent spreading of antibody solutions over the microscope slide.

2.7.2 Immunohistochemistry and Immunocytochemistry

Endogenous peroxidase activity was quenched by incubation in 3% hydrogen peroxide solution for 10 mins at room temperature followed by washing in PBS for 5 mins. Non-specific antibody binding was blocked by incubating the tissue sections or cells in normal horse serum for 20 mins. These were then incubated overnight at 4°C with the primary antibody diluted as appropriate in normal horse serum followed by three washes in PBS for 5 mins. Biotinylated secondary antibody was added for 30 mins at room temperature followed by three washes with PBS. This procedure was followed by incubation with biotin-streptavidin-peroxidase complex for 30 mins and three 5 min washes in PBS. The tissues/cells

were then incubated with diaminobenzidine tetrahydrochloride (DAB) solution for 2 – 10 mins and washed in running tap water for 5 mins. Cells were counterstained with Harris haematoxylin for approximately 10 secs and mounted onto microscope slides in a drop of DPX mounting medium. Tissues were counterstained with Harris haematoxylin for 1 min, washed in running tap water for 3 mins and placed into 1% acetic acid for 10 secs followed by a further wash in running tap water for 2 mins. They were then dehydrated in ethanol solutions (70% EtOH-15 secs, 2X 100% EtOH 30 secs) and cleared in xylene before being carefully mounted under glass coverslips in a drop of DPX mounting medium avoiding air bubbles. The slides were then examined and photographed under a light microscope.

2.7.3 Immunofluorescence

Non-specific antibody binding was blocked by incubating tissues or cells in normal horse serum for 20 mins at room temperature. Primary antibodies were incubated overnight at 4°C and slides washed in PBS for 5 mins three times. The sections/cells were incubated with Fluoroscein isothiocyanate (FITC)- or tetramethyl rhodamineisothiocyanate (TRITC)-conjugated secondary antibodies for 30 mins followed by three 5 minute washes in PBS. Nuclei were stained by incubation with a 1 μg/ml solution of Hoechst 33258 (Sigma) for 5 minutes. Negative control tissue sections/cells were treated in an identical manner, but omitting the primary antibody. The tissue sections were then carefully mounted under glass cover slips and mounted onto microscope slides in a drop of Gelvatol mounting medium. The slides were examined under an Hg-arc Zeiss Axiophot fluorescence microscope. The microscope was coupled to a Coolview 12 cooled charge-couple device (CCD) camera (1024 x 1024, 12-bit pixels; Photonic Science, Robertsbridge, UK) controlled by Image Pro-Plus software v3.0; Media Cybernetics, Rockville, MD).

2.8 Western Blotting

2.8.1 Lysate preparation

Cells were grown to approximately 70-80% confluence in T75 culture flasks. The medium was removed and the cells washed three times in PBS. One ml of extraction buffer was added to the flask, the cells were scraped and placed into 1.5

ml eppendorf tubes and incubated on ice for 15 mins. The samples were then centrifuged at 13,000 rpm at 4°C, the supernatant was transferred to a fresh tube and the cell pellet was discarded.

2.8.2 Measurement of protein content

In order to measure the protein concentration of the cell extracts The Bradford assay (BioRad) was employed according to the manufacturers instructions.

2.8.3 Polyacrylamide gel electrophoresis

Protein samples (30 μg) were loaded onto polyacrylamide gels and electrophoresis was carried out using BioRad electrophoresis apparatus. The gel apparatus was assembled according to the manufacturers instructions and 0.5mm or 1.5mm thick resolving gels of the required percentage were prepared and overlayed with 1 ml of water to ensure a level surface of the gel. The resolving gel was then allowed to set for at least 1 hour after which the water was poured off and a stacking gel poured on top. A comb was quickly inserted and the gel was left to set for approximately 30 mins. The composition of the gels were as follows:

Reagent	Resolving Gel	Resolving Gels	Stacking Gel
	7.5%	12%	4%
1.5M Tris pH 8.8	1.25 ml	1.25 ml	-
1M Tris pH 6.8	-	-	500 μl
10% SDS	50 μl	50 μl	40 μl
50% glycerol	100 μl	100 μl	-
0.5M EDTA	20 μl	20 μl	16 μl
Acrylamide	830 μl	1.992 ml	530 μl
dH_2O	2.695 ml	1.533 ml	2.89 ml
10% AMPS	50 μl	50 μl	40 μl
TEMED	5 μl	5 μl	10 μl

The protein samples were prepared by mixing with 2x loading buffer and denatured at 100°C for 5 mins prior to loading onto the gel. One of the lanes was loaded with 5 μl of Rainbow high molecular weight marker (Amersham International). Electrophoresis was carried out at 100 V for 2 hours in 1X running buffer.

2.8.4 Protein transfer and blotting

Once electrophoresis was complete, the apparatus was dismantled, the stacking gel discarded and the resolving gel carefully removed and placed into transfer buffer for at least 10 mins. Immobilon-P (Millipore) membrane was prepared by wetting in 100% methanol for a few seconds followed by washing in dH_2O for 2 mins and then allowed to equilibrate with the transfer buffer for at least 10 mins. Two pieces of Whatman 3MM paper were cut to exact gel size and also soaked in transfer buffer. The resolving gel was then assembled in the transfer apparatus (BioRad) as shown in Figure 2-1. Proteins were transferred at 45 V overnight at 4°C. The apparatus was dismantled and the membrane was blocked in 5% skimmed milk powder (Marvel)/0.1% Tween 20 (Sigma) in PBS for 30 mins at room temperature. Immunodetection of specific proteins was performed by incubation with primary antibody for 1 hour at room temperature, in PBS containing 2% skimmed milk powder/0.1% Tween 20 (Sigma). Membranes were then incubated with peroxidase-conjugated anti-mouse IgG for 45 minutes at room temperature. Membranes were washed in PBS with 0.1% Tween 20 between antibody incubations. Antibody binding was detected using the ECL chemiluminescence kit (Amersham Pharmacia Biotech) according to the manufacturers instructions. Membranes were then wrapped in Saran Wrap and exposed to Hyperfilm MP autoradiography film (Amersham Pharmacia Biotech) for various lengths of time (2 secs to 10 mins) for visualisation.

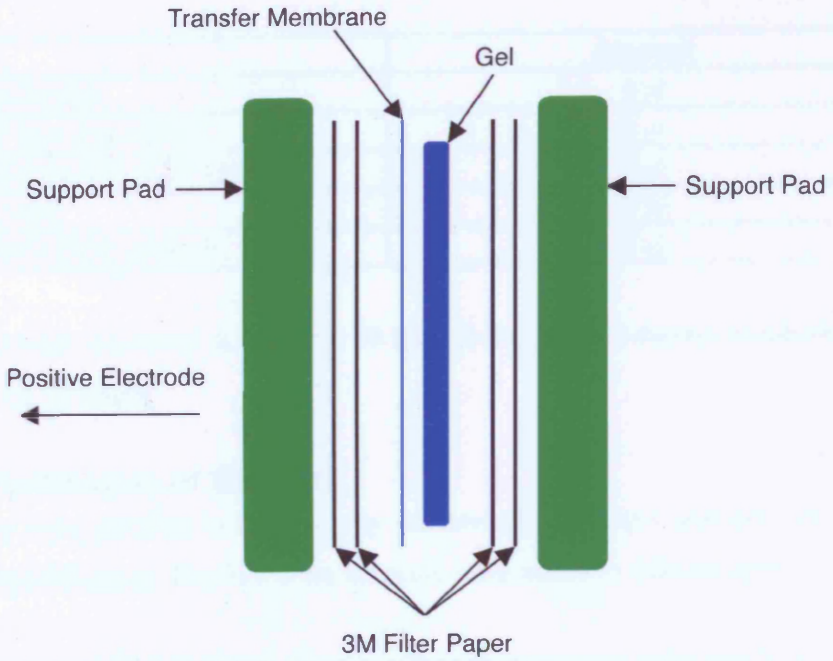

Figure 2-1 Western blotting protein transfer apparatus set up.

2.9 Microarray Analysis

To compare differences in gene expression between PrE2.8 cells grown at 33°C and at 39°C for 4 days, cDNA microarray analysis was employed.

2.9.1 Cy-dye labelling and reverse transcription of total RNA

Four µg of total RNA from each sample (RNA extracted from cells grown at 33°C (control sample) and 39°C (test sample)) was simultaneously reverse transcribed and labelled with either cy-3 or cy-5 fluorescent dye. Reactions were set up for each sample as follows:

Reagent	Amount
Total RNA	4 µg
Random primer	2 µl
sd H_2O	8 µl

Samples were incubated at 65°C for 5 mins followed by a further incubation at 28°C for 1 min. The following reactions were then set up for each sample:

Reagent	Amount
5x reaction buffer	4 µl
10x dNTP mix (low dCTP)	2 µl
Cy (3 or 5)-labelled dCTP (1 mM)	2 µl
DTT (0.1 mM)	2 µl
Superscript II (200 units/µl)	2 µl

Reactions were incubated at 25°C for 10 mins followed by a further incubation at 37°C for 18-20 hours.

2.9.2 Purification of Samples

Reactions were purified to remove any un-incorporated dyes and prevent non-specific hybridisation. The following reagents were added to each sample:

Reagent	Amount
EDTA (0.5 M)	3.75 µl
CoT 1 DNA (1µg/µl)	12.5 µl
NaOH (1 M)	3 µl

Reactions were heated at 70°C for 10 mins after which 400 µl of 0.5X SSPE was added and they were then transferred to a 0.1 µm Ultrafree-MC spin column (Millipore) and spun at 6,500 rpm in a microcentrifuge. The solutions were then transferred to Microcon YM-30 spin column (Millipore) and spun at 13,000 rpm in a microcentrifuge for 7 mins, plus additional short spins of 30 secs until the reaction volume was approximately 30 µl. This was followed by a further addition of 400 µl of 0.5X SSPE and the samples were re-spun at 13,000 rpm to a volume of approximately 30 µl. Samples were then used immediately or stored at –4°C until required.

2.9.3 Pre-hybridisation

Poly-L-Lysine-coated (Sigma) glass microscope slides were pre-hybridised by incubation in hybridisation buffer at 65°C for 18-20 hours in a humid box. The slides were then washed as follows:

Solution	Temperature	Incubation Time
2x SSC	32°C	1 min
2x SSC	32°C	2 min
1x SSC	Room temperature	1 min
Formamide/2x SSC	65°C	3 min

This was followed by short washes for a few seconds each in a series of graded alcohol solutions at room temperature: 70% EtOH (X2); 80% EtOH (X1); 100% EtOH (X1). The slides were then dried using an invertible air duster followed by incubation at 37°C until ready for hybridisation.

2.9.4 Hybridisation Reactions

The following components were added to the purified samples:

Reagent	Amount
EDTA (500 mM)	1.25 µl
20x SSPE (pH 7.4)	15 µl
2% Tween	2.5 µl

The control and test samples were then combined and mixed by pippetting. They were then heated to 99°C for 2 min followed by a 3hour incubation at 65°C in a Hybaid PCR machine. The samples were then placed into a 0.1 Ultrafree-MC spin column and centrifuged at 3,000 rpm for 5 min. The samples were then re-heated at 99°C for 2 min followed by 65°C for 10 min and 37°C for 20 min. The sample was then placed onto a glass microscope slide, containing an array of 5,800 genes, and a 22x66 mm Hybrislip that had been pre-warmed at 37°C and treated with an antistatic gun was placed on top. This was placed into a sealed hybridisation chamber and hybridised in a water bath at 65°C for 48 hours.

Following hybridisation the slides were washed as follows, after which the array slide was rapidly dried with canned air prior to analysis:

Solution	Temperature	Wash Time
2x SSC	32°C	1 min
2x SSC	32°C	2 min
1x SSC/50 nM EDTA	Room temperature	1 min
0.05x SSC	Room temperature	1 min

2.9.5 Microarray Image Analysis

The microarray slide was placed into a Genepix microarray scanner (Axon Instruments, Foster City, CA) and the image analysed using the Genepix Pro 3.0 image analysis software (Axon Instruments, Foster City, CA) according to the manufacturers instructions.

2.9.6 Microarray Data Analysis

Following image analysis the resulting data were analysed using the Significance Analysis of Microarrays (SAM) software (Stanford University, CA) according to the manufacturers instructions.

2.9.7 Verification of Significant Gene Expression by RT-PCR

Genes found to be significantly over- or under-expressed were verified by RT PCR and immunocytochemistry.

3 IDENTIFICATION OF DIFFERENTIALLY EXPRESSED GENES IN THE PRE2.8 CELL LINE

3.1 Introduction

Differential gene expression has important functional implications in normal cell growth, differentiation, and in pathological conditions. In order to identify candidate genes that may be involved in prostate epithelial cell differentiation, differential display (DD) (Liang and Pardee, 1992) was employed using a model cell culture system, the PrE2.8 prostate epithelial cell line (Daly-Burns *et al* , in preparation). The cells were grown at the permissive and non-permissive temperatures for a period of 7 days after which total RNA was extracted and differential gene expression was analysed.

Differential display is a useful tool for identifying and cloning differentially expressed genes and was first described by Liang and Pardee (1992) as a method for analysing gene expression in eukaryotic cells and tissues. This method involves the reverse transcription of the mRNAs with oligo-dT primers anchored to the beginning of the ploy(A) tail. The anchored primers used in this study employ one 'anchoring' base (A, C and G) at the 3'-end, to anneal to specific subsets of mRNAs. This generates three different cDNA fractions corresponding to the presence of either a U, G or C respectively, immediately upstream of the poly(A)$^+$ region. Reverse transcription was followed by the PCR reaction in the presence of a second 10mer, arbitrary in sequence. The amplified cDNA subpopulations of 3' termini of mRNAs, as defined by this pair of primers, were then 'displayed' side by side on a high resolution denaturing gel so that differential gene expression was immediately visible (Figure 3-1). By changing primer combinations using all the anchored oligo-dT primers with 80 arbitrary 10mers would statistically cover the majority of mRNAs in a eukaryotic cell

(Liang and Pardee, 1992). Furthermore, DD can examine several different RNA samples simultaneously and so is ideal for time course, dose-response and multiple treatment studies. Other advantages of DD include its simplicity, sensitivity, reproducibility and speed.

Following DD PCR, bands of interest, corresponding to potentially up and down-regulated genes were excised from the denaturing gels, re-amplified and cloned. The cloned genes were then sequenced in order to identify them and this was followed by RT-PCR in the PrE2.8 cell line in order to confirm the differential expression of the identified genes.

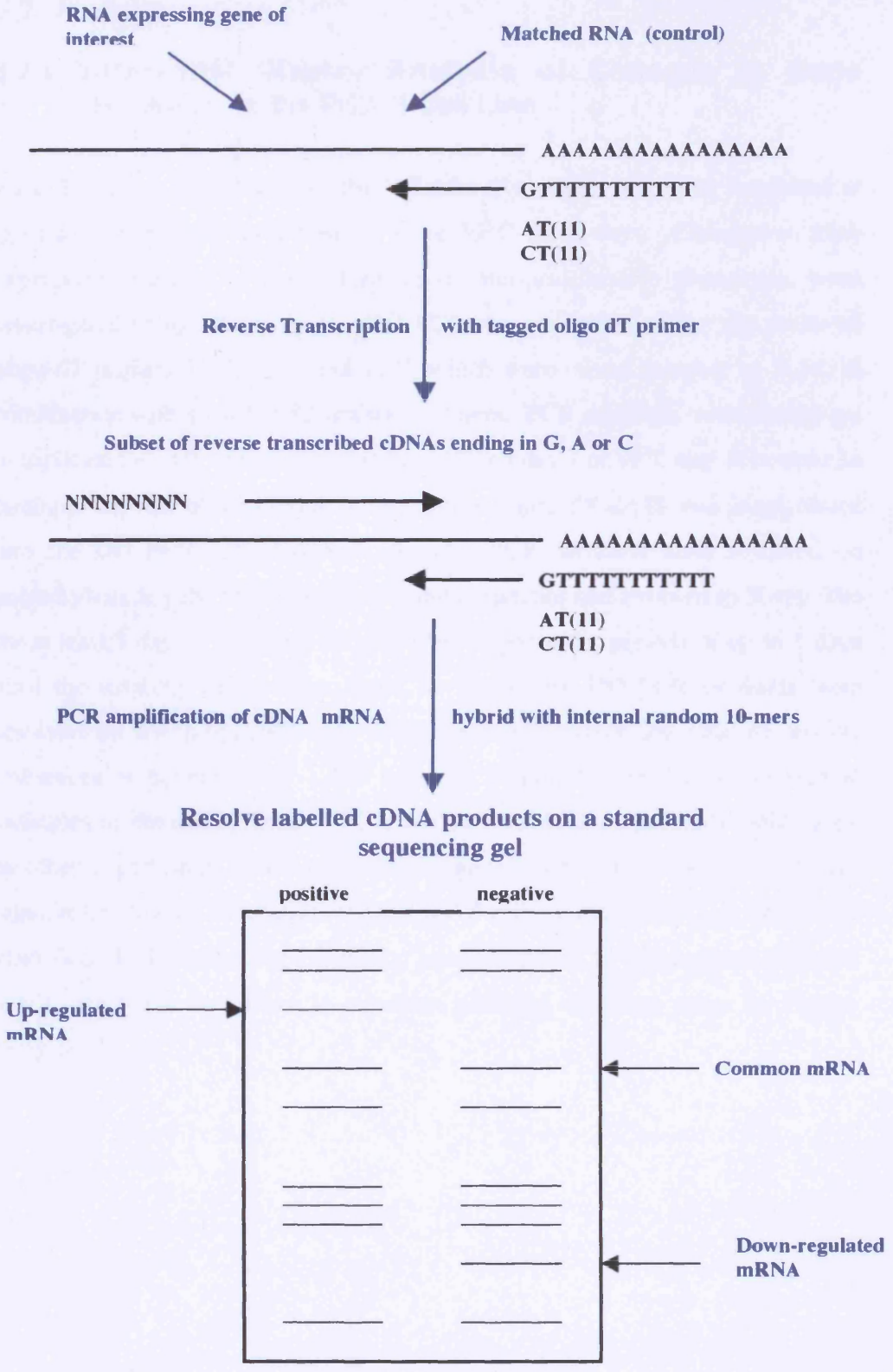

Figure 3-1: Schematic of Differential Display PCR.

3.2 Results

3.2.1 Differential Display Analysis of Changes in Gene Expression of the PrE2.8 Cell Line

Total RNA was isolated from the PrE2.8 cells, which had been incubated at growth temperatures of either 33°C or 39°C for 7 days. Changes in gene expression induced by a proliferative or non-proliferative phenotype, were investigated using DD analysis. DD PCR was performed using the anchored oligo-dT primers $T_{11}G$, $T_{11}A$ and $T_{11}C$, which were mixed together as $T_{11}M$, in combination with a total of 83 arbitrary 10mers. PCR reactions were carried out in triplicate for each sample (obtained at 33°C on day 7 or 39°C day 7) in order to minimise the risk of identifying false positive bands. ^{35}S-dATP was incorporated into the DD PCR reactions and after the PCR products were resolved on polyacrylamide gels, these were dried under vacuum and exposed to X-ray film for at least 1 day. If required, the gels were exposed for periods of up to 5 days until the majority of products could be visualised. DD PCR products were resolved on 6% polyacrylamide sequencing gels which are able to resolve sequences of between 200 – 500 bases in length. Figure 3-2 shows typical examples of autoradiographs of PCR products resolved on polyacrylamide gels. In other experiments bands representing genes that were either up or down-regulated following incubation of the PrE2.8 cells at either 33°C or 39°C were identified. If differences in expression levels appeared to occur across triplicate bands then these were taken to represent potential candidate genes for further analysis.

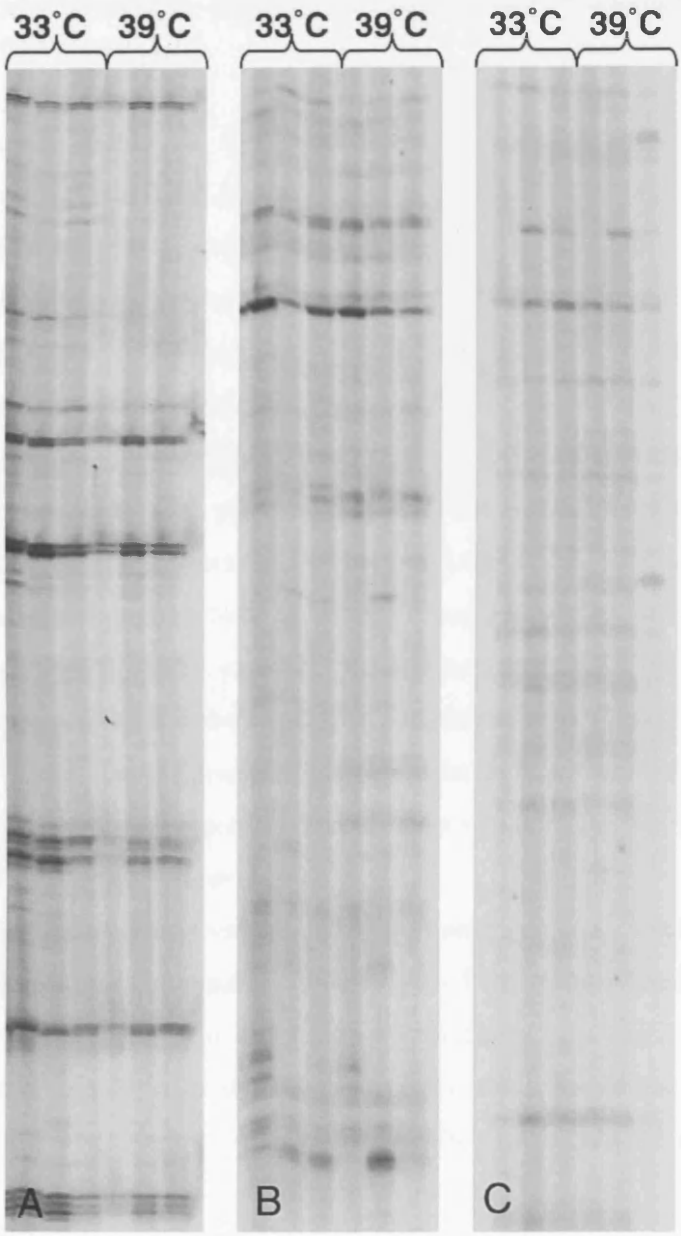

Figure 3-2: Autoradiographs of polyacylamide gels showing DD PCR products.

To assess reproducibility, the cDNA representing each sample was synthesised in three independent reactions. DD PCRs were carried out for each sample (33°C at day 7 or 39°C at day 7) using the $T_{11}M$ primer in combination with an arbitrary 10-mer. Autoradiographs are shown for PCRs using the primers $T_{11}M$ and the 10mers C6 (A), C8 (B) and C10 (C).

3.2.2 Identification and Isolation of Differentially Expressed PCR Products

The autoradiographs of the polyacrylamide gels as shown in Figure 3-2, illustrating the banding patterns of the DD PCR products, were carefully examined in order to identify bands representing genes that were differentially expressed by the PrE2.8 cell line incubated at the two growth temperatures. A total of 25 differentially expressed bands were chosen for further analysis. Once candidate bands were identified, the autoradiographs were carefully positioned over the original dried polyacrylamide gel using fluorescent markers in order to assist orientation. By piercing a pin through the autoradiograph and polyacrylamide gel, the position of the band on the gel was located and a razor blade was used to cut the band of interest from the gel. In order to verify that the appropriate band had been removed, the polyacrylamide gel, was re-exposed to X-ray film. Figure 3-3A shows typical examples of experiments where candidate genes of interest were identified on autoradiographs. Following location of the appropriate bands on the polyacrylamide gels and the excision of these bands, re-exposure verified their removal.

The DNA excised from the polyacrylamide gels was then re-amplified using PCR and resolved on agarose gels. Figure 3-3B shows bands, named by the arbitrary primer that was used to amplify them, run on 1.5% agarose gels alongside a 1kb DNA marker. This revealed the sizes of the amplified cDNA products and whether the re-amplification PCR had been successful.

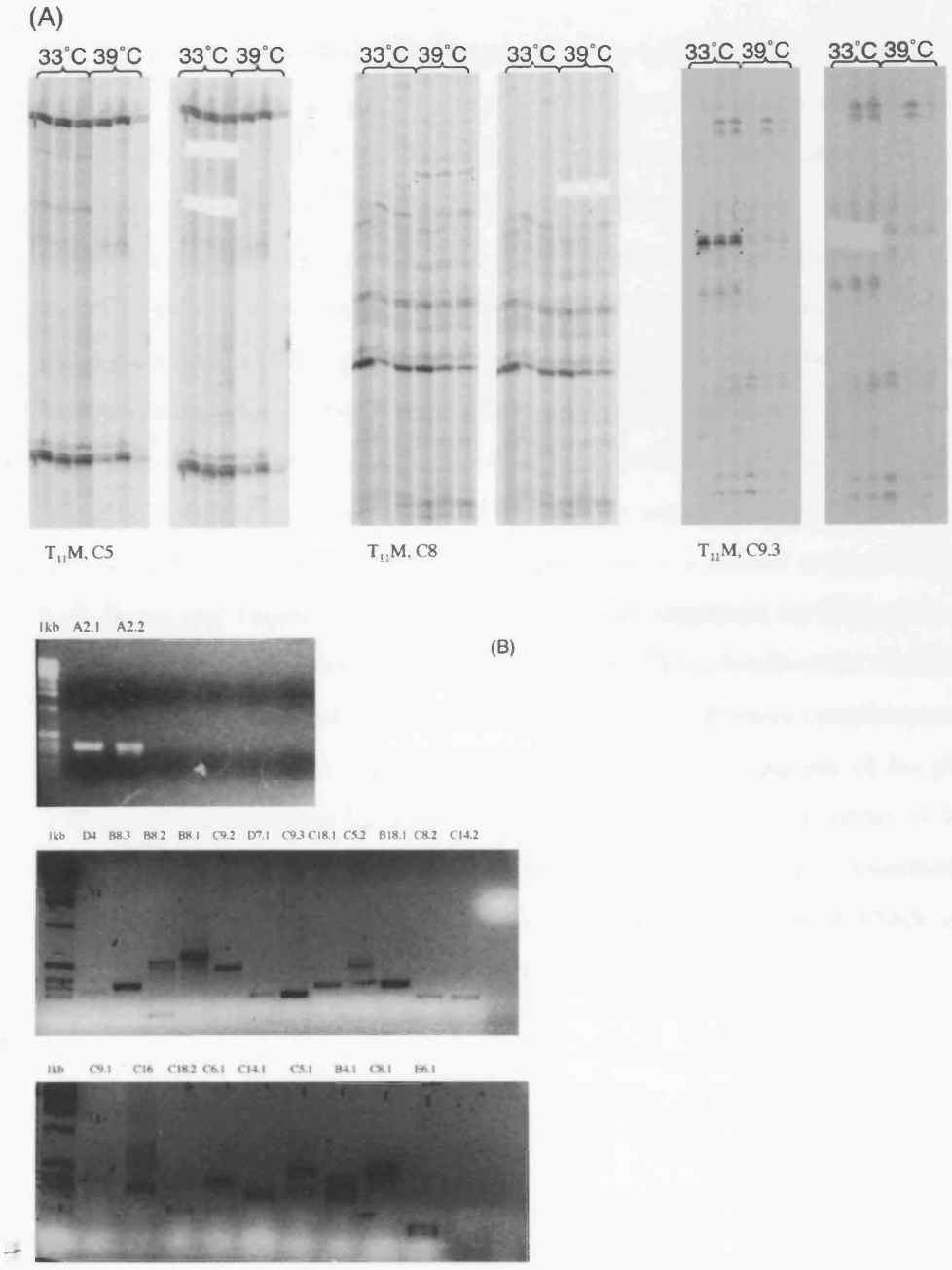

Figure 3-3: Excision of differentially expressed DNA from polyacrylamide gels (A) and re-amplification of putative differentially expressed cDNAs (B).

(A) Autoradiographs of differentially expressed bands before and after excision are shown and primer pairs used to amplify the DNA fragments are indicated. Putative differentially expressed bands were cut from dried polyacrylamide gels and precise excision of the appropriate fragment confirmed by re-exposing the dried gel to x-ray film. (B) Extracted DNA extracted was re-amplified using the same primer pair as used in the DD PCR and resolved on 1.5% agarose gels.

3.2.3 Cloning of Differential Display cDNA Fragments

The successfully amplified DNA fragments were subcloned into a pGEM-T Easy cloning vector. This vector is a convenient tool for the cloning of PCR products. The addition of a 3' terminal thymidine to both ends of the insertion site greatly improves the efficiency of ligation of a PCR product into the plasmid by preventing the recircularisation of the vector and providing a compatible overhang for PCR products generated by thermostable polymerases, such as AmpliTaq DNA polymerase. This enzyme adds a single deoxy-adenosine, in a template-independent fashion, to the 3'-ends of the amplified fragments.

The cloned PCR products that were transfected into E. coli were grown on LB agar plates. The presence of an insert was tested for by using blue/white selection. White colonies indicated the presence of a correct colony containing both insert and vector. Colony DNA was then amplified by PCR in order to verify that these white colonies contained inserts. Ten colonies from each sample cloned were picked at random for the PCR screening. Primers complementary to the T7 and SP6 promoter regions flanking the multiple cloning site of the pGEM-T Easy vector were used for amplification. Figure 3-4 shows examples of cloned cDNA for the C16 and A2.2 DD bands that were successfully transfected as revealed by expression across 10 clones. This analysis revealed which clones contained an insert and therefore could be used for further analysis.

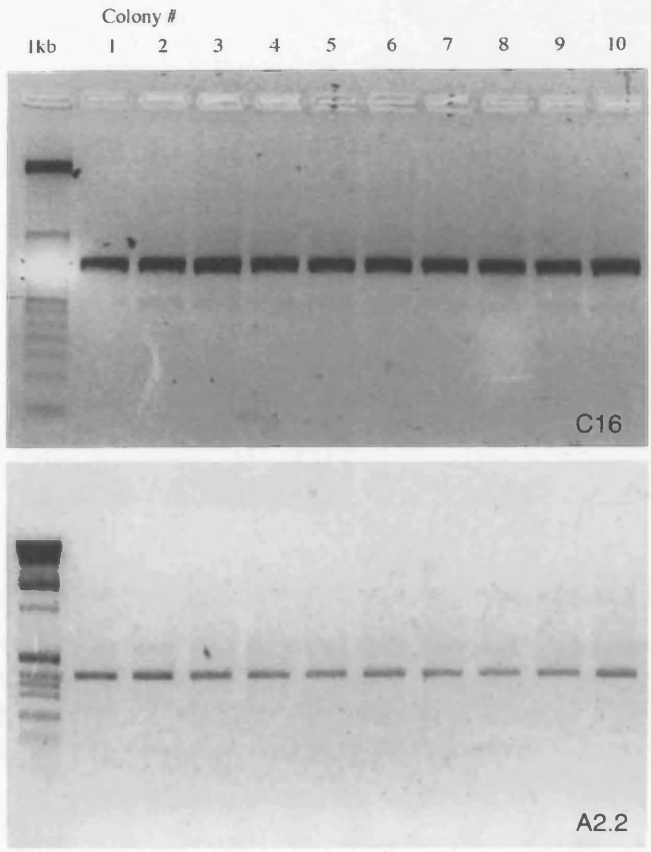

Figure 3-4: Colony PCRs of cloned cDNA fragments.

A total of 10 colonies for each cloned PCR product were selected for screening by colony PCR. This screen was carried out in order to verify the presence of insert DNA prior to minipreparation of DNA for sequencing.

3.2.4 Minipreparation of Cloned cDNA Fragments

Of the ten colonies per sample screened by PCR for the presence of inserts, 6-8 were then chosen for minipreparation of DNA to be sequenced. The miniprep DNA was digested with the *Eco*RI restriction enzyme which allowed release of the insert from the multiple cloning region. Digested samples were visualised on 1.5% agarose gels. Figure 3-5 shows examples of cloned DNA for the D7 or A2.2 bands that were digested with the *Eco*RI restriction enzyme. The larger bands represent the vector DNA whilst the smaller bands represent the insert DNA obtained from the previous DD analysis. This revealed whether the minipreparation of DNA had been successful and if so, whether the insert DNA had been successfully digested from the vector.

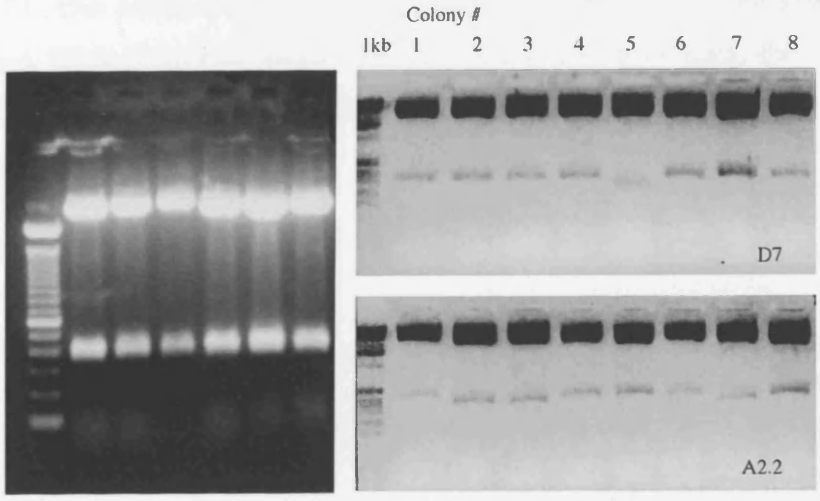

Figure 3-5: Minipreparation and restriction analysis of the cDNA clones.

(A) Miniprepped DNA samples were run on 1.5% agarose gels. (B,C) Restriction endonuclease patterns of independent clones from the same target band which have been digested with *Eco*RI. Restriction enzyme digests were carried out in order to identify colonies containing DNA inserts.

3.2.5 Sequencing and Identification of Differentially Expressed cDNA Clones

Successfully digested miniprep DNA was sequenced in order to identify the differentially expressed genes. Three clones for each candidate gene were sequenced in both forward and reverse directions using the T7 and SP6 promoter sequences as primers for the sequencing reaction. These forward and reverse sequences were aligned using the Autoassembler software package. Sequencing was carried out from three separate clones for each gene in order to verify identification. If initial attempts were unsuccessful, sequencing of cDNA clones was repeated until a good, readable sequence was obtained. For a number of genes a readable sequence was not obtained and these candidate genes were therefore not selected for further investigation. Successful DNA sequencing of the cDNA clones revealed the *Eco*RI restriction site, the poly(A) tail of the gene and the primers used in both the sequencing and the original DD PCR reaction.

Figure 3-6 shows the DNA sequence of the DD PCR product C14.2. The three sequences obtained for this gene, and others, were compared with the Genbank/EMBL non-redundant nucleotide (nr) and expressed sequence tag (EST) databases with the BLAST algorithm (blastn) available via the world wide web at

the NCBI. This enabled the sequences obtained for these candidate genes to be identified. Table 2 lists the genes identified, their respective sizes, the results of BLAST searches and the up- or down-regulation of gene expression in the PrE2.8 cell line.

TTAAGCTTTTTTTTTTTTACATAAGTTTTACAAGATAATACATTTTTACAG
TGACCTGATGTGGATACAACTTTGCAACTTGGCAAAAAGCAAATCTTAAC
TTACATTATAATTAATTTGCTGCTACACATCTCTGATTCTCAATTTTGGC
AAGTACAACAGGTTAAGGGTTCTATTTAGTGTCCCCTTCTGATGAATATG
ATGATCTTGAACCCATTCTTCCTCCTCAAGCACGCAAATCGAATTC

Figure 3-6: DNA sequence of the DD PCR product C14.2.

The sequence of the above PCR product was determined using cycle sequencing on an automated ABI Prism sequencer. A BLAST search revealed homology to S.pombe chromosome III cosmid. The *Eco*RI restriction sites in the multiple cloning region of the pGEM-T Easy vector are shown in blue. The sequence of the primers used for DD PCR and subsequent re-amplification ($T_{11}A$ and the arbitrary 10mer, C14) are shown in red.

3.2.6 Confirmation of Differential Gene Expression by RT-PCR

In order to verify that the bands isolated from the DD polyacrylamide gels represented differentially expressed genes, primers were designed to the sequences obtained and RT-PCR was carried out using reverse transcribed RNA from the PrE2.8 cell line grown at either 33°C or 39°C over a time course of 4, 7, 10 and 14 days of growth. RT-PCR confirmation of differential gene expression revealed that only 3 of the 25 genes identified by sequencing were differentially expressed (Table 1). Two genes found to be up-regulated at 39°C in the PrE2.8 cell line, when the cells appear to be differentiating, were the S100 calcium binding protein A8 (S100A8) and the small proline-rich protein 1B (SPR 1B). A gene found to be down-regulated at 39°C was cyclo-oxygenase 2 (COX 2) (Figure 3-7).

Table 1: Summary of putative differentially expressed genes.

DD band names, sizes of re-amplified DNA products, BLAST search results and RT-PCR confirmation results are listed.

DD Band Name	Size of Re-amplified DNA (bp)	Blast Search Result	Confirmation of Differential Expression
A2.1	400	Human myosin regulatory light chain	No change
A2.2	390	S100 calcium binding protein A8	Up-regulated
A19	-		
B8.1	610	Not sequenced due to lack of material	
B8.2	590	Not sequenced due to lack of material	
B8.3	400.	Not sequenced due to lack of material	
B9	360	BAC clone	No change
B10	345	Human Newcastle disease virus inducible protein	No change
C5.1	500	Cyclo-oxygenase 2	Down-regulated
C5.2	400	Human cytochrome c oxidase subunitII	No change
C6	396	Human mitochondrial complete genome	No change
C8.1	510	Arabidopsis thaliana DNA chromosome 3 clone	No change
C8.2	290	PAC clone	No change
C9.1	-		
C9.2	490	Human mitochondrial complete genome	No change
C9.3	250	Small nuclear ribonucleoprotein polypeptide B	No change
C14.1	300	S. pombe chromosome III cosmid	No change
C14.2	250	BAC clone	No change
C16	350	Small proline-rich protein 1B	Up-regulated
C18.1	310	Alpha tubulin	No change
C18.2	200	Alpha tubulin	No change
D4	345	PAC clone	No change
D7	290	Heat shock protein	No change
E6	150	BAC clone	No change
E7	-		

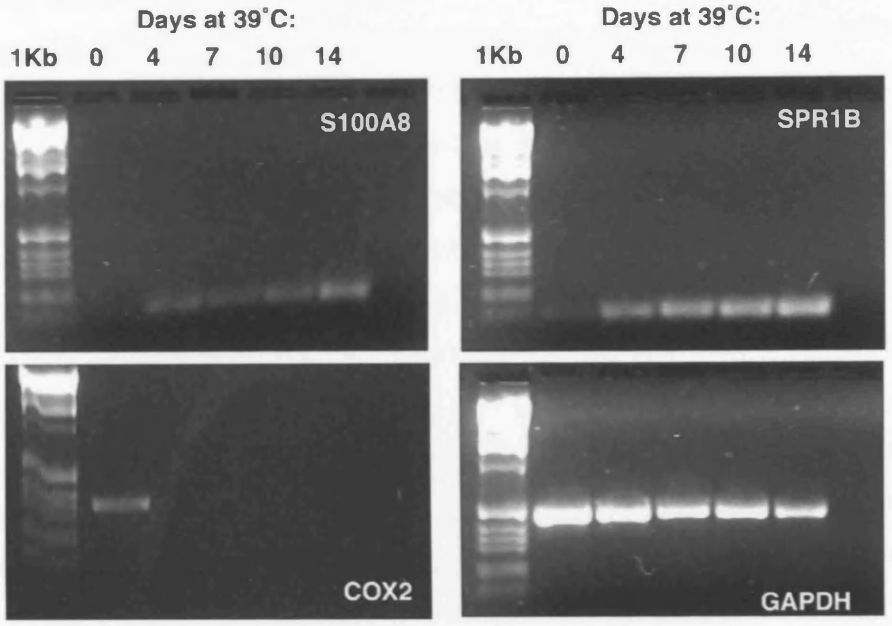

Figure 3-7: Confirmation of differentially gene expression by RT-PCR.

In order to verify that the bands identified through differential display were differentially expressed in the PrE2.8 cell line, RT-PCR was performed using 25-35 cycles on reverse transcribed RNA from cells incubated at 33°C or 39°C after 4, 7, 10 and 14 days of culture. Amplifications are shown for genes showing differential expression following confirmation by RT-PCR: S100A8 (calcium binding protein S100A8), SPR1B (small proline-rich protein 1B) and COX2 (cyclo-oxygenase 2). GAPDH was used as a control. The last lane of each RT-PCR shown represents a negative PCR control.

3.3 Discussion

Changes in gene expression between a proliferative and a differentiated phenotype in the PrE2.8 cells were investigated using differential display. Twenty five bands, representing potentially up- and down-regulated genes, were chosen for further analysis. These genes were cloned and sequenced for identification and differential gene expression was then confirmed using RT PCR. However, this revealed that only three of the genes were truly up-, or down-regulated using this technique. These discrepancies may have been due to a number of features of the differential display technique.

A major drawback of the technique is the generation of a relatively large number of 'false positives' as was demonstrated in this study. A false positive

occurs when the expression pattern of a clone isolated from a differentially expressed cDNA band on a polyacrylamide gel cannot be reproduced using independent techniques such as RT-PCR. Differential display is a multi-step process where false positives can be generated at several stages, from the running of the experimental model and RNA extraction, through to cloning of candidate genes and confirmation of differential expression. False positive results in part could be attributed to degraded RNA or contaminating DNA. Although DNAse I treatment was applied to the mRNA prior to DD PCR, a trace amount of DNA may remain. In some cases, during the PCR process, contaminating DNAs of the same size as the band of interest may be produced and amplified that cannot be removed by gel purification. These contaminating DNAs may clone and amplify more efficiently than the band of interest, since they may be more abundant, resulting in the differentially expressed mRNAs to be obscured and the DD band to be scored as a false positive. There is also increasing evidence in the literature that single bands with differential appearance on gels, represent a mixture of several cDNA fragments of identical size but different sequence (Li et al., 1994a; Vogeli-Lange et al., 1996). Thus the cDNA clones obtained from one particular differential may be derived from several different mRNAs, including both differentially and constitutively expressed ones. Also, despite the advent of better gel systems with improved resolution, it is still possible to unintentionally excise more than one band from the polyacrylamide gel and thus re-amplify and clone a mixture of cDNAs.

In some instances the candidate bands excised from polyacrylamide gels fail to re-amplify, as was the case with DD bands A19, C9.1 and E7. Re-amplification problems can be caused if the gel is not sufficiently washed, causing excess urea and acrylamide to inhibit the PCR reaction. It is also recommended that the DD bands of interest should be excised and re-amplified as soon as possible so as to minimise degradation of DNA. Despite the majority of candidate genes in this study being established as false positives, three candidate genes were confirmed as being differentially expressed in the PrE2.8 cell line. Two genes found to be up regulated during differentiation of the cells at 39°C, were identified as the S100 calcium binding protein A8 (S100A8) and the small proline rich protein 1B (SPR1B). These genes are both located on chromosome 1q21.

This region consists of a collection of genes known to play an important role in terminal differentiation of the human epidermis and has been designated the epidermal differentiation complex (EDC) (Mischke et al., 1996). In addition, the 1q21-23 region is deleted in uterine and bladder adenocarcinomas and is the target for translocation in breast adenocarcinoma (Solomon et al., 1991).

SPR1B belongs to the first family of EDC genes. This family consists of 13 genes, involucrin, loricrin and the three classes of small proline rich proteins comprising 2 SPR1 and 8 SPR2 genes as well as 1 SPR3 gene. These encode structural proteins of the human epidermis (Gibbs et al., 1993). The second family of the EDC consists of profilaggrin and trichohyalin. These genes encode intermediate filament associated proteins that are synthesised in the granular layer of the epidermis and adjoin the keratin filaments of keratinocytes during cornification (Fietz et al., 1992). The third family of genes of the EDC is comprised of the S100 family of calcium binding proteins named which has at least 19 members. They were initially characterised as low molecular weight (10-12 kd) acidic proteins and named by their solubility in 100% ammonium sulphate ("S100"). These genes are thought to play a part in signal transduction and cell cycle progression during terminal differentiation of keratinocytes. The calcium binding proteins S100A7, S100A8 and S100A9 have been shown to be up regulated in psoriatic epidermis and primary human keratinocytes undergoing aberrant differentiation (Hoffmann et al., 1994; Saintigny et al., 1992). Other proteins of this family are abnormally expressed in various tumours such as breast carcinomas as well as tumours of the bladder and colon (Lee et al., 1992; Pedrocchi et al., 1994). The S100 proteins are involved in numerous functions ranging from the control of cell cycle progression and cell differentiation to enzyme activation and regulation of muscle contraction (Schafer and Heizmann, 1996). Thus they appear to have a wide variety of functions in normal and diseased states and are expressed in a cell- and disease-specific manner.

A third gene found to be differentially expressed in the PrE2.8 cell line is cyclooxygenase 2 (COX-2) whose expression was decreased upon differentiation of the cells. Two cyclooxygenase genes have been cloned (COX-1 and COX-2) that share >60% identity at the amino acid level. Both enzymes catalyse the conversion of arachidonic acid to prostaglandins. COX-1 is constitutively expressed in many mammalian tissues and is involved in the physiological

production of prostaglandins for maintaining normal homeostasis. On the other hand, expression of COX-2 is low or not detectable in most healthy tissues, but can be highly induced in response to cell activation by hormones, pro-inflammatory cytokines, growth factors and tumour promoters. The expression of COX-2, but not COX-1, has been found to be increased in a variety of tumours including bladder, colorectal, breast and prostate tumours.

This study has identified changes in gene expression in the PrE2.8 cell line between a proliferative and a non-proliferative phenotype, through differential display analysis. The genes SPR1B and S100A8 are up regulated at 39°C and may be early markers of normal epithelial cell differentiation in the human prostate. To date these genes have not been previously studied in this tissue. COX-2 is down regulated in the cell line at 39°C and is known to show increased expression in prostate cancer. However, its role in normal prostate epithelial cell differentiation is not fully understood. In vivo analysis of these genes in prostate tissue will further elucidate their role in normal prostate epithelial cell differentiation.

4 EXPRESSION OF CD44 IN PRE2.8 CELLS AND PROSTATE TISSUE

4.1 Introduction

Differential display analysis of changes in gene expression between a proliferative and differentiated phenotype in the PrE2.8 cells revealed only three genes with confirmed differential expression (discussed in chapter 3). In order to further investigate the PrE2.8 cell line as a model of prostate epithelial cell differentiation, a candidate gene approach was employed. Among the genes investigated, CD44 revealed an intriguing pattern of gene expression in the PrE2.8 cells, exhibiting an interesting pattern of alternatively spliced isoforms between the proliferative and non-proliferative phenotype. CD44 expression was therefore further investigated in this model system.

CD44 is a transmembrane glycoprotein that is widely expressed in virtually all cell types. It functions as an extracellular matrix receptor and is involved in cell-cell and cell-matrix interactions. CD44 may also participate in growth regulation by presenting growth factors to their cell surface receptors (Lesley et al., 1993). The CD44 protein is encoded by a single gene, located on chromosome 11p13, that consists of 20 exons. However, through extensive alternative splicing of exons 6–14 (also referred to as exons v2-v10), the extracellular membrane domain is highly variable, producing multiple protein isoforms that are expressed in a tissue specific manner (Screaton et al., 1992; Tolg et al., 1993). The shortest isoform of CD44 (CD44s) lacks all variable exons. It has a wide tissue distribution, and is the most common form expressed on haematopoietic cells. Larger splice variants dominate on several normal epithelia and tumours (Fonseca et al., 2000; Heider et al., 1995; Hudson et al., 1995; Hudson et al., 1996; Matsumura and Tarin, 1992). Additional diversity of CD44 isoforms results from post-translational modifications with *N*- and *O*-linked sugars and glycosaminoglycan side chains (Skelton et al., 1998).

CD44 has been implicated in a number of normal and disease processes, including intracellular adhesion and tumour metastasis. Normal human salivary gland was found to be negative for the v4/5 isoform but positive for the variant exons v3 and v6, where it might be involved in the regulation of growth and renewal of the tissue (Fonseca et al., 2000). Keratinocytes express various CD44 isoforms, including forms containing exons v2-v10, v3-v10, v4-v10, v6-v10 and v8-v10 (Brown et al., 1991; Hudson et al., 1995).

Expression of variant isoforms has been implicated in various human malignancies, including colorectal (Heider et al., 1993b), stomach (Heider et al., 1993a), breast (Matsumura and Tarin, 1992), squamous cell carcinoma (Hudson et al., 1996) and prostate cancer (Nagabhushan et al., 1996). In the prostate, CD44s and v6 expression is inversely correlated with tumour stage, grade and ploidy (Nagabhushan et al., 1996). In addition, there have been reports that loss of CD44 s and v6 may be useful prognostic markers in prostate cancer patients treated by radical prostatectomy (Kallakury et al., 1998; Noordzij et al., 1997). Further studies have revealed reduced CD44 expression in prostate cancer metastasis as well as in the corresponding primary tumours (Noordzij et al., 1999). More recently, (Iczkowski et al., 2003) demonstrated an increase in expression of variants v7-v9 in prostate cancer. In rat, expression of the v4-v7 isoform is involved in pancreatic carcinoma and metastasis (Gunthert et al., 1991).

Previous reports of CD44 expression in non-malignant human prostate have shown that basal and intermediate epithelial cells express CD44 (Heider et al., 1995; Noordzij et al., 1997; Tran et al., 2002) but little is known about changes in expression of variant isoforms during different stages of epithelial differentiation. The aim of this experiment was to investigate the expression of CD44 in the PrE2.8 conditionally immortalised cell line. At the permissive temperature they display basal cell characteristics where as at the non-permissive temperature the cells may be undergoing differentiation towards a luminal cell type. It would therefore be of interest to study the expression of CD44 in the PrE2.8 cells at the two growth temperatures, since it is a marker of the basal cell population. RT-PCR revealed a very interesting expression pattern of the CD44 gene in the PrE2.8 cells. Several isoforms of the gene were expressed by the cells and these were identical at the two growth temperatures. However, the largest of the CD44

isoforms showed a significantly higher level of expression at 39°C than at 33°C. This suggested that this isoform may play a role in the differentiation of the PrE2.8 cells and this was investigated further in these cells, as well as in primary prostate epithelial cell cultures and in prostate tissue.

4.2 Results

4.2.1 CD44 isoforms expressed by the prostate epithelial cell line PrE2.8

The expression of the CD44 isoforms in the PrE2.8 cell line were investigated using RT-PCR. Total RNA was isolated from the PrE2.8 cells, which had been incubated at growth temperatures of either 33°C or 39°C for a period of 4, 7, 10 and 14 days. This was reverse transcribed and RT-PCR was carried out using primers positioned at exons 3 and 18 (designated P1 and P2), which flank the variable region of the CD44 gene. A schematic diagram of the gene is shown in Figure 4-1A. The amplified PCR products were electrophoresed on a 1.5% agarose gel and are shown in Figure 4-1B). All lanes show a band of approximately 500 bp, corresponding to the standard form of the CD44 gene, which lacks all variable exons and is 549 bp in length. Three further major CD44 isoforms are expressed at the two growth temperatures. However, there is an increase in the relative expression levels of the largest isoform at the non-permissive temperature.

In order to identify the CD44 exons expressed in each isoform, exon-specific RT PCR was carried out using a forward primer designed for the 5′ side of the constant region of the CD44 gene (primer P1) together with a 3′ primer designed for each of the variant exons v1-v10 (Figure 4-1B(b)). From the number of bands per lane and the stepwise increase in band size, it is possible to deduce which CD44 isoforms are expressed. No product was seen with the v1 primer, but all other lanes contained one or more PCR products. The PCR product labelled (i) in Figure 4-1 appears to contain exons v2-v10. Band (ii) contains exons v6-v10, since it is absent from the v1 to v5 lanes and the band labelled (iii) contains exons v8-v10, as it is absent from lanes v1-v7. Band (iv) represents the standard isoform of CD44. The composition of the bands was confirmed by sequencing of the PCR products and a schematic of the variant forms identified is shown in Figure

4-1A(i-iv). Sequencing of band (ii) revealed that this product actually contains v3-v10 and not v2. There is therefore an additional minor band containing v2. Because variant exons v3-v5 were observed only in the largest band, v3-v10, v5 was chosen as a marker for this isoform as any positive staining for v5 would indicate cells expressing this variant.

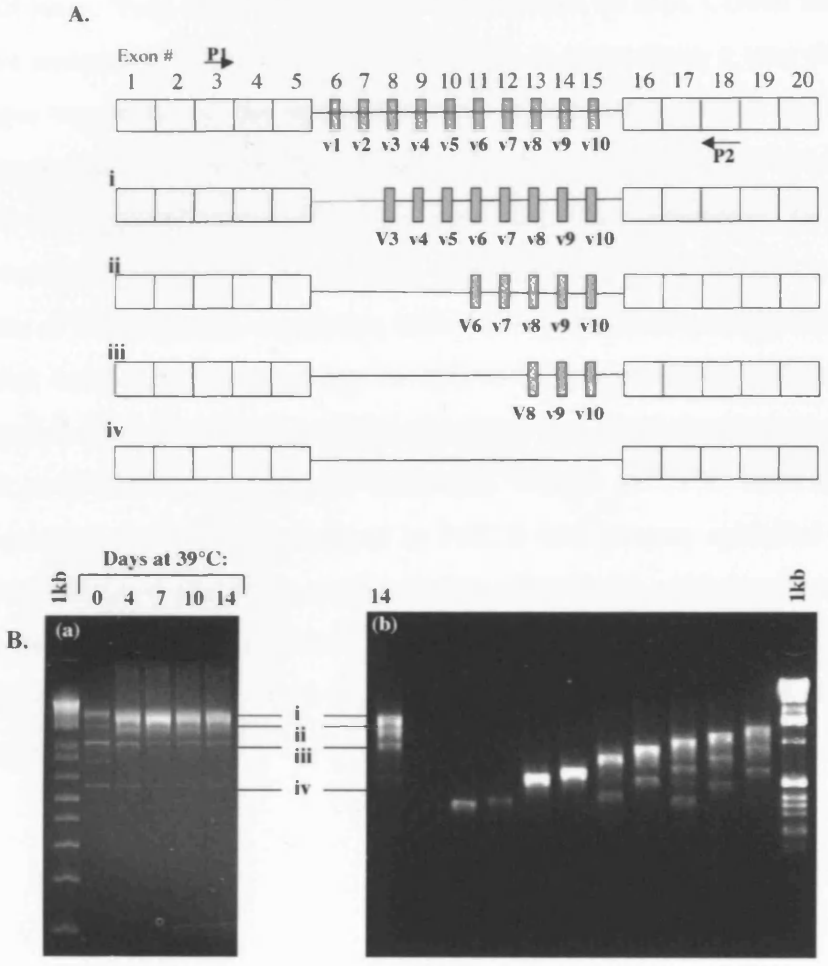

Figure 4-1: RT PCR analysis of CD44 in PrE2.8 cells.

PCR products were resolved on a 1.5% agarose gel. **(A)** Schematic representation of the CD44 gene and the variant isoforms expressed by the PrE2.8 cells and primary cultures of BPH based on sequencing of CD44 PCR products (i-iv). **(B)** Isoform expression of CD44 expressed in the PrE2.8 cells at 33C and at 39C over a 14-day time course **(C)**. RT PCR of PrE2.8 cells grown at 39C for 14 days, using internal primers for each variant exon with the common primer P1. Band i represents expression of variant exons v3-10, band ii, variant exons v6-10, and band iii variant exons v8-10. Band iv represents the standard form of CD44.

4.2.2 CD44 protein expression in Pre 2.8 and BPH cell cultures

Cell extracts of PrE2.8 and primary cultures of BPH were resolved on SDS-PAGE gels, transferred to Immobilon P membrane and probed with E1/2, which recognises all isoforms of CD44. Equal amounts of protein (30 μg) were loaded in all lanes. Very weak expression of the standard 90 kDa, CD44s was observed in all samples (Figure 4-2B arrow) although in some cases it was only seen on longer exposure of the autoradiograph. Three other CD44 isoforms were expressed at 33°C by the Pre 2.8 cells. The most abundant form has a molecular mass of approximately 160 kDa with the least abundant variant being approximately 250 kDa. As the cells differentiate at 39°C, there is a shift in the levels of CD44 protein expression with the largest isoform being more abundant at this temperature and by day 14 this is the major CD44 variant expressed (Figure 4-2A). The CD44 isoforms also have an altered electrophoretic mobility with a reduction in apparent molecular weight at 39°C than at 33°C. A comparison of the bands produced by PrE2.8 with primary epithelial cell culture from BPH tissue revealed a similar pattern of isoforms, with 3 variant bands and the standard form. The variant bands were expressed at similar levels to each other and they had the same apparent molecular weight as PrE2.8 cells at 33°C (Figure 4-2).

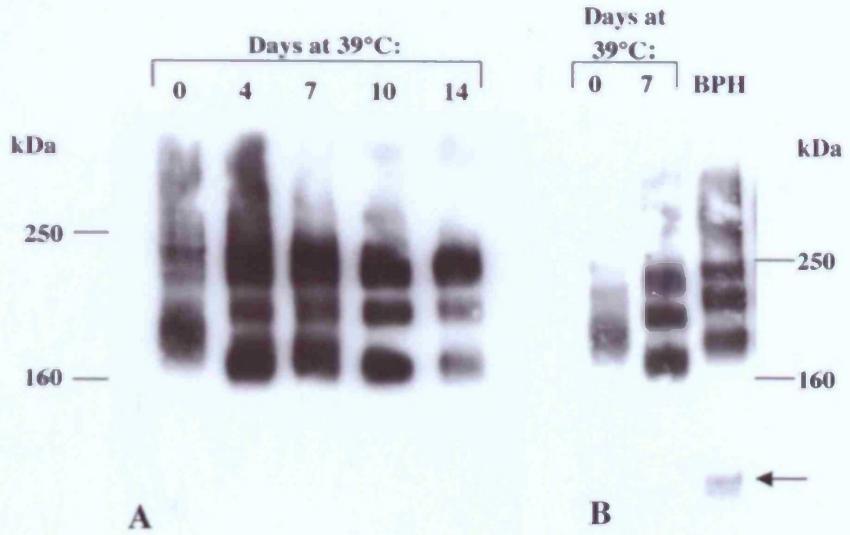

Figure 4-2: CD44 protein expression in PrE2.8 and BPH cells.

(A) Western blotting analysis of CD44 protein (E1.2, anti-total CD44) in PrE2.8 cells grown at 33°C and 39°C. At 39°C the larger protein isoform (~250 kD) is expressed more abundantly than at 33°C, where the smallest variant isoform is the major band. At 39°C the CD44 isoforms have an altered electrophoretic mobility with a reduction in apparent molecular weight. (B) CD44 protein expression in PrE2.8 cells compared with BPH cells. Primary BPH cells show a similar pattern of expression of CD44 isoforms to those expressed by PrE2.8 cells at 39°C, but with higher apparent molecular weight.

4.2.3 Cell surface expression of CD44 protein during differentiation of Pre 2.8 cells and in BPH cell cultures

Immunohistochemistry was used to investigate the cell surface expression and distribution of CD44 in PrE2.8 cells. At 33°C, when the cells are predominantly proliferative, weak expression of total CD44 protein is observed at cell-cell boundaries and is stronger at the surface of cells in the process of mitosis (Figure 4-3A). Only occasional very weak inter-cellular staining for v5-containing isoforms was detected, although there was strong staining in some cells that appear to be overlying other basal cells (Figure 4-3B). When the cells are switched to the non-permissive temperature of 39°C, the increase in cell size is accompanied by an increase in total CD44 protein expression with strong intercellular staining of almost all cells (Figure 4-3D). Strong expression of v5 is now detected at cell-cell borders, indicating that at least some of the newly

expressed CD44 consists of the v3-v10-containing isoform (Figure 4-3E). Primary cultures of BPH cells consist of a mixed population of cells at various stages of the differentiation process. Total CD44 was expressed on the surface of the majority of cells, while the strongest expression of CD44v5 was seen by a minority of cells that, again, were overlying other cells (Figure 4-3C and F).

4.2.4 CD44 protein expression in prostate tissue

To confirm that the CD44 isoforms expressed in prostate cells were also expressed in prostate tissue, RNA was isolated from fresh samples of BPH and normal prostate. DNA sequencing of RT-PCR products revealed the same pattern of isoform expression as found in the cell cultures. Prostate tissues were therefore examined for the distribution of the major v3-v10 isoform. Because exons v3, v4 and v5 will be found only where the v3-v10 isoform is expressed, an antibody to v5 was used as a marker. Eight BPH samples were stained for keratin 14, keratin 19 and CD44 v5 and the sections were scored for distribution of staining. A typical example of expression pattern of double staining for keratin 14 and the CD44 v5-containing isoform in prostate tissue is shown in Figure 4-3G. Positive staining for CD44 v5 was observed in all eight samples. CD44 v5 was expressed in basal cells that were negative for keratin 14 in all samples (example shown in Figure 4-3G) and five samples also showed areas of keratin 14 positive cells that were negative for CD44 v5. In addition, areas of basal cell hyperplasia expressed very high levels of CD44 v5 and were negative for keratin 14 (Figure 4-3I). Interestingly, CD44 v5 was also expressed in epithelial cells located in an intermediate position above the keratin 14-expressing basal layer but below the luminal layer (Figure 4-3G, arrowhead). These cells are taller than typical basal cells and appear to be leaving the basal layer. This expression pattern was almost identical to that observed previously (Hudson et al., 2001) for keratin 19 in human prostate tissue (Figure 4-3H). To confirm that the staining patterns were not due to aberrant growth of cells in BPH, a further six tissue samples were obtained from tissues collected from young male cadavers. In all cases alternating staining patterns for CD44v5 and K14 were found and this was observed in all three glandular zones, central, peripheral and transition zones (Daley-Burns *et al* , in preparation).

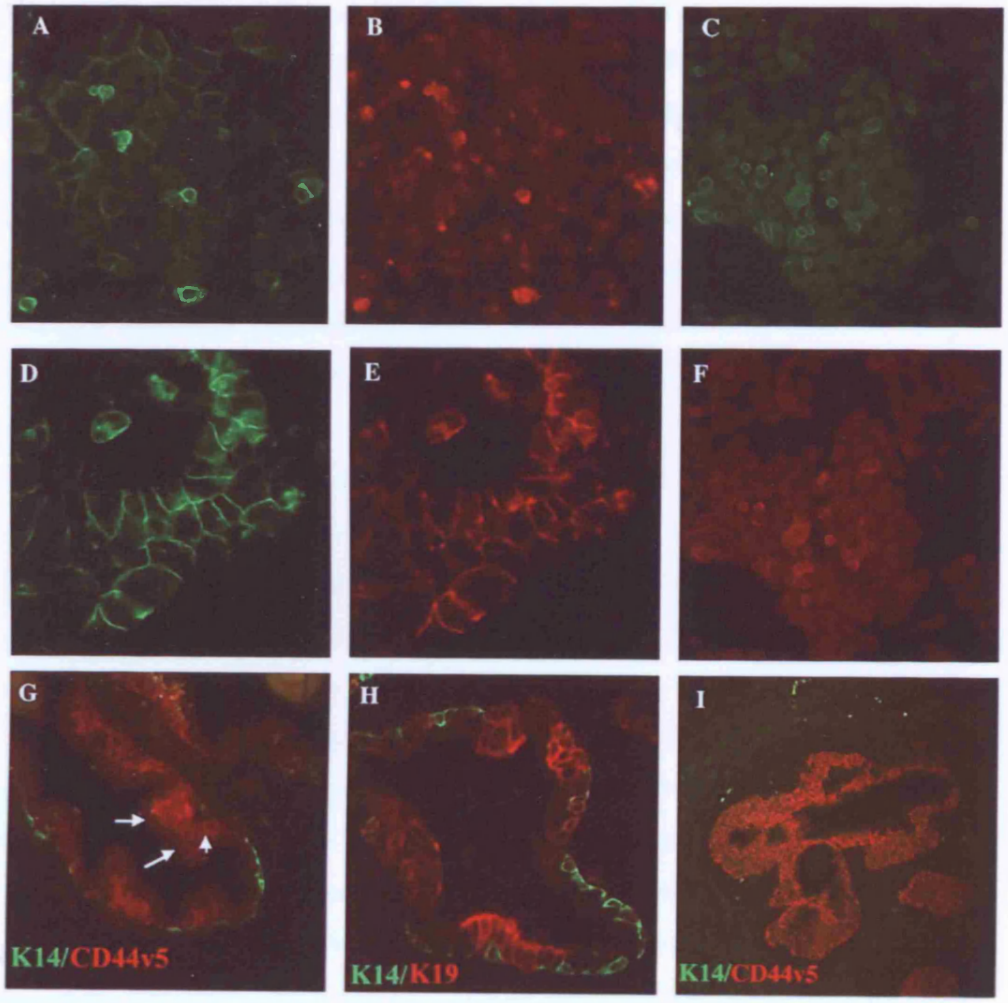

Figure 4-3: Immunofluorescent staining for cell surface CD44 in prostate cells and tissue.

PrE2.8 cells grown at 33°C (A, B) or switched to 39°C for 7 days (D, E) or primary cultures of BPH epithelial cells (C, F) stained for total CD44 (antibody E1.2) (A, C, D) or CD44v5 (B, E, F). Paraffin-embedded BPH tissue (G, H, I) double stained for K14 (green) and CD44v5 (red). In BPH tissue (G), CD44v5 (red) is seen in cells not expressing K14 (green) in a similar pattern to that seen for K19 (H, red). Arrowheads in G indicate limit of luminal cells. CD44v5 is seen in areas of K14-negative basal cell hyperplasia in BPH tissue (I). Original magnifications: A-H X 400; J X 200.

4.3 Discussion

The expression of CD44 during normal human prostate epithelial cell differentiation was investigated. RT-PCR analysis and DNA sequencing revealed four CD44 isoforms expressed by both the immortalised PrE2.8 cells and primary cultures of BPH. The shortest isoform corresponds to the standard form of the gene whereas the three other isoforms represent alternatively spliced CD44 variants. None of these variants expressed exon v1, which is consistent with the report that this exon contains a stop codon (Screaton et al., 1993). The CD44 transcripts expressed were also observed at the protein level as determined by Western blot analysis, the largest isoform being expressed more abundantly by day 14 at 39°C when PrE2.8 cells are further along the differentiation pathway (Alam et al., 2004). Three major isoforms were expressed at similar levels in primary cultures of BPH epithelial cells. However, these cultures contain a mixed population of proliferating and differentiating cells and it was only by using a model in which differentiation could be induced that we could examine the changes in expression of the isoforms.

Whereas RT PCR revealed that the CD44 variants expressed by the cells were all of equal size, an apparent shift in molecular weight was observed by Western blot analysis. This may be due to differences in post-translational modification of the CD44 protein. CD44 contains a number of *N*- and *O*-linked glycosylation sites all of which contribute to further diversity in protein expression. The results show that the isoforms expressed by PrE2.8 cells grown at the non-permissive temperature have an increased electrophoretic mobility and therefore a lower molecular mass, compared to those grown at 33°C and to the primary BPH cultures. This difference may be the result of altered glycosylation of the CD44 variants, perhaps caused by aberrant activity of glycosylation enzymes at 39°C.

The *in vitro* studies suggested that the CD44 v2-v10 isoform may play a role in the differentiation of normal prostate epithelial cells as demonstrated by the PrE2.8 cell culture model system. In order to confirm whether the v5-containing CD44 isoform may also play a role *in vivo*, the expression of the v5-containing variant in prostate tissue specimens was investigated. Positive staining for CD44 v5 was seen in basal epithelial cells in BPH and normal prostate tissues.

This is consistent with reports that CD44 isoforms are expressed by the proliferating compartments of epithelia, specifically the basal layer (Mackay et al., 1994). However, many v5-positive cells were negative for keratin 14, a marker for the least differentiated basal cells. Also in a number of patients, v5-positive staining was seen in epithelial cells that lay above the basal layer but below the luminal layer. These cells were larger and taller than the characteristically small spindle-shaped basal cells. This suggests that the v5-positive cells may be in the process of differentiation from the basal to the luminal layer. It has previously been shown that this cell type also stains positive for keratin 19 and has thus been postulated that they represent an epithelial cell population that are in the process of differentiation (Hudson et al., 2001).

Taken together, these results provide evidence of early differentiation-associated changes in CD44 expression during normal prostate epithelial cell differentiation. More importantly, the CD44 v5-containing isoform may be a marker of cells in the early stages of this differentiation process. CD44 has previously been used as a target for separating basal from luminal prostate cells using immunomagnetic bead-based cell-sorting (Collins et al., 2001). We have now extended this to show that different isoforms of CD44 are in fact expressed in different basal cell populations. The identification of a CD44 isoform as a cell surface marker specific for the transit amplifying population in the prostate will provide a valuable tool for the further characterisation of the differentiation process. Furthermore, the results confirm that the PrE2.8 prostate epithelial cell line provides a model for the study of the differentiation process in the normal human prostate. This led to a more global approach to the study of gene expression in the PrE2.8 cell model using cDNA microarray analysis.

5 MICROARRAY ANALYSIS OF DIFFERENTIAL CHANGES IN GENE EXPRESSION IN THE PRE2.8 CELL LINE

5.1 Introduction

Analysis of temperature-dependent changes in gene expression in the PrE2.8 cells, as determined by differential display (Chapter 3), resulted in only three genes that were positively identified to be differentially expressed. The technique also yielded a high number of false positive results. In order to overcome this problem, and to gain a global picture of the changes occurring in gene expression in the PrE2.8 cells during proliferation and differentiation, microarray analysis was employed.

Microarrays allow the simultaneous analysis of changes in expression levels of thousands of genes within a test and reference sample and offer an insight into cellular function. Various types of DNA microarrays exist, such as cDNA arrays and oligo arrays. In this case, cDNA arrays were employed. Figure 5-1 outlines the general principle of the technology: mRNA from the sample of interest is converted into cDNA in a reverse transcription reaction that incorporates one specific fluorescent dye. The sample of interest by consensus is labelled with Cy5 dye, which fluoresces at a wavelength of 635 nm, and is visualised as a red colour in the scanned computerised image of the array slide. A control or reference mRNA source is also converted to cDNA. This time the reaction incorporates a different fluorescent dye, Cy3, which fluoresces at a wavelength of 532 nm and is

visualised as a green colour. The two different labelled samples are then mixed and hybridised together onto the microarray where the labelled cDNA sequences bind to their respective probes on the array. Since two differently labelled cDNAs are applied to the same array, competitive hybridisation occurs for each probe.

The level of hybridisation of labelled cDNA to each array probe is determined by laser-scanning the array. The lasers stimulate the Cy5 and Cy3 dyes at their corresponding wavelengths and the amount of emission/fluorescence is measured. This relates to the amount of sample bound to each probe on the array. If a gene is expressed at a high level in the experimental sample, but at a low level in the control/reference sample, the spot on the array will be predominantly red. If a gene is expressed at a low level in the experimental sample but a high level in the control/reference sample, the spot on the array will be predominantly green. Equal levels of gene expression in the sample of interest and reference sample results in a yellow spot on the array due to equal amounts of red and green hybridisation.

The microarrays used in the following experiments were obtained from the Institute of Cancer Research (UK) (http://icr.ac.uk/array.array.html) and consisted of 5,603 IMAGE cDNA clones acquired from the Human Genome Mapping Project Resource Centre (http://www.hgmp.mrc.ac.uk) and from Research Genetics (http://www.resgen.com). The arrays contained cDNA clones with defined biological functions which were selected in preference to anonymous expressed sequence tags (ESTs) (5,321 known function; 282 anonymous ESTs). mRNA, extracted from total RNA, from PrE2.8 cells grown at 39°C for 4 days was labelled with Cy5 (experimental sample) and mRNA from the cells grown at 33°C (control/reference sample) was labelled with Cy3.

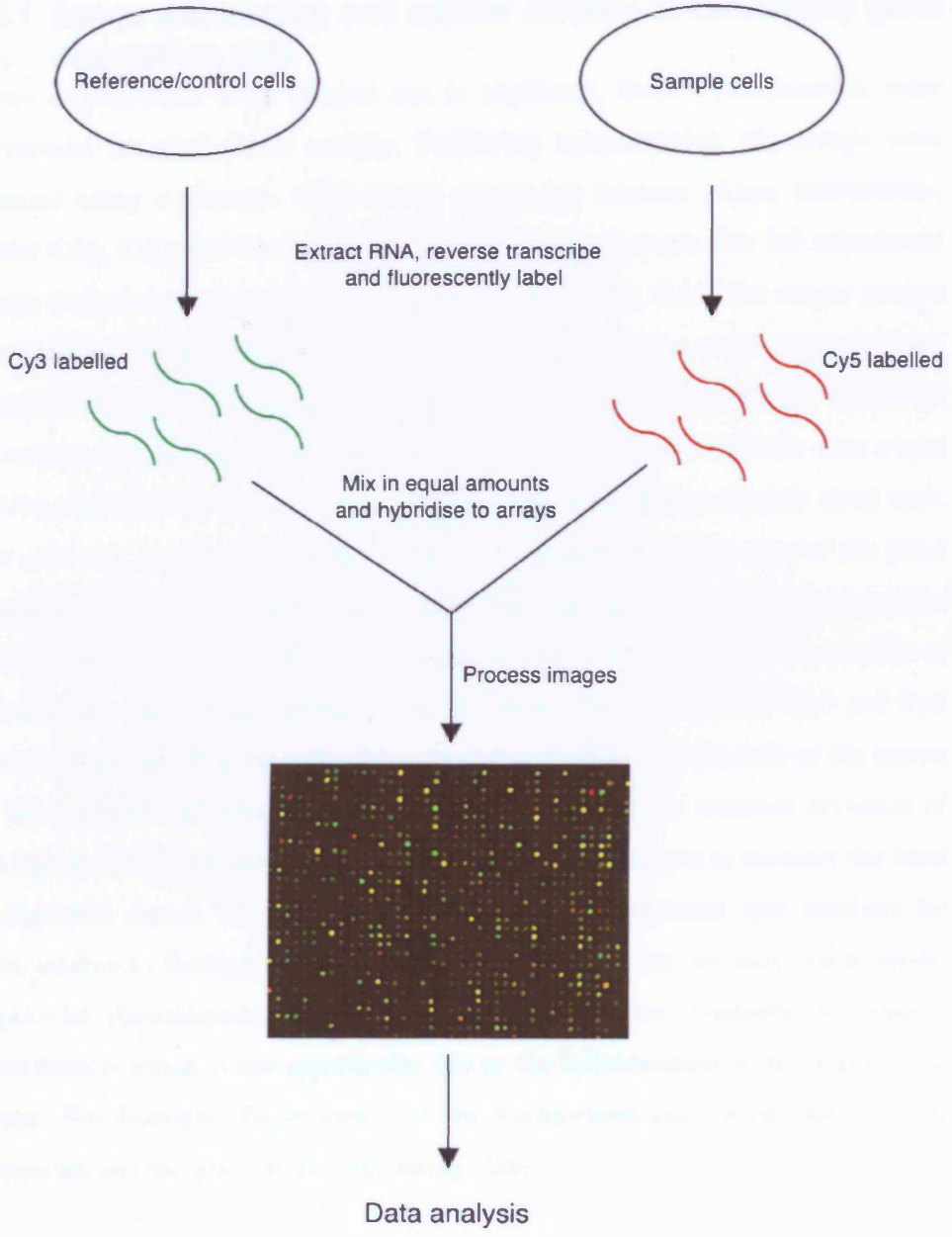

Figure 5-1: Schematic of microarray process.

5.2 Results

5.2.1 Image processing and scatter display of microarray gene expression data

Array experiments were carried out in triplicate; three hybridisations were performed for each RNA sample. Following hybridisation, the arrays were scanned using a Genepix 4000 Series microarray scanner (Axon Instruments, Foster City, CA) and the image analysed using the Genepix Pro 3.0 microarray image analysis software (Axon Instruments, Foster City, CA). The output images are stored as 16-bit image files, one for each dye, which are viewed as 'raw data' (Figure 5-2). The image processing stage extracts measures of transcript abundance hybridised to each gene spotted on the array. The software uses a spot finding algorithm to define the location and edge boundaries of each array spot. For each dye, the signal for any given spot is measured by the sum of the pixel intensities for each emission wavelength within the spot. The sum represents the total amount of cDNA hybridized to the spotted DNA sequence. A number of calculations can also be derived from the measured intensities of Cy3 and Cy5 dye for each spot. For example, the ratio of the medians and the ratio of the means of the Cy3 and Cy5 channels can be derived, as well as the standard deviation of the values. The algorithm also defines an area around the spot to measure the local background signal. This was subtracted from the foreground spot intensity for data analysis. Background correction was carried out because each spots' measured fluorescence intensity, in each of the two channels, includes a contribution which is not specifically due to the hybridisation of the target to the probe. For example, fluorescence of the background may occur due to other chemicals and the glass of the microarray slide.

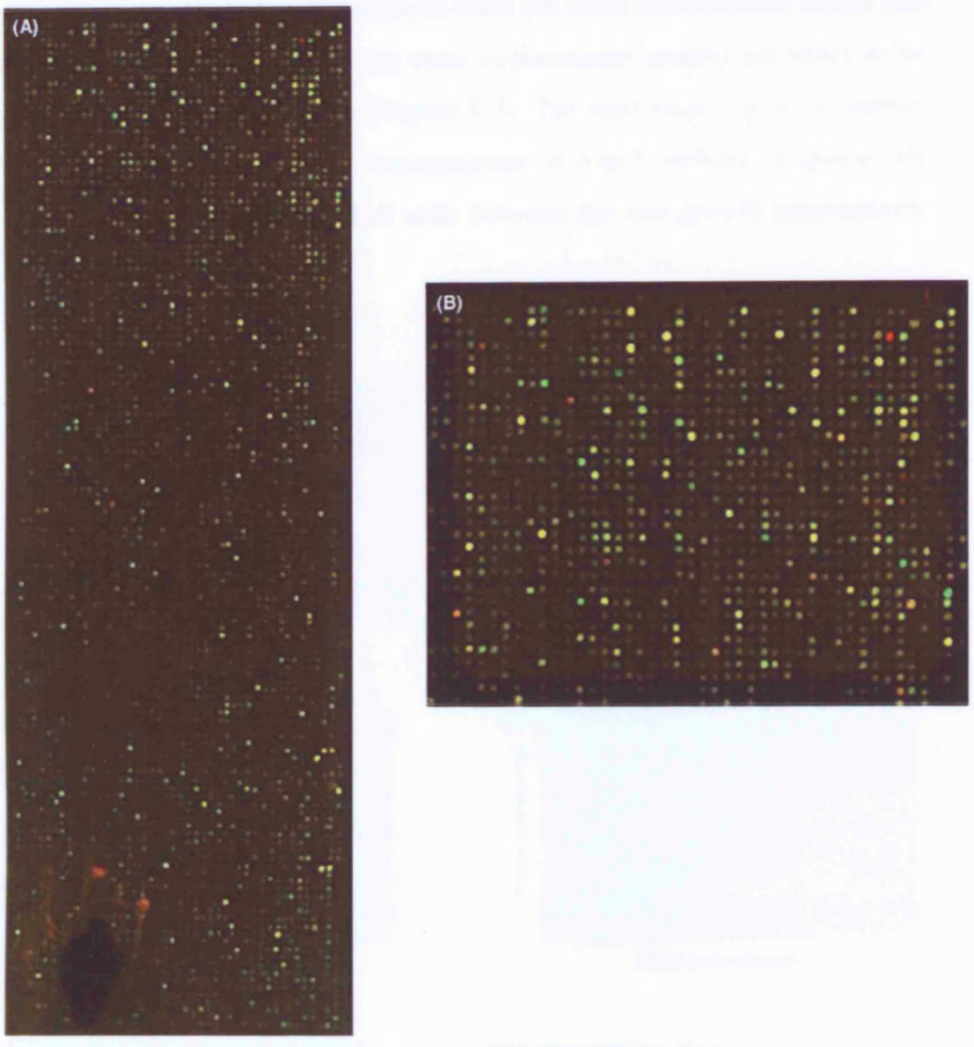

Figure 5-2: Scan of microarray slide.

Following hybridisation, arrays were scanned using a Genepix 4000 Series microarray scanner (Axon Instruments, Foster City, CA) and the image analysed using the Genepix Pro 3.0 microarray image analysis software (Axon Instruments, Foster City, CA). The output images were stored as 16-bit image files (A). (B) shows an enlarged area of image (A).

A control array experiment was also performed in which RNA extracted from the reference/control sample (PrE2.8 cells cultured at 33°C) was divided into two, labelled with Cy3 or Cy5 dyes then mixed and co-hybridised to the array. The Cy3 and Cy5 intensity data from this experiment can be viewed by plotting the background-subtracted $\log_2$ intensities for the Cy5 sample verses the Cy3 sample for each gene spotted on the array. In this case, all intensity ratios should equal one, i.e. have a $\log_2(Cy3) = \log_2(Cy5)$ relationship between the intensities.

This data can be compared to that derived from the three experimental arrays and in this way, verify that outliers in the three experimental graphs are likely to be due to differential gene expression (Figure 5-3). The next stage was to normalise the gene expression data prior to determination of which outliers, or genes, are differentially expressed in the PrE2.8 cells between the two growth temperatures of 33°C and 39°C.

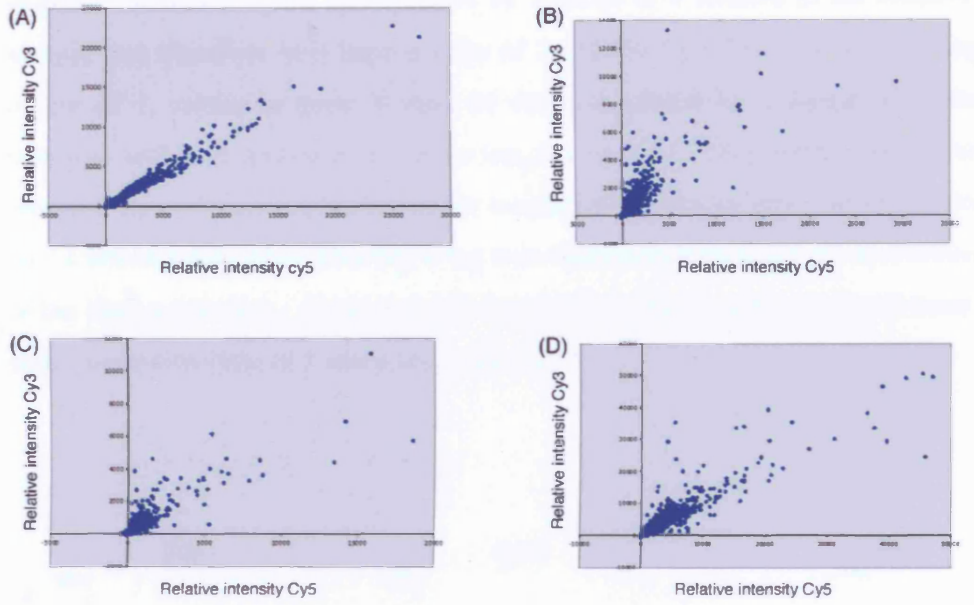

Figure 5-3: Scatter plots of cDNA microarray expression data.

The graphs show relative intensities of Cy3 verses Cy5 dyes for (A) the control hybridisation of PrE2.8 (33˚C) cDNA labelled with Cy3 and PrE2.8 (33˚C) labelled with Cy5. Experimental hybridisations were carried out with PrE2.8 (33˚C) labelled with Cy3 and PrE2.8 (39˚C) labelled with Cy5; these experiments were replicated three times (B, C, D).

5.2.2 Log transformation of gene expression data

The log ratio of the median intensity values for each feature on the array is used for data analysis. This is preferable to using raw intensity values (Figure 5-4) since these are not normally distributed where as log transformed intensities approach a normal distribution. This can be seen in Figure 5-5 where the linear or log intensity ratios of Cy3 and Cy5 gene expression ratio of three sets of data are plotted. Although they are different, with different mean and median values, the

actual shape and spread of the sets of data in the histograms is very similar, i.e. the two data sets have similar standard deviations. Therefore, log transformation aids the comparison between arrays and the array normalisation processes. Log ratios also facilitate the interpretation of relative increases or decreases in gene expression from different samples. Logarithms to base 2 are used rather than natural or decimal logarithms (log to base 10), which allows the interpretation of gene expression ratio changes between genes from different samples. For example, gene X may be up-regulated by a factor of 2 relative to the reference sample and therefore will have a ratio of 2 (15000 Cy5/7500 Cy3) and a $\log_2$ (ratio) of 1, where as gene Y may be down-regulated by a factor of 2, and therefore will have a ratio of 0.5 and a $\log_2$ (ratio) of –1. This gives a much more intuitive view of gene expression as the magnitudes for under and over expression are identical whilst also allowing a log transformation into a normal distribution of the expression data. A gene whose expression value is unchanged will have a gene expression ratio of 1 and a $\log_2$ (ratio) of 0.

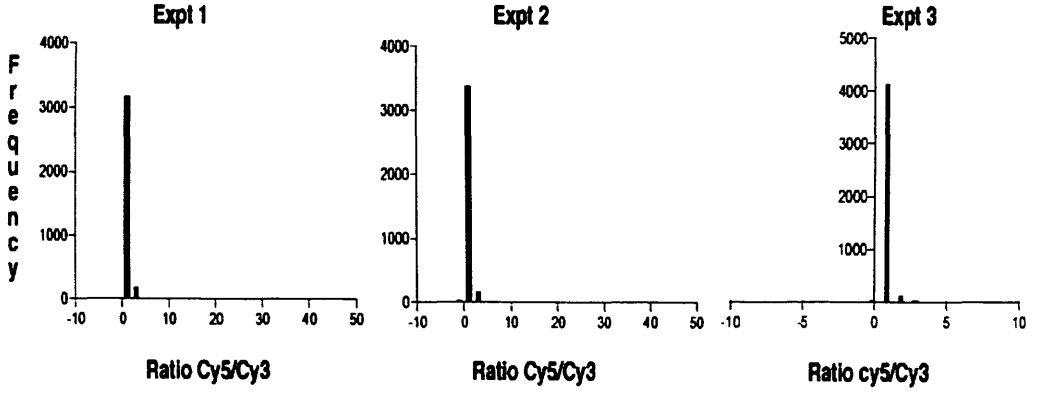

Figure 5-4: Histograms of unlogged microarray expression data.

Histograms are plotted showing the frequency of gene expression ratios (Cy5/Cy3) for the three replicate microarray experiments. The majority of spots on each array have a gene expression ratio of approximately 0.

5.2.3 Data normalisation

Like all other biological experiments, gene expression measurements using microarrays are subject to both random and systematic variations which affect measured gene expression levels. For example, experimental differences in the absolute amounts of mRNA used for each array, efficiency of reverse transcription reactions and differences in array hybridisations and washing can occur. Systematic differences between the physical properties of the two fluorescent dyes can also occur such as heat and light sensitivity as well as excitation and emission half lives. Therefore the process of normalisation is used to minimise systematic variations in the gene expression levels of the two samples hybridised to the array and to allow the comparison of such data across arrays, prior to data analysis.

A number of methods exist for data normalisation and are based on certain assumptions about the underlying data (Quackenbush, 2001). Normalisation methods take advantage of the fact that when log transformed, gene expression data approaches a normal distribution and therefore the entire gene expression data distribution can be shifted to the left or right of the population mean or median without changing the standard deviation.

The Global normalisation method was used normalise the gene expression data obtained from the three replicate experiments. This normalisation method assumes that the Cy5 and Cy3 intensities on a slide are related by a constant factor (Cy5 = kCy3) and that the $\log_2$ expression ratio of the average (mean) or median gene of the population is zero or the Cy5/Cy3 ratio for the average gene is 1 (i.e. the expression levels of the majority of genes will not change when comparing two mRNA populations and only a small proportion of genes are expected to be differentially expressed). Therefore:

$$\text{Log}_2 (\text{Cy5}/(\text{kCy3})) = \log_2 (\text{Cy5}/\text{Cy3}) - a$$

where, as indicated above, a common choice for 'a' is the median or mean of the $\log_2$ ratios of all the data (i.e. $a = \log_2 k$). These calculations were carried out using the Microsoft Excel software. Figure 5-5 shows the expression data of the three data sets before and after global normalisation. After normalisation, the data sets should be centred around a $\log_2$ ratio of zero in order that the three replicate experiments can be compared with each other for data analysis. From Figure 5-5 it can be seen that following global normalisation of the expression data, the

average gene expression ratios are not exactly centred at zero. This is particularly prominent in experiment three (Figure 5-5 C (ii)).

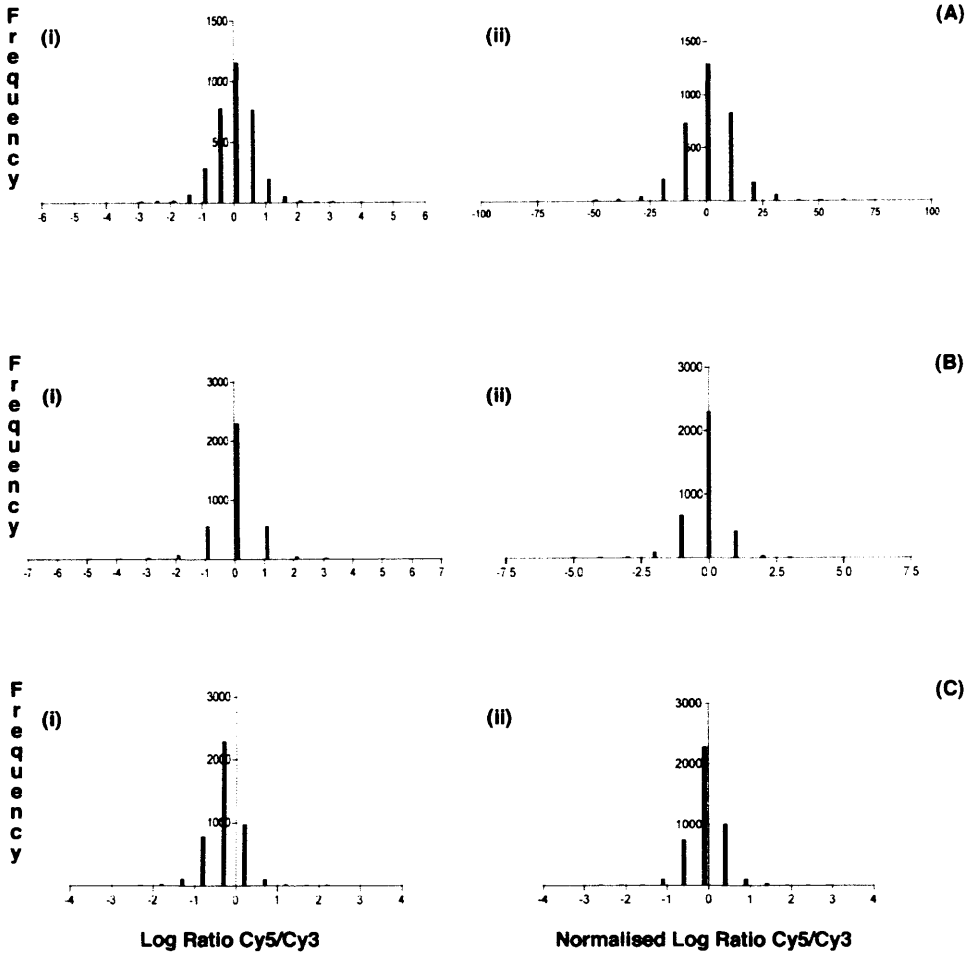

Figure 5-5: Histograms of log_2 expression data before and after normalisation.

Histograms are plotted showing the frequency and distribution of log_2 transformed gene expression ratios (Cy5/Cy3) for the three replicate microarray experiments (A, B, C), before (i) and after (ii) global normalisation.

In order to rectify this, a more advanced method of normalisation was used known as LOWESS (Locally Weighted Least Squares) normalisation (Cleveland WS, 1979) using the statistical package R (Ihaka & Gentleman, 1996). This method works on the observation that when looking at data from an individual slide, there is not an absolute linear relationship between log_2 ratio values and intensity. Lowess is a scatter plot smoother method which is used to produce location-specific estimates of the log2 ratios for various intensities and uses these

as distinct local normalisation values dependent on overall intensity. Essentially, LOWESS divides the scatter-plotted values into subgroups and produces a low-degree polynomial to this subset of data (Figure 5-6).

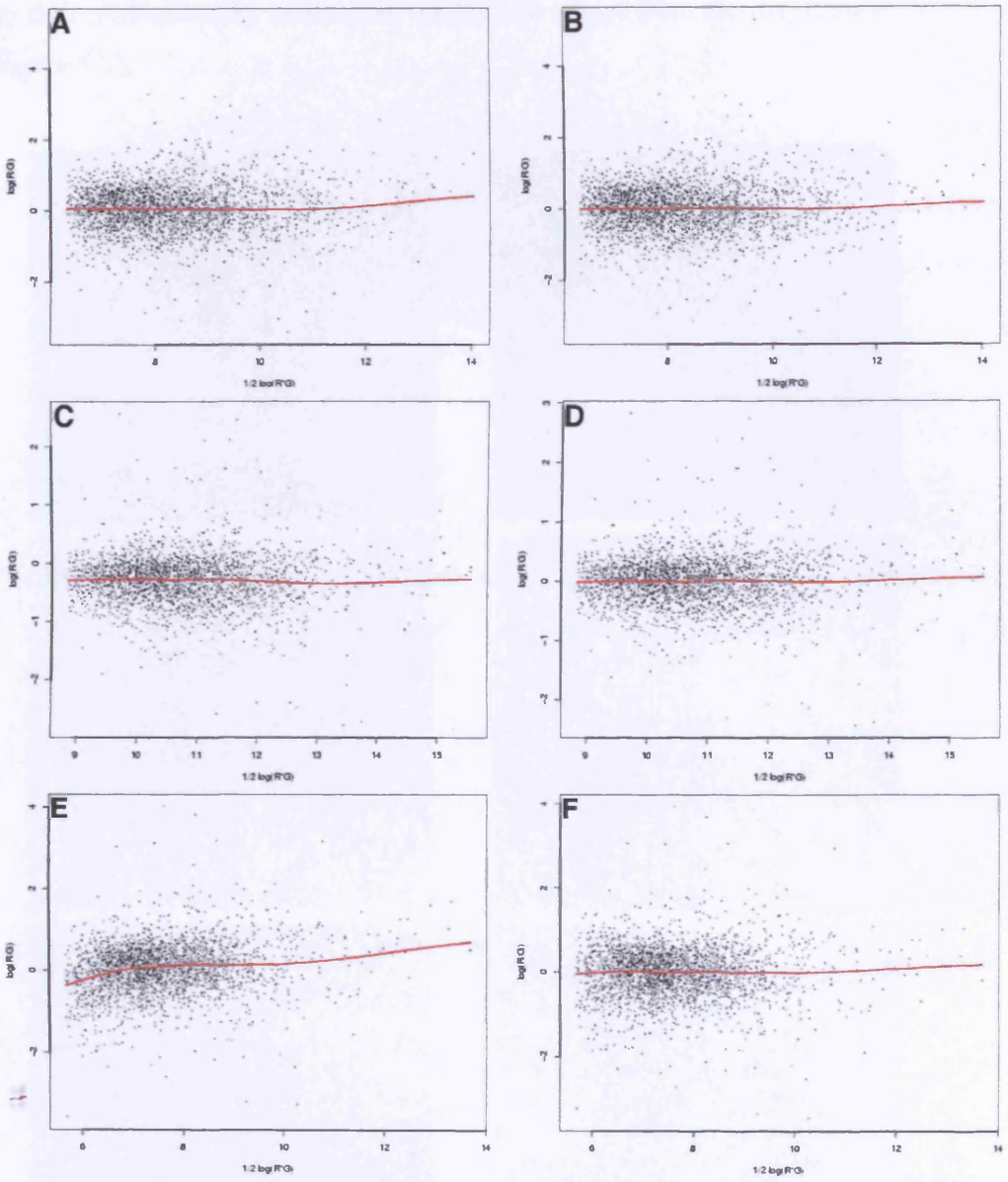

Figure 5-6: Lowess normalisation of microarray data.

Graphs show Lowess scatter plots of microarray expression data for the three replicate microarray experiments before (A, C, E) and after (B, D, F) Lowess normalisation.

A third normalisation method was used in parallel with the Lowess method which takes into account the variability in hybridisation of dyes across the array,

i.e. hybridisation is not uniform over the array and there may also be areas of high background hybridisation. A way of making such systematic differences visible is by applying the 2dimensional (2d) normalisation method (Wernisch et al., 2003). This method fits a trend surface to log ratio values over the array sets. Log_2 ratios are then normalised by subtracting the surface values from the log_2 ratio values (Figure 5-7).

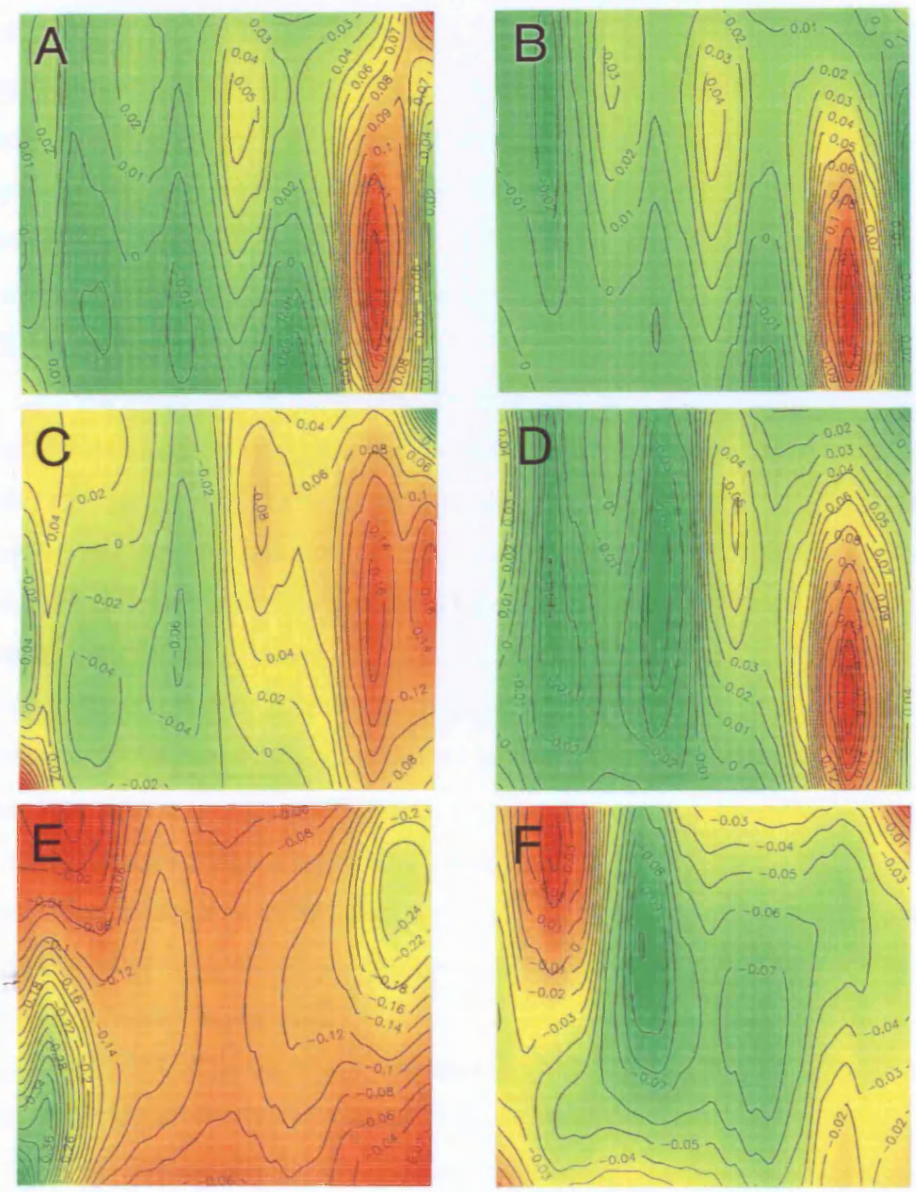

Figure 5-7: 2d normalisation of microarray data.

Images show 2d Lowess surface fitted to log ratio values from the three replicate microarray experiments before (A, C, E) and after (B, D, F) normalisation.

5.2.4 Data analysis

Following normalisation, the microarray expression data was analysed to identify statistically significant differential gene expression. An analysis of variance (ANOVA) approach was used, as proposed by (Kerr et al., 2000), using a statistical software package known as R. To account for the multiple sources of variation in a microarray experiment, the following model is implemented by R:

$$\mathbf{Log}\ (y_{ijkg}) = \mu + A_i + D_j + V_k + G_g + (AG)_{ig} + (VG)_{kg} + \varepsilon_{ijkg}$$

Where μ is the overall average signal, A_i represents the effect of the i^{th} array, D_j represents the effect of the j^{th} dye, V_k represents the effect of the k^{th} variety, G_g represents the effect of the g^{th} gene, $(AG)_{ig}$ represents a combination of array i and gene g (i.e. a particular spot on a particular array), and $(VG)_{kg}$ represents the interaction between the k^{th} variety and the g^{th} gene. The error terms ε_{ijkg} are assumed to be independent and identically distributed with mean 0 (Kerr et al., 2000).

The array effects A_i account for differences between arrays averaged over all genes, dyes and varieties. The dye effects D_j account for differences between the average signal from each dye; one dye may be inherently brighter than the other, and this is taken into account in the analysis. The terms V_k account for overall differences in the varieties. Such differences could arise if some varieties have more transcription activity in general, or because of differential concentration of mRNA in the labelled sample. The terms G_g account for average effects of individual genes spotted on the arrays in the experiment. The $(AG)_{ig}$ account for the average effect of the spot on array i for gene g. Essentially this is a "spot" effect, and may arise because there is not complete control over the amount and concentration of cDNA immobilized from one array to the next (Kerr et al., 2000). All of these effects are generally not of interest, but account for sources of variation in microarray data.

ANOVA analysis of gene expression data revealed 47 genes up-regulated in the PrE2.8 cell line at 39°C and 52 genes down-regulated at this temperature (Table 2). Differential gene expression of a number of genes was confirmed by sequencing and RT-PCR (Figure 5-8). To understand the biological significance of overall changes in gene expression, the differentially expressed genes were categorised into functional groups (Figure 5-9).

Table 2: List of differentially expressed genes detected by microarray analysis.

Up-regulated genes are shown in red, down-regulated in green.

CLONE ID	GENE NAME	P VALUE	FOLD CHANGE
562729	S100 calcium-binding protein A8 (S100A8)	3.17E-51	16.020225
813614	Small proline-rich protein 1B (SPR1B)	1.14E-30	8.715104
119530	inward rectifier potassium channel	5.52E-27	7.668213
204335	brain mRNA homologous to 3'UTR of human	2.49E-23	6.697957
814798	Aldehyde dehydrogenase 6 (ADH)	3.57E-23	6.657645
812965	V-myc avian myelocytomatosis viral oncogene	1.14E-16	5.088454
842863	RTP/dDrg-1/NDRG1	4.24E-11	3.881768
729942	small proline rich protein II	7.97E-11	3.825207
2556976	tissue inhibitor of metalloproteinase 3 (TIMP3)	5.09E-10	3.660203
188036	bullous 230 kDa pemphigoid antigen (BPAG1)	4.14E-09	3.475968
811096	Integrin beta-4 subunit (INTB4)	8.54E-09	3.412956
810960	serine protease-like protease	1.25E-08	3.380107
244307	Plasminogen activator inhibitor, type I	1.03E-07	3.198071
417226	similar to gb:K02276 myc proto-oncogene	1.89E-07	3.14558
810131	Keratin 19	9.25E-07	3.010106
840708	Superoxide dismutase 2, mitochondrial	1.24E-06	2.985414
489519	Tissue inhibitor of metalloproteinase 3	1.23E-05	2.791254
772878	Keratin 10	1.75E-05	2.761044
868212	Transforming growth factor, beta-induced	2.17E-05	2.742902
757873	Cyclin-dependent	3.61E-05	2.700271

	kinase 5, regulatory subunit		
590369	similar to gb:X12701 plasminogen activator	5.62E-05	2.662983
345957	Cytostatin A (CSTA)	2.09E-04	2.552578
51865	Carbonic anhydrase II	2.16E-04	2.549545
841664	Caveolin, caveolae protein, 22kD	5.14E-04	2.47667
122428	Jun B proto-oncogene (JunB)	5.59E-04	2.469739
161456	Serum amyloid A protein precursor	6.10E-04	2.462339
2266734	Laminin-5 beta3 chain	6.22E-04	2.460694
77577	Fos-related antigen 2	8.99E-04	2.429715
415851	RhoE (ARHE)	1.54E-03	2.384366
814595	RACK-like protein PRKCBP1	1.69E-03	2.376335
460398	Small inducible cytokine A3	3.08E-03	2.325879
201727	B cell lymphoma protein 6	3.08E-03	2.325732
786067	M-phase inducer phosphatase 2	3.92E-03	2.305528
505225	Arg/Abl-interacting protein ArgBP2a ArgBP2a	5.50E-03	2.276827
298268	B-cell translocation gene 1, anti-prolif (BTG)	5.51E-03	2.276684
51448	Activating transcription factor 3	8.77E-03	2.237247
194214	TGIF protein	9.39E-03	2.231452
842820	inducible poly(A)-binding protein	1.29E-02	2.204303
208718	Annexin I (lipocortin I)	1.36E-02	2.200065
35077	APEG-1	2.02E-02	2.166405
589362	Clusterin (complement lysis inhibitor; t	2.20E-02	2.159021
297392	Metallothionein 1L	2.77E-02	2.139192
741497	Neutrophil gelatinase-associated lipocal	2.82E-02	2.137818
35185	Gamma-aminobutyric acid (GABA) A receptor	2.91E-02	2.135053

768031	KIAA0303	3.09E-02	2.129965
815781	KIAA0201	4.49E-02	2.097898

CLONE ID	GENE NAME	P VALUE	FOLD CHANGE
214006	Histone H2B/l (His)	2.34E-28	0.1242249
488964	Histone H2A.2	5.20E-26	0.1350787
52076	clone 23876 neuronal olfactomedin-related	1.80E-21	0.1605503
66317	Histone H1D	4.39E-16	0.2017631
970590	Ribosomal protein L37	8.05E-14	0.2243501
789091	Histone 2A-like protein (H2A/l)	1.58E-13	0.2275674
144834	E-MAP-115	1.92E-13	0.2285337
250654	SPARC/osteonectin	6.99E-13	0.2349687
781089	PTTG1 pituitary-tumour transforming gene	1.40E-11	0.2511353
815526	V-myb avian myeloblastosis viral oncogene	3.25E-11	0.2560321
342640	KIAA0101 (KIA)	2.08E-10	0.2674162
36393	T-complex protein 1, alpha subunit	6.65E-10	0.274979
769921	cyclin-selective ubiquitin carrier protein	1.33E-09	0.2796725
796694	effector cell protease receptor-1 EPR-1	4.85E-09	0.2888255
129865	AURORA/IPL1-related kinase	1.18E-07	0.3138659
380797	putative RNA binding protein RNPL	1.86E-07	0.3177405
742132	Interferon-induced 17 KD Protein	2.25E-06	0.3407656
810142	Major histocompatibility complex, class	2.27E-06	0.3408335
365641	DNA primase polypeptide 1 (49kD)	1.03E-05	0.3563402
530282	NADH dehydrogenase	1.46E-05	0.3601765
242578	tastin	3.68E-05	0.3705727
970591	High-mobility group (nonhistone chromoso	1.26E-04	0.385318
379920	Thymidine kinase 1, soluble	1.61E-04	0.3884757
796646	Ornithine decarboxylase 1	1.94E-04	0.3908095
978715	similar to gb:K00558 Tubulin alpha-1 CHA	2.02E-04	0.3913712
789204	translocation protein-1	2.39E-04	0.3935074
306358	Eukaryotic initiation factor 4A-LIKE NUK	3.62E-04	0.3989898
208161_1	Tyrosine 3-monooxygenase/tryptophan 5-mo	6.78E-04	0.4075865
878798	BETA-2-microglobulin precursor	1.28E-03	0.4166855

755093	neuronal apoptosis inhibitory protein	1.54E-03	0.4193681
810142_1	Major histocompatibility complex, class	2.17E-03	0.4245433
753620	Insulin-like growth factor binding protein	3.00E-03	0.4295576
241826	non-histone chromosomal protein HMG-17	3.44E-03	0.4316979
39798	Serine hydroxymethyltransferase	4.59E-03	0.4362667
1476053	Replication protein A	7.77E-03	0.4449367
853906	MHC class I protein HLA-A	9.47E-03	0.4482777
843049	CDC21 Homologue	1.03E-02	0.4496614
783696	Ornithine aminotransferase	1.21E-02	0.4525226
471196	Weakly similar to putative	1.24E-02	0.4529436
856447	Gamma-interferon-inducible protein IP-30	1.35E-02	0.454435
815501	Laminin, beta 2	1.41E-02	0.4552018
796278	General transcription factor IIH, polype.	2.01E-02	0.4615597
449058	roundabout 1	2.24E-02	0.4634822
630013	DNA repair protein MSH2.	2.68E-02	0.4667963
280507	Hypoxanthine phosphoribosyltransferase 1.	2.74E-02	0.4672098
436121	Adrenal specific 30 KD protein	3.29E-02	0.470685
47681	putative splice factor transformer2-beta.	3.42E-02	0.4713933
839623	Neuroblastoma RAS viral (v-ras) oncogene.	3.45E-02	0.4715956
77805	Coatomer beta subunit	4.21E-02	0.4753881
837923	putative ribulose-5-phosphate-epimerase.	4.27E-02	0.4756727
884766	Testis enhanced gene transcript.	4.31E-02	0.4758585
760148	Uroporphyrinogen decarboxylase.	4.33E-02	0.4759556

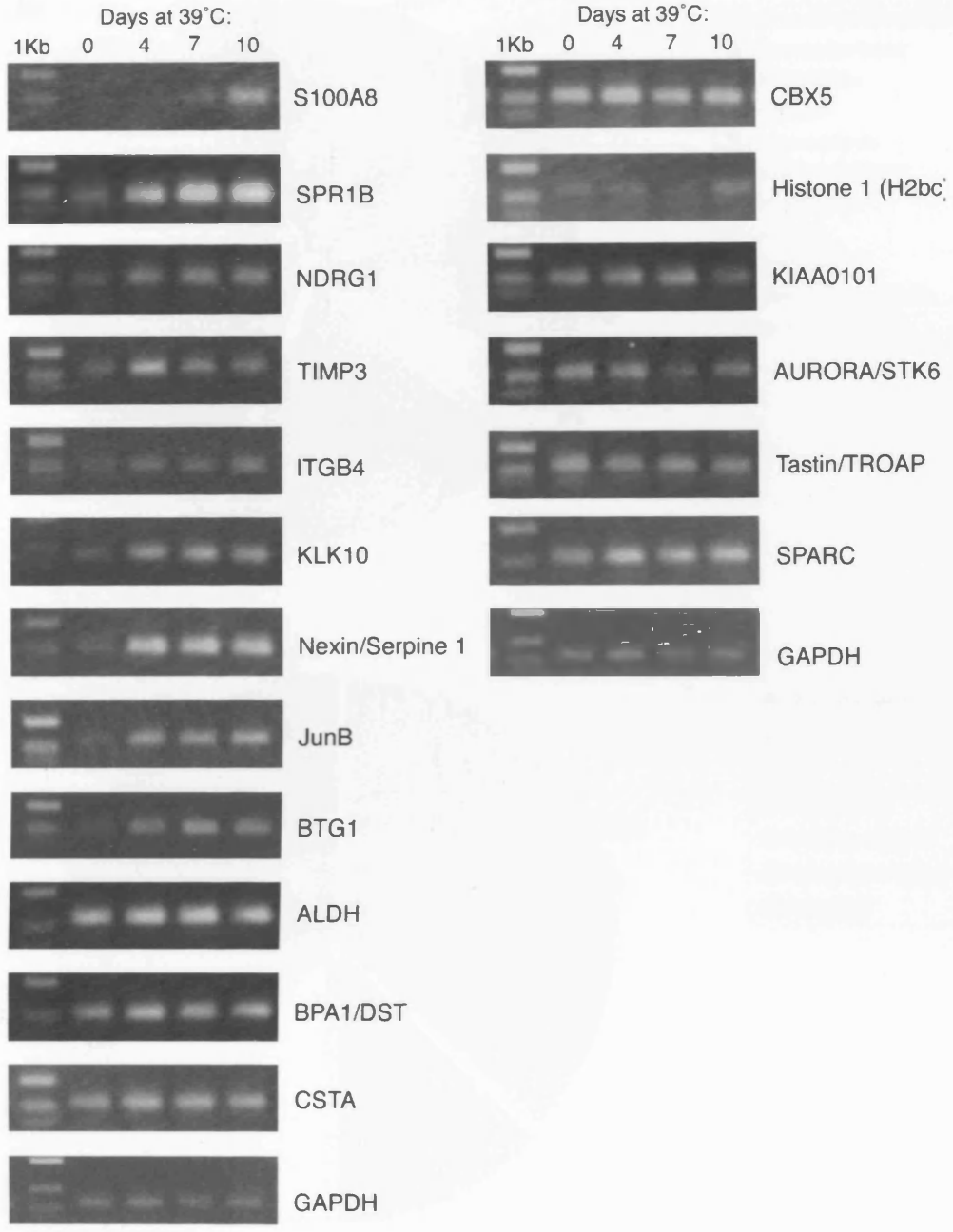

Figure 5-8: Expression of mRNA species in the PrE2.8 cell line cultured at 33°C then transferred to 39°C and sampled over 10 days.

RT-PCR analysis was carried out for a range of target sequences identified in microarray experiments to be either (A) up-regulated or (B) down-regulated in PrE2.8 cells following incubation of the cell line at 33°C and then transferred to 39°C for 4, 7 and 10 days. PCR products were resolved on 1.4% agarose gels.

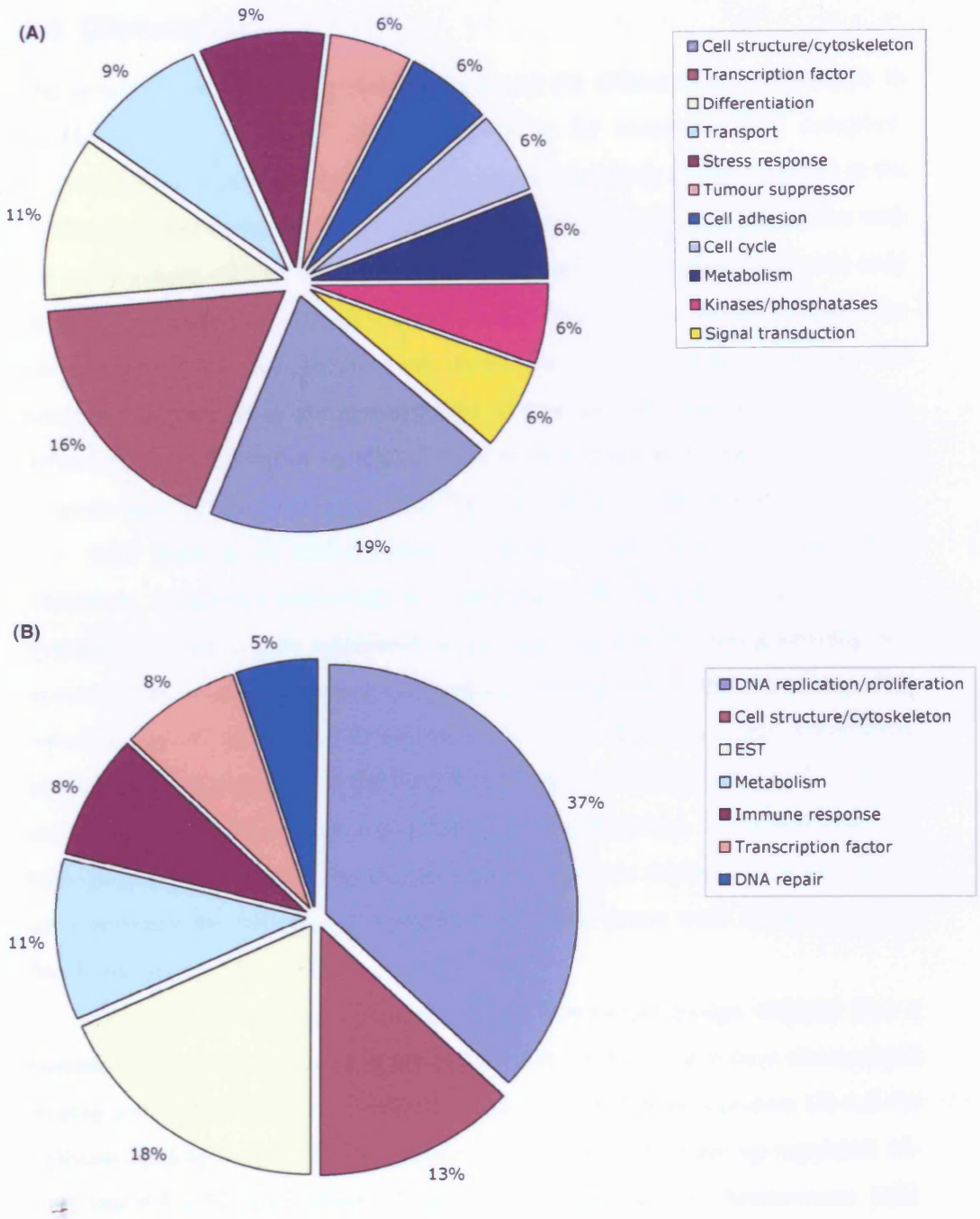

Figure 5-9: Pie charts of gene functional groups.

Differentially expressed genes were categorised into functional groups. The pie charts show the percentage of genes in each functional group for over-expressed (A) and under-expressed (B) genes.

5.3 Discussion

The genetic reprogramming that brings about the differentiated phenotype in human prostate epithelial cells is likely to be extensive and complex. Differentiation of prostate epithelial cells remains a poorly defined process at the biochemical and molecular level; changes in signalling pathways, interaction with the extracellular matrix, metabolic process and apoptotic pathways remain only partially characterised. Hence understanding these events would enhance the knowledge of the mechanisms of maintenance of prostate epithelial cell homeostasis, as well as the pathogenesis of prostate tumourigenesis. Typically, differentiation of prostate epithelial cells is accompanied by the expression of prostate specific genes such as PSA, PAP and the androgen receptor. However, few other markers of differentiation in this cell type have been identified. Therefore, microarray technology in combination with the PrE2.8 cell line model system was used to gain additional insight into the genetic reprogramming that accompanies prostate epithelial cell maturation. Analysis of the microarray data revealed that 47 genes (0.8%) out of the 5,603 on the array, were statistically significantly up-regulated in the Pre2.8 cells when switched from 33°C to 39°C, and 52 genes (0.9%) were significantly down-regulated. To understand the biological significance of the overall changes in gene expression in the Pre2.8 cells between the two growth temperatures, these genes were categorised into functional groups (Figure 5-9).

Of particular interest, analysis of the functional groups showed that a number of genes up-regulated in the PrE2.8 cells at 39°C, have been documented to play a role in cellular differentiation. The small proline-rich protein 1B and the calcium binding protein S100A8 (discussed in chapter 6) were up-regulated 16-fold and 8.7-fold, respectively. Both genes are located on chromosome 1q21 within a gene complex designated the "epidermal differentiation complex"; genes within this chromosomal region are up-regulated during differentiation of keratinocytes (Mischke et al., 1996). An additional gene showing over-expression was Drg-1 (differentiation-related gene 1), up-regulated 3.8-fold in the PrE2.8 cell line at 39°C. The gene has been mapped to chromosome 8q24.2 and encodes a cytoplasmic 43 kDa protein. Drg-1 was also identified as a reducing and tunicamycin-resoponsive gene (RTP) (Kokame et al., 1996); (Sato et al., 1998) as

well as an N-myc downstream-regulated gene 1 (NDRG1). van Belzen *et al* (1997) originally described Drg-1 to be expressed in normal colon cells at the terminal stage of differentiation, just preceding apoptosis and shedding of cells in the colon lumen (van Belzen et al., 1997). Drg-1 is expressed predominantly in epithelial cells and by most organ systems including the digestive tract, immune, reproductive, and urinary systems with the kidney, and in particular the prostate and ovary exhibiting the highest levels (Lachat et al., 2002). Although, cellular expression of Drg-1 has been found to be mainly cytoplasmic, a strong association with the plasma membrane has also been noted, predominantly adjacent to adherens junctions and desmosomes, whilst in other epithelia, such as the prostate, predominant nuclear staining has been detected. Also, in the prostate Drg-1 has been shown to be expressed mainly by luminal epithelial cells (Lachat et al., 2002), consistent with reports that this is a differentiation-related gene. Furthermore, over-expression of Drg-1 has been reported in a variety of cancers, including prostate, breast, lung, brain, liver and renal cancers (Cangul et al., 2002). However, the exact biological function of Drg-1 remains obscure and further studies of its expression in normal and aberrant prostate epithelial cell differentiation will help elucidate its role in differentiation and as a marker of this process.

The up-regulation of differentiation-related genes in the PrE2.8 cell line was accompanied by a concomitant decrease in genes involved in DNA replication and repair. Genes involved in chromatin assembly were down-regulated including the histones H2A, H2B and H1D. Similarly, and consistent with DNA repair being most active in rapidly proliferating cells, DNA repair genes, such as DNA repair protein MSH2. Genes with a role in DNA synthesis and replication included DNA primase polypeptide 1 and replication protein A.

An additional functional category that showed significant enrichment at 39°C in the PrE2.8 cell model were genes involved in maintaining cell structure and cytoskeleton. Genes up-regulated included keratin 19 and keratin 10. This is consistent with observations that in the epidermis, keratin 10 expression is associated with the loss of proliferative capacity and the onset of terminal differentiation (Kartasova et al., 1992). In addition, keratin 19 has been implicated in the differentiation of a number of epithelial cell types, such as oral epithelium and mammary gland ducts (Stasiak et al., 1989). In the prostate, (Hudson et al.,

2001) identified a sub-population of keratin 14-negative basal epithelial cells which expressed keratin 19 and continued expression into the luminal layer. It was therefore postulated that keratin 19 may be a potential marker for the amplifying non-stem-cell basal population. Genes active in extracellular matrix (ECM) formation were also up-regulated. Differentiating epithelium must adhere to the newly synthesized basal lamina, components of the ECM, in order to establish polarity (Streuli, 1999). Interactions between epithelial cells and the ECM are crucial for biological processes such as cell migration, proliferation and differentiation. In line with this, microarray analysis revealed the up-regulation of tissue inhibitor of matrix metalloproteinase 3 (TIMP-3), integrin beta-4 subunit and laminin 5β3 in the PrE2.8 cells at 39°C. TIMP-3 binds to the ECM and it has also been reported to initiate apoptosis. In addition, laminin 5-mediated activation of α3β1 integrins has been reported as a key step in the differentiation process of colon epithelial cells (Gout et al., 2001). These results suggest that increased expression of ECM-associated genes is a feature of prostate epithelial cell differentiation.

The study of normal prostate epithelial cell differentiation has been hindered by a lack of model systems. However, the PrE2.8 cell line may provide a suitable and highly informative alternative for such studies. Furthermore, organization of the microarray data into functional groups enabled changes in biological processes to be more clearly visualized. This approach revealed that prostate epithelial cell differentiation is likely a highly organized and complex process. Elucidating the role of the signal transduction molecules and transcription factors triggering such events may reveal the pathways driving these reprogramming events. The challenge of future studies will be to dissect the contribution of these individual pathways and their interaction to the overall maturation program.

6 EXPRESSION OF S100A8 IN PRE2.8 CELLS AND PROSTATE TISSUE

6.1 Introduction

The S100 proteins comprise a family of 20 low molecular weight (9-13 kDa) proteins that share a common structure defined in part by the Ca^{2+}-binding EF-hand motif. Thirteen S100 proteins (S100A2-A4, S100A6-A12, S100A15, S100B and S100P) are located within the epidermal differentiation complex, on human chromosome 1q21, so called due to the involvement of genes in this region in the differentiation of basal keratinocytes (Mischke et al., 1996). Within cells, most S100 proteins exist as homodimers, however, some form heterodimers, as is the case with the S100A1/S100B, S100A8/S100A9, S100B/S100A6, S100A1/S100A4 and the S100B/S100A11 dimers (Deloulme et al., 2000; Hunter and Chazin, 1998; Isobe et al., 1981; Propper et al., 1999; Tarabykina et al., 2000; Wang et al., 2000; Yang et al., 1999a). Upon calcium binding, they interact with target proteins to regulate cell function.

The S100 proteins are expressed in a discriminate fashion in specific cells and tissues, and act intracellularly as Ca2+-signalling or Ca2+-buffering proteins. However, the most unusual characteristic of certain S100 proteins is their occurrence in the extracellular space. Several S100 proteins, such as S100B, S100A4, S100A8, S100A9, S100A12 and S100A13, are secreted and act in a cytokine-like manner. For example, the S100A8/A9 heterodimer acts as a chemotactic molecule in inflammation (Newton and Hogg, 1998), S100B exhibits neurotrophic activity (Huttunen et al., 2000) and S100A4 has angiogenic effects (Ambartsumian et al., 2001). A multiligand receptor mediating the extracellular activities of S100 proteins was recently identified; S100B binds to the extracellular domain of the receptor for advanced glycation end products (RAGE)

and activates different intracellular signalling pathways, including MAP-kinase or NFκB (Arumugam et al., 2004; Hoffmann et al., 1999; Hsieh et al., 2003; Sorci et al., 2003). In addition to Ca2+, many S100 proteins display high affinities towards Zn^{2+} and Cu^{2+} ions, which could influence their activity in the extracellular space.

Whilst the exact functions of the S100 protein family remain to be characterised, these proteins have been implicated in a number of processes such as the immune response, differentiation, cytoskeleton dynamics, enzyme activity, Ca2+ homeostasis, growth and cancer. Observations of alterations in S100 protein expression both within primary and metastatic disease are suggestive of a potential marker of diagnostic and prognostic outcome (Diederichs et al., 2004).

Expression of S100A8 and S100A9 has been observed in neutrophils, activated macrophages and endothelial cells, in the epidermis, particularly in the course of psoriasis, and also in malignant disorders as well as in inflammatory brain diseases and Alzheimer's disease (Akiyama et al., 1994; Kerkhoff et al., 1998; Passey et al., 1999; Postler et al., 1997). The S100A8/ S100A9 complex has been found in sera from patients with cystic fibrosis, rheumatoid arthritis, and chronic bronchitis as well as at sites of acute inflammation (Kerkhoff et al., 1998; Passey et al., 1999). During the inflammatory process, the S100A8/S100A9 heterodimer may be involved in leukocyte trafficking through the transport of arachidonic acid to target cells (Kerkhoff et al., 1999).

S100A8 and S100A9 expression has also been reported in monocytes during the early stages of differentiation (Lagasse and Clerc, 1988) and in infiltrating monocytes, but not in resident tissue macrophages (Zwadlo et al., 1988). This suggests that the expression of S100A8 and S100A9 and the formation of the S100A8/S100A9 complex are related to a definite functional stage of macrophages and participate in the inflammatory response. In addition, deletion of the S100A8 gene results in embryo resorption by day 9.5 post-coitum in 100% of homozygous null embryos (Passey et al., 1999). These observations indicate that S100A8 has a role in the prevention of maternal rejection of the implanting embryo, and also of protecting the embryo from immune attack by maternal cells.

Microarray analysis of gene expression levels in the PrE2.8 conditionally immortalised cell line revealed that the calcium binding protein S100A8 was over-expressed 16-fold at 39°C, when the cells appear to undergo changes

consistent with differentiation, compared with 33°C when the cells are predominantly proliferating. The small proline-rich protein 1B (SPR1B) was also over-expressed by the PrE2.8 cells (8.7-fold). However, due to the lack of availability of an antibody targeting SPR1B, we chose to concentrate on further investigating the gene and protein expression levels of S100A8 in the PrE2.8 cell line, as well as its distribution in human prostate tissue.

6.2 Results

6.2.1 Expression of S100A8 in PrE2.8 cells

Microarray analysis of gene expression in the PrE2.8 cell line revealed that the small proline–rich protein 1B (SPR1B) and the Ca^{2+}-binding protein S100A8 were significantly over-expressed in cells cultured at 39°C compared with 33°C. The differences in S100A8 and SPR1B gene expression levels were confirmed by semi-quantitative RT-PCR. PrE2.8 cells were incubated at growth temperatures of either 33°C or 39°C for periods of up to 4, 7, 10 or 14 days; RNA was then extracted at the time points indicated. Following reverse transcription of total RNA isolated from the PrE2.8 cells, the amplified PCR products were electrophoresed on a 1.5% agarose gel as shown in Figure 6-1. PCR products revealed bands corresponding to S100A8 and SPR1B, respectively, expressed at 39°C. In comparison, very weak or no expression was observed in PrE2.8 cells cultured at 33°C throughout the time-course whereas strongly elevated levels of S100A8 and SPR1B gene expression were observed at 39°C at all time points examined i.e. 4-14 days. In light of these observations, S100A8 expression in both the PrE2.8 cells and in prostate tissue was further examined.

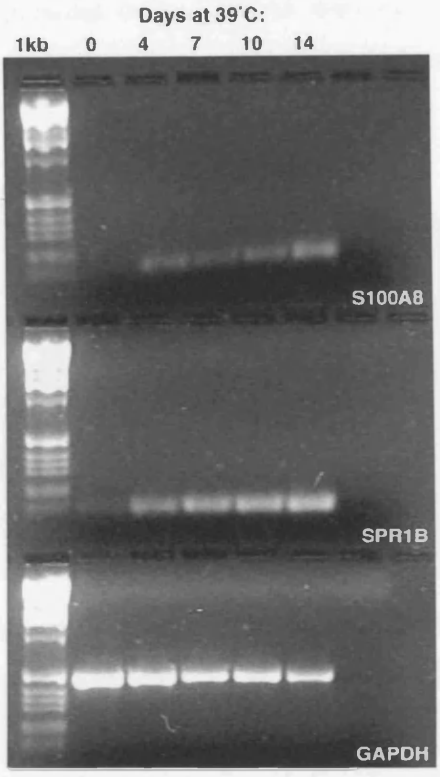

Figure 6-1: RT PCR analysis of S100A8 and SPR1B in PrE2.8 cells.

RT PCR was performed using 25-35 cycles on reverse transcribed mRNA from PrE2.8 cells incubated at 33°C or 39°C after 4, 7, 10 and 14 days of culture. PCR products were resolved on a 1.5% agarose gel. Amplifications are shown for S100A8 and SPR1B. GAPDH was used as a control.

6.2.2 S100A8 protein expression in PrE2.8 cells

Immunohistochemistry was used to investigate the protein expression and distribution of S100A8 in PrE2.8 cells. At 33°C, when the PrE2.8 cells are mainly proliferating, very weak or no expression of S100A8 was observed. However, when the cells were switched to the non-permissive temperature of 39°C, cytoplasmic staining of S100A8 protein was observed in 100% of PrE2.8 cells (Figure 6-2), indicating that S100A8 may be involved in the differentiation process of human prostate epithelial cells. It is well documented that S100A8 and S100A9 exist as a heterodimer in many cell types. The expression of the S100A8/S100A9 complex was therefore also investigated in the PrE2.8 cells. However, at both the permissive (33°C) and non-permissive temperature (39°C), no S100A8/S100A9 expression was detected in these cells. The absence of positive staining towards the S100A8/S100A9 complex may be due to the fact

that in human prostate epithelial cells, S100A8 does not form a heterodimer complex with S100A9, or that the latter protein is not expressed at all in human prostate epithelial cells.

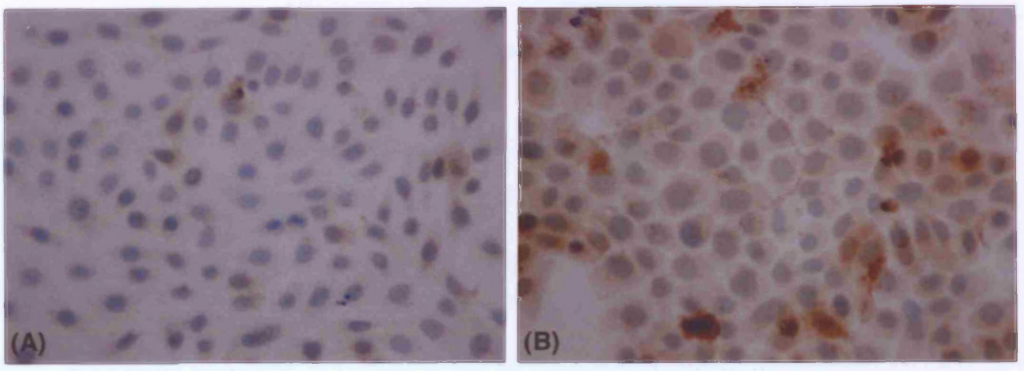

Figure 6-2: Immunocytochemistry of S100A8 protein in PrE2.8 cells.

S100A8 protein was detected in the PrE2.8 cell line using immunocytochemistry. Cells were incubated at 33°C or 39°C for 4 days. S100A8 protein was weakly expressed in a small number of cells at 33°C (A) whereas moderate to strong positive staining (brown) was observed in almost all cells at 39°C (B).

S100A8 protein expression was further investigated in the PrE2.8 cells using Western blot analysis. Cell extracts of PrE2.8 cells were cultured at 33°C or 39°C for periods of up to 4, 7, 10 or 14 days were resolved on SDS-PAGE gels, transferred to Immobilin P membrane and probed with anti-S100A8 antibody. Equal amounts of protein (estimated to be 30 μg) were loaded in all lanes. Under the conditions employed in this study, a band that would signify the presence of S100A8 protein was not apparent in extracts of the PrE2.8 cells cultured at 33°C, thus agreeing with the above observations of little or no gene expression under these conditions. However, in PrE2.8 cells cultured at 39°C protein expression levels increased progressively in a time-related fashion resulting ultimately in the observation that protein extracts obtained following 14-day culture exhibited the most abundant S100A8 levels, as indicated by the 8 kDa band (Figure 6-3).

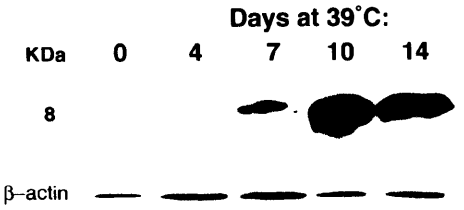

Figure 6-3: S100A8 protein expression in PrE2.8 cells.

Western blotting analysis of S100A8 protein in PrE2.8 cells grown at 33°C and 39°C. No protein expression is detected at 33°C or 39°C at day 4. However, by day 7, S100A8 is strongly expressed, with days 10 and 14 showing the most abundant expression. β-actin was used as a control.

6.2.3 S100A8 protein expression in prostate tissue

Paraffin embedded samples were obtained from patients undergoing transurethral resection of the prostate. Eight BPH samples and seven from patients suffering from prostate cancer were stained for S100A8 and the sections were analysed for staining distribution. Examples are shown in Figure 6-4 and Figure 6-5. All the BPH and benign regions of cancer samples analysed in this study were observed to exhibit some positive staining for S100A8. A staining pattern whereby protein expression appeared to be restricted to the secretory luminal cells of the prostate gland was apparent (Figure 6-4, A). This was further characterised by the observation that the strongest expression occurred at the outer luminal tips of the luminal cells (Figure 6-4, B). From these observations in these tissue samples, one could surmise that the intracellular protein is packaged into vesicles prior to being secreted into the glandular lumen. In support of this idea are the observations of a very dense S100A8 staining pattern in the lumen of several acini (Figure 6-4, B, C). This suggests that the S100A8 protein is secreted into the lumen of the prostate gland. Although positive staining was observed in luminal cells, the basal cells and stroma of the corresponding prostate tissues were consistently negative for S100A8 protein.

S100A8 protein expression was significantly reduced in the tumour samples examined with the majority of tissues being negative for S100A8. However, occasional positive staining was observed in a small number of epithelial cells (Figure 6-5, (a)). Interestingly, despite negative staining in tumours, strong positive staining was observed in cells of blood vessels within cancerous areas as

well as in occasional cells within the tumour region, which may represent infiltrating monocytes. These observations are consistent with reports of S100A8 and S100A9 expression in infiltrating monocytes, but not in resident tissue macrophages (Zwadlo et al., 1988).

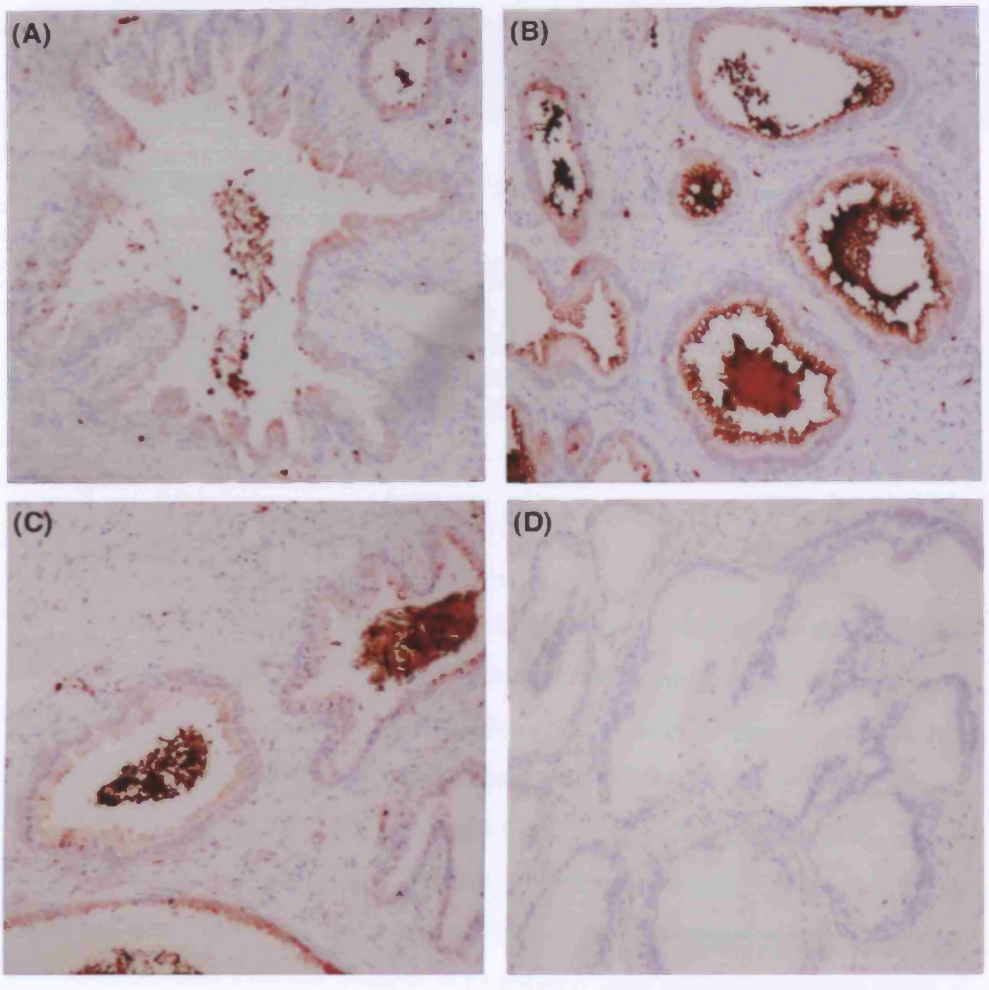

Figure 6-4: Immunocytochemistry of S100A8 protein in prostate tissue.

Paraffin-embedded prostate tissue from patients with BPH was stained for S100A8 protein. Positive staining is shown in brown. Cytoplasmic staining was observed which was restricted to the luminal cells (A). Expression was most abundant in the outer luminal tips of the luminal cells (B). A dense staining pattern was also observed in the lumen of several acini (B, C). D shows the negative control.

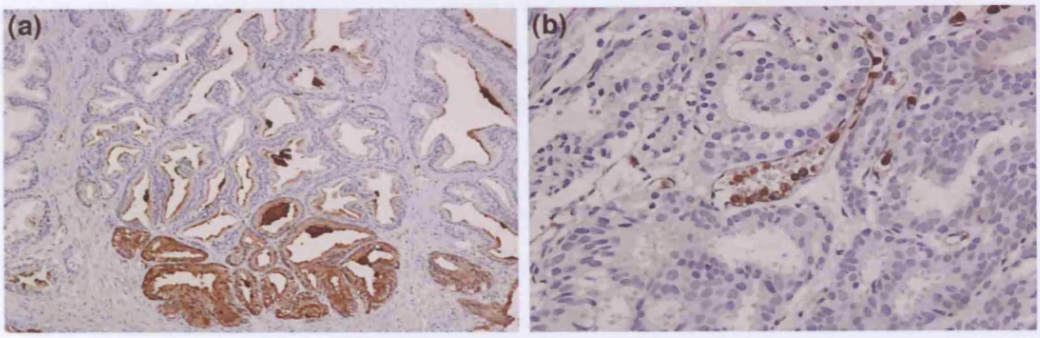

Figure 6-5: Immunocytochemistry of S100A8 protein in prostate tumour tissue.

Paraffin-embedded prostate tumour tissue was stained for S100A8 protein. Positive staining is shown in brown. The majority of tumour samples were negative for S100A8. However, occasional staining was observed a small number of glands (a). In addition, S100A8 protein was detected in cells within blood vessels as well as in occasional cells within tumours (b).

6.3 Discussion

The distribution and expression levels of the calcium binding protein S100A8 in the PrE2.8 cell line and in human prostate tissue were investigated. Microarray analysis and RT-PCR revealed that S100A8 is expressed at very low levels in the PrE2.8 cells at the proliferative temperature of 33°C. However, at 39°C, when the PrE2.8 cells appear to be undergoing changes consistent with cellular differentiation, S100A8 gene expression is elevated 16-fold. This was further characterised at the protein level where immunohistochemical analysis demonstrated that S100A8 protein is expressed very weakly or not at all in the majority of PrE2.8 cells at 33°C; at 39°C, all PrE2.8 cells strongly express S100A8 protein. Consistent with the immunohistological findings, immunoblot detection of S100A8 revealed minimal expression at 33°C, but elevated expression was observed in the PrE2.8 cells at 39°C cultured over the time course of 4-14 days. These results are suggestive of a role of S100A8 during the process of human prostate epithelial cell differentiation.

The presence of S100A8 within the cluster of genes known as the epidermal differentiation complex on chromosome 1q21, further supports this hypothesis. This Chromosomal band consists of three gene families involved in terminal differentiation of the human epidermis. They encode precursor proteins of the

cornified cell envelope, including SPR1B, intermediate filament-associated proteins and thirteen members of the S100 family (Mischke et al., 1996). SPR1B belongs to a family of small proline-rich (SPR) proteins consisting of two SPR1 genes (SPR1A and –1B), seven SPR2 genes (SPR2A to –2F) and one SPR3 gene, all located on chromosome 1q21 within the epidermal differentiation complex (Mischke *et al* , 1999). In this study, SPR1B was over-expressed 8.7-fold by the PrE2.8 cells at 39°C. The SPR genes are cross-bridging, structural proteins involved in the cornification of the cell envelope, a structure synthesized at late stages of keratinocyte differentiation, of stratified squamous epithelia (Cabral et al., 2001; Steinert, 1998). Despite few reports in the literature regarding the expression and possible functions of SPR1B, expression has also been reported in non-squamous cells such as mammary epithelium (Anisowicz et al., 1999), Chinese hamster ovary (Tesfaigzi and Carlson, 1996) and smooth muscle cells (Koizumi et al., 1996), suggestive of a role other than cell cornification. For example, in the breast, SPR1B is expressed in normal epithelium but expression is down-regulated or inactivated in breast tumours. Interestingly, SPR1B expression in breast tumours could be re-activated by phorbol 12-myristate 13-acetate (PMA) or UV irradiation via a transcriptional mechanism, suggesting SPR1B and its downstream targets may be useful for therapeutic manipulation in these cancers (Anisowicz et al., 1999).

The expression and possible functions of the S100 proteins have been more extensively studied. For example, in normal epidermis, S100A8 and S100A9 have been reported to be expressed at low levels, however in psoriatic tissue, both proteins are expressed at high levels (Broome et al., 2003). Also, in the psoratic epidermis, both proteins are expressed at the plasma membrane, consistent with the idea that some S100 proteins may be secreted (Katz and Taichman, 1999). The expression pattern of S100A8 in BPH tissue samples in this study showed the protein is restricted to the luminal cells of the prostate epithelium, with the strongest expression being observed at the tips of the luminal cells. This suggests that the intracellular protein may be packaged into vesicles prior to being secreted into the glandular lumen. In support of this idea are the observations of a very dense S100A8 staining pattern in the lumen of several acini. This further suggests that the S100A8 protein is secreted into the lumen of the prostate gland. This is

consistent with reports that several S100 proteins, including S100A8, are secreted into the extracellular space where they have further effects on target proteins (Marenholz et al., 2004). For example, in the form of an S100A8/S100A9 complex, the protein propagates inflammation and enhances CD11b expression in human monocytes through the targeting of arachidonic acid to inflammatory cells. The non-oxidised S100A8 homodimer has been reported as a potent chemotactic agent for leukocytes by binding to heparan sulphate glycosaminoglycans on endothelial cells. The extracellular S1000A8/S100A9 heterodimer has also been reported to inhibit immature monomyelocytic HL-60 cell proliferation and mitogen-stimulated lymphocyte proliferation, and to have cytostatic activity towards bacteria and fungi (Donato, 2003).

Several members of the S100 family have also been implicated to play a role in certain tumour types. For example, S100A4 expression has been reported in several cancers such as breast (Nikitenko et al., 2000), lung, (Takenaga et al., 1997), gastric (Yonemura et al., 2000), medulloblastoma (Hernan et al., 2003), prostate (Gupta et al., 2003) and bladder (Davies et al., 2002). More specifically, S100A4 has been suggested to play a role in tumour invasion. This hypothesis is supported by studies in which inhibition of the S100A4 gene by antisense RNA in a highly metastatic cell line, resulted in a decrease in cell motility and invasiveness in vitro (Takenaga et al., 1997). S100A4 is thought to exert its tumour-promoting activity through the inhibition of p53 (Grigorian et al., 2001). S100A7 has also been found to be expressed in tumours such as squamous cell carcinoma (Alowami et al., 2003), melanoma (Brouard et al., 2002), gastric cancer (El-Rifai et al., 2002) and breast cancer (Enerback et al., 2002). In breast cancer, S100A7 is predominantly expressed in the pre-invasive component of primary breast cancer (Enerback et al., 2002) and is one of the most abundantly expressed genes in ductal carcinoma in situ (Leygue et al., 1996). Furthermore, the S100A7 protein product has been found to be nuclear and cytoplasmic as well as being secreted in breast tumours (Al-Haddad et al., 1999). S100A2 on the other hand is typically down-regulated in carcinomas compared with normal tissues. This expression profile has been observed in breast (Ilg et al., 1996), prostate (Gupta et al., 2003) and lung tumours (Feng et al., 2001). It has therefore been hypothesized that S100A2 may be a tumour suppressor and down-regulation of the gene is thought to occur primarily via hypermethylation of the promoter at

CpG sites (Wicki et al., 1997). Interestingly, re-expression of S100A2 in head and neck squamous cell carcinoma lines was reported to exert an inhibitory influence on cell motility, possibly via an effect on the polymerisation/depolymerisation dynamics of the actin microfilamentary cytoskeleton (Nagy et al., 2001).

However, there is sparse information with regards to the role of S100A8 and cancer. Nonetheless, recent reports indicate that S100A8 and S100A9 are over-expressed in gastric cancer (El-Rifai et al., 2002), skin carcinogenesis (Gebhardt et al., 2002) and at the invasive margin of colorectal carcinoma (Stulik et al., 1999). It remains to be elucidated whether S100A8, or indeed SPR1B, may also play a role, not only in normal epithelial differentiation in the prostate, but also in the aberrant differentiation observed in prostate carcinoma.

7 DISCUSSION

7.1 Summary

The identification of markers that would point to the early development and progression of invasive adenocarcinoma of the prostate remains an important challenge. This project set out to identify markers associated with the early steps in prostate epithelial cell differentiation using the PrE2.8 cell line as a model system. Such markers might improve the understanding of the aetiology of BPH and prostate cancer. It is believed that in most tissues or organs, stem cells are a rare sub-population of the total cells. Stem cells possess a much greater capacity for proliferation than other cells, give rise to other cell types within that tissue and are responsible for maintaining regenerative capacity. There is also a hypothesis that either aberrant stem cells or cells that acquire stem-cell-like characteristics, give rise to cancer (Al-Hajj and Clarke, 2004; Fiala, 1968; Reya et al., 2001). However, changes occurring in cells and signalling pathways further along the differentiation process could also give rise to BPH and/or prostate cancer. This study has identified a number of genes that are associated with epithelial cell differentiation. These genes may provide valuable targets for future therapies aimed at inhibiting aberrant cellular proliferation and inducing cellular differentiation.

7.2 The use of cell lines in prostate disease research

Immortalised cell lines represent a valuable tool in scientific research and possess advantages when compared to the use of primary cells. Primary prostate cells are limited in their lifespan and display characteristics that may differ from batch to batch based on differing genotype and/or phenotype due to their different original donors. Although the important need to examine and elucidate mechanisms in real cells is unquestioned, one is also reliant on a continuous supply of fresh tissues. Overcoming such limitations would require that enormous numbers of tissue samples need to be obtained from large cohorts of individuals. This approach

would be required to overcome the problems of limited primary-cell lifespan and inter-individual variation. These limitations would in all probability make the identification of underlying biological mechanism(s) much more difficult to ascertain and/or delineate. Some of these limitations can be overcome by the use of immortalised cell lines since they exhibit an infinite capacity to proliferate in culture, allowing them to be well characterised. However, cell lines also have disadvantages. With increasing time in culture, such cells often acquire progressive changes due to an accumulation of genomic alterations. It is therefore necessary to monitor these changes and to use cell lines, where possible, within a number of passages to limit these changes.

From the mid-1970s, many groups have established immortalised prostate epithelial-cell lines. The most widely used prostate cancer cell lines PC3 (Kaighn et al., 1978), LNCaP (Horoszewicz et al., 1980) and DU145 (Stone *et al* , 1977) exhibit an advanced cancer phenotype and were all derived from metastases. In recent times, efforts have been made to develop a more representative cell model for experimental studies aimed towards understanding prostatic disease states, including the immortalisation of human prostate epithelial cells by expression of c-Myc (Gil et al., 2005). Although these newer cell lines provide useful tools for identifying genes that may play a role in carcinogenesis, many of these represent cells with either a secretory luminal or non-secretory intermediate luminal phenotype. The relevance of such a terminally differentiated phenotype to explore mechanisms of carcinogenesis may be questionable. Hitherto, appropriate *in vitro* cell models of prostate growth and differentiation that would allow for the identification of lineage-specific markers have not existed.

7.3 The PrE2.8 cell line as a model of differentiation

Derived from BPH tissue, the PrE2.8 epithelial-cell line was immortalised by transfection with a temperature-sensitive SV40 large T-antigen construct. Thus, at a permissive temperature of 33°C, these cells proliferate whereas at 39°C, the cells cease to proliferate and apparently undergo prostate epithelial-cell differentiation. Their growth characteristics have similarities to those of primary cultures in that at 33°C they appear as tightly-packed colonies while at 39°C, PrE2.8 cells become less dense and increase in size. Keratin-staining profiles have been used to

correlate such morphological changes with differentiation. The observation of a down-regulation of K14 compared to increases in the expression of cell differentiation-associated markers, including K8/K17/K19, $p21^{Waf1/Cip1}$ and PSCA in cells grown at the non-permissive temperature point to the usefulness of this cell line. The up-regulation of PSCA is of particular interest since it is a prostate-specific cell surface antigen and has been shown to be a marker of an intermediate sub-population of transit amplifying cells (Tran et al., 2002). This observation lends further support to the PrE2.8 cell line as a model system of the early stages of prostate epithelial cell differentiation. The lack of further prostate-specific differentiation markers in these cells, such as AR and PSA, is therefore not surprising since almost all tissue-specific differentiation markers are expressed in terminally differentiated cells. Thus, PrE2.8 cells provide a relatively reproducible tool to examine previously unidentified lineage-specific markers in cells isolated from prostate tissue itself. The objective of this project was to identify the differences in gene expression between PrE2.8 cells cultured at 33°C (a proliferative basal cell phenotype) and 39°C (a differentiated phenotype).

7.4 Expression analysis

Initial investigations used differential display to investigate differences in gene expression. This method was applied to RNA transcripts isolated from PrE2.8 cells cultured at either 33°C or 39°C. From a panel of 25 potential genes, three candidates were subsequently verified using semi-quantitative RT-PCR. Of these three candidate genes, two (calcium-binding protein S100A8 and small proline-rich protein 1B (SPR1B)) were up-regulated and one (cyclooxygenase-2 (COX-2)) was down-regulated in the PrE2.8 cells at 33°C. The genes encoding S100A8 and SPR1B are located on chromosome 1q21 in a region termed the epidermal differentiation complex (EDC) (Marenholz et al., 1996). Interestingly, both genes are up-regulated during differentiation of keratinocytes. On the other hand, COX-2 has been shown to be involved in the catalytic conversion of arachidonic acid to prostaglandins and is over-expressed in a variety of tumours including bladder, colorectal, breast and prostate cancers (Eltze et al., 2005; Kundu et al., 2001; Srinath et al., 2003; Wu et al., 2004). Whilst this candidate gene does not represent a novel marker of epithelial-cell differentiation, the observation that this

tumour progression-associated marker is down-regulated in the PrE2.8 differentiated phenotype, provides evidence supporting the concept that PrE2.8 cells differentiate at 39°C. Although differential display identified some candidate genes for further investigation, this method is limited by the high proportion of false positives that subsequently have to be eliminated using RT-PCR.

To identify additional markers of prostate epithelial cell differentiation, the more recently developed technology of microarray analysis was applied. Using this approach, several genes were found to be either up-regulated (n=47) or down-regulated (n=52) in this PrE2.8 model of cell differentiation. To facilitate mechanistic analysis, these genes were grouped according to function (Figure 5-9). Interestingly, several genes previously associated with cellular differentiation were identified to be up-regulated in the cells grown at 39°C, including S100A8 and SPR1B. In addition, the gene, Drg-1 (differentiation-related gene 1), originally described to be expressed in normal colon cells at the terminal stage of differentiation, just preceding apoptosis and shedding of cells in the colon lumen (van Belzen et al., 1997), was also up-regulated.

S100A8 and SPR1B are located on chromosome 1q21 in a region designated the EDC (Marenholz *et al* , 1996). This 2 Mb region consists of three gene families: the first family consists of thirteen genes, involucrin, loricrin and the three classes of small proline-rich (SPR) proteins comprising two SPR1 genes, eight SPR2 genes and one SPR3 gene. They encode structural proteins of the cornified cell envelope in the human epidermis (Eckert and Green, 1986; Gibbs et al., 1993; Kartasova et al., 1988; Yoneda et al., 1992), providing the skin with a protective barrier against dehydration and other environmental factors (Roop, 1995; Simon et al., 1994). The second gene family of the EDC consists of profilaggrin and trichohyalin. These genes encode intermediate filament-associated proteins that are synthesized in the granular layer of the epidermis and conjoin with the keratin filaments during cornification (Fietz et al., 1992; McKinley-Grant et al., 1989). The third gene family of the EDC consists of the S100 family of small calcium-binding proteins (Mischke et al., 1996). It was initially suggested that these genes are likely to be involved in signal transduction and cell cycle progression (Kligman and Hilt, 1988). Several functional roles for the S100A genes have since been proposed as discussed in Chapter 6. Interestingly, it has been shown that the S100A genes begin to be expressed at an

early stage of keratinocyte differentiation, while expression of the cornified precursors begins later in differentiation (Mischke, 1998). The expression of S100A8, and indeed SPR1B, in the PrE2.8 cells at 39°C suggests that members of the EDC may also be involved in the early stages of prostate epithelial cell differentiation. These observations lend further support for the PrE2.8 cells as a model for the study of early changes in gene expression during prostate epithelial cell differentiation. In addition, it has been suggested that due to the co-localisation of these functionally and structurally related genes in the EDC, and their co-ordinated expression during epidermal differentiation, these gene families may be subject to coordinated transcriptional control mechanism (Mischke, 1998; Zhao and Elder, 1997). Further investigation of the transcription factors identified in this study through microarray analysis, and their possible involvement in the control of S100A8 expression may shed light onto the pathways/mechanisms involved in prostate epithelial cell differentiation; these pathways may be deregulated during BPH and prostate cancer and represent an avenue of investigation into the initiation of these disease processes.

More recently, S100A8 and S100A9 have been shown to be up-regulated in prostate cancer (Hermani et al., 2005). The expression of S100A8 and A9 appeared to be significantly increased in adenocarcinoma compared with surrounding benign prostatic tissue, with increased expression of the S100 proteins in high-grade compared with low-grade tumours. In addition, positive staining of the S100 proteins was observed in prostatic intraepithelial neoplasias (Hermani et al., 2005). These findings are in contrast to the present study however, where, as shown in Chapter 6, the expression of S100A8 was markedly reduced in the prostate cancer specimens examined compared with benign prostatic tissue, and S100A9 was not detected. Hermani *et al* (2005) also observed expression of S100A8 and A9 in basal cells of benign prostate tissue and in luminal cells of adenocarcinoma. Again, this is in contrast to the present study (Chapter 6) where positive S100A8 staining was seen in the luminal cells of benign prostatic epithelium. These discrepancies, however, may be due to the fact that different antibodies were used in both studies; re-examination of the expression pattern of S100A8 and A9 using a panel of anti-S100A8/A9 antibodies will need to be carried out in order to resolve such discrepancies. Interestingly, Hermani *et al* (2005) found significantly increased concentrations of S100A9 in

the serum of cancer patients compared with the serum of patients with BPH and healthy individuals, suggesting that this protein may also represent a novel marker for the diagnosis of prostate cancer. It is intriguing that S100A8 was not detected, particularly in light of observations in the present study that suggest that S100A8 may also be secreted into the serum. The intense staining patterns of S100A8 in secretory luminal cells, in particular, in the outer luminal tips, together with a very dense S100A8 staining pattern in the lumen of several acini, suggest that S100A8 may also be secreted. Examination of S100A8 in the serum of healthy subjects compared with that of patients with BPH and prostate cancer could, if shown, represent an additional prognostic/diagnostic marker.

In this study, a candidate gene approach was also employed in order to further investigate the PrE2.8 cell line as a model of prostate epithelial cell differentiation. Among the genes investigated, CD44 revealed an intriguing pattern of gene expression in the PrE2.8 cells. Depending on whether the proliferative or non-proliferative phenotype was being examined, an interesting pattern of alternatively spliced isoforms was observed. CD44 expression was therefore further investigated in this model system.

CD44 is a transmembrane glycoprotein that is widely expressed in virtually all cell types. It functions as an extracellular matrix receptor and is involved in cell-cell and cell-matrix interactions. CD44 may also participate in growth regulation by presenting growth factors to their cell surface receptors (Lesley et al., 1993). The CD44 protein is encoded by a single gene that consists of 20 exons, located on chromosome 11p13. However, through extensive alternative splicing of exons 6–14 (also referred to as exons v2-v10), the extracellular membrane domain is highly variable, producing multiple protein isoforms that are expressed in a tissue-specific manner (Screaton et al., 1992; Tolg et al., 1993). It was found that an alternatively spliced CD44 v2-v10 isoform was expressed specifically in a subset of basal cells, many of which were negative for keratin 14, a marker for the least differentiated basal cells. This v5-containing isoform was also observed in epithelial cells that are situated just above the basal layer and below the luminal layer. This observation is suggestive that the v5-positive cells may be in the process of differentiation from the basal to the luminal layer. It has previously been shown that this cell type also stains positive for keratin 19. It has been postulated that these cells represent an epithelial cell population in the

process of differentiation from the stem cell compartment to the terminally differentiated luminal cell layer (Hudson et al., 2001). Further investigation of the CD44 v2-v10 isoform in a larger panel of prostate tissue, normal as well as cancer, will reveal whether this variant is specifically expressed in normal prostate epithelial cell differentiation. More importantly, the CD44 v2-v10 isoform represents a putative marker of the transit amplifying (TA) population of prostate epithelial cells and as it is expressed at the cell surface, represents a valuable tool for the isolation and separation of TA cells from stem cells and fully differentiated luminal cells.

7.5 Further work

The discoveries uncovered in this project have revealed a number of avenues to be further investigated in order to evaluate putative genes, and pathways, involved in the control of human prostate epithelial cell differentiation. Microarray analysis revealed a number of genes up-regulated in the PrE2.8 cell line at 39°C when the cells appear to undergo changes consistent with early differentiation. Further investigation of these gene families in prostate tissue will give a better insight into the sequence of events controlling the differentiation process. The arrays used in this study contained 5,603 IMAGE cDNA clones. However, repeating these experiments using arrays with a greater number of targets, such as Affymetrix GeneChip arrays, which contain ≥60, 000 transcripts, would provide a more in depth analysis of the changes in gene expression occurring in the PrE2.8 cells at 39°C. An additional point to note is that the present study investigated gene expression in PrE2.8 cells grown at 39°C for a period of 4 days. A time-course experiment, where RNA is extracted from cells grown at 39°C from day 1 to day 14, would provide information on genes and regulatory pathways that are up- or down-regulated early on in this model system, as well as changes in gene expression further along the time course/differentiation process. These genes, if validated through confirmation of protein expression in prostate tissue, could potentially provide markers of subpopulations of epithelial cells at different stages of the differentiation process in the prostate.

Cell surface markers, such as the CD44 v2-v10 isoform identified in this study, would be of particular value as tools to isolate subpopulations of cells

along the differentiation pathway. This would allow these subpopulations to be characterised further. For example, growing these cells in culture to investigate whether they can undergo terminal differentiation, thus confirming their progenitor cell status. In addition, subpopulations of isolated cells believed to be at the very early stages of the differentiation pathway could be further characterised in xenograft experiments. For example, such subpopulations could be grown as xenografts in mice, together with stromal cells, in order to investigate whether these cells are able to differentiate further, or even regenerate into a prostate gland.

Other genes identified in this study and/or future studies may shed light on the mechanisms driving the differentiation pathway. Manipulation of these genes and/or pathways will also provide valuable information about the differentiation process, both in normal and diseased prostate. For example, these genes may represent potential targets for the development of new drugs for the treatment of proliferation-related prostate epithelial-cell disorders. The PrE2.8 cell line could be used as an initial screening assay to verify these gene targets; compounds that may block/inhibit genes involved in the normal pathway of differentiation may be useful as potential drugs for the treatment of BPH/prostate cancer, if those same genes are involved in these diseases. In addition, over-expression of putative genes in cell lines would be of interest in order to evaluate the function of these genes and potentially identify genes that are crucial to the differentiation process.

Additional studies that could be carried out include *in vivo* gene knockout experiments. Key genes identified through microarray analysis and verified in prostate tissue could be deleted in mouse models. This would be a valuable method of evaluating the consequences of such deletions on the differentiation process in prostate epithelial cells as well as on the development and functioning of the prostate gland. Finally, the delineation of a central underlying pathway in differentiation might result in the development of targets for intervention or prevention of prostatic disease states.

8 REFERENCES

Abrahamsson, P. A. (1996). Neuroendocrine differentiation and hormone-refractory prostate cancer. Prostate Suppl *6*, 3-8.

Akiyama, T. H., Sasagawa, T., Suzuki, M., and Titani, K. (1994). A method for selective isolation of the amino-terminal peptide from alpha-amino-blocked proteins. Anal Biochem *222*, 210-216.

Al-Haddad, S., Zhang, Z., Leygue, E., Snell, L., Huang, A., Niu, Y., Hiller-Hitchcock, T., Hole, K., Murphy, L. C., and Watson, P. H. (1999). Psoriasin (S100A7) expression and invasive breast cancer. Am J Pathol *155*, 2057-2066.

Al-Hajj, M., and Clarke, M. F. (2004). Self-renewal and solid tumor stem cells. Oncogene *23*, 7274-7282.

Alam, T. N., O'Hare, M. J., Laczko, I., Freeman, A., Al-Beidh, F., Masters, J. R., and Hudson, D. L. (2004). Differential expression of CD44 during human prostate epithelial cell differentiation. J Histochem Cytochem *52*, 1083-1090.

Alowami, S., Qing, G., Emberley, E., Snell, L., and Watson, P. H. (2003). Psoriasin (S100A7) expression is altered during skin tumorigenesis. BMC Dermatol *3*, 1.

Alvi, A. J., Clayton, H., Joshi, C., Enver, T., Ashworth, A., Vivanco, M. M., Dale, T. C., and Smalley, M. J. (2003). Functional and molecular characterisation of mammary side population cells. Breast Cancer Res *5*, R1-8.

Ambartsumian, N., Klingelhofer, J., Grigorian, M., Christensen, C., Kriajevska, M., Tulchinsky, E., Georgiev, G., Berezin, V., Bock, E., Rygaard, J., *et al.* (2001). The metastasis-associated Mts1(S100A4) protein could act as an angiogenic factor. Oncogene *20*, 4685-4695.

Anisowicz, A., Sotiropoulou, G., and Sager, R. (1999). Re-expression of SPR1 in breast cancer cells by phorbol 12-myristate 13-acetate (PMA) or UV irradiation is mediated by the AP-1 binding site in the SPR1 promoter. Mol Med *5*, 526-541.

Arumugam, T., Simeone, D. M., Schmidt, A. M., and Logsdon, C. D. (2004). S100P stimulates cell proliferation and survival via receptor for activated glycation end products (RAGE). J Biol Chem *279*, 5059-5065.

Aumuller, G., Seitz, J., and Bischof, W. (1983). Immunohistochemical study on the initiation of acid phosphatase secretion in the human prostate. Cytochemistry and biochemistry of acid phosphatases IV. J Androl *4*, 183-191.

Aumuller, G., Seitz, J., Lilja, H., Abrahamsson, P. A., von der Kammer, H., and Scheit, K. H. (1990). Species- and organ-specificity of secretory proteins derived from human prostate and seminal vesicles. Prostate *17*, 31-40.

Baum, C. M., Weissman, I. L., Tsukamoto, A. S., Buckle, A. M., and Peault, B. (1992). Isolation of a candidate human hematopoietic stem-cell population. Proc Natl Acad Sci U S A *89*, 2804-2808.

Bello, D., Webber, M. M., Kleinman, H. K., Wartinger, D. D., and Rhim, J. S. (1997). Androgen responsive adult human prostatic epithelial cell lines immortalized by human papillomavirus 18. Carcinogenesis *18*, 1215-1223.

Bentvelsen, F. M., Brinkmann, A. O., van der Schoot, P., van der Linden, J. E., van der Kwast, T. H., Boersma, W. J., Schroder, F. H., and Nijman, J. M. (1995). Developmental pattern and regulation by androgens of androgen receptor expression in the urogenital tract of the rat. Mol Cell Endocrinol *113*, 245-253.

Biagini, G., Preda, P., Lo Cigno, M., Soli, M., and Bercovich, E. (1982). Ultrastructural aspects of human prostate in benign prostatic hyperplasia. Prostate *3*, 99-108.

Bjerknes, M., and Cheng, H. (1999). Clonal analysis of mouse intestinal epithelial progenitors. Gastroenterology *116*, 7-14.

Bonkhoff, H. (1996). Role of the basal cells in premalignant changes of the human prostate: a stem cell concept for the development of prostate cancer. Eur Urol *30*, 201-205.

Bonkhoff, H., and Remberger, K. (1993). Widespread distribution of nuclear androgen receptors in the basal cell layer of the normal and hyperplastic human prostate. Virchows Arch A Pathol Anat Histopathol *422*, 35-38.

Bonkhoff, H., and Remberger, K. (1996). Differentiation pathways and histogenetic aspects of normal and abnormal prostatic growth: a stem cell model. Prostate *28*, 98-106.

Bonkhoff, H., Stein, U., and Remberger, K. (1994a). Multidirectional differentiation in the normal, hyperplastic, and neoplastic human prostate: simultaneous demonstration of cell-specific epithelial markers. Hum Pathol *25*, 42-46.

Bonkhoff, H., Stein, U., and Remberger, K. (1994b). The proliferative function of basal cells in the normal and hyperplastic human prostate. Prostate *24*, 114-118.

Bosch, F. X., Leube, R. E., Achtstatter, T., Moll, R., and Franke, W. W. (1988). Expression of simple epithelial type cytokeratins in stratified epithelia as detected by immunolocalization and hybridization in situ. J Cell Biol *106*, 1635-1648.

Bright, R. K., Vocke, C. D., Emmert-Buck, M. R., Duray, P. H., Solomon, D., Fetsch, P., Rhim, J. S., Linehan, W. M., and Topalian, S. L. (1997). Generation and genetic characterization of immortal human prostate epithelial cell lines derived from primary cancer specimens. Cancer Res *57*, 995-1002.

Broome, A. M., Ryan, D., and Eckert, R. L. (2003). S100 protein subcellular localization during epidermal differentiation and psoriasis. J Histochem Cytochem *51*, 675-685.

Brothman, A. R., Lesho, L. J., Somers, K. D., Wright, G. L., Jr., and Merchant, D. J. (1989). Phenotypic and cytogenetic characterization of a cell line derived from primary prostatic carcinoma. Int J Cancer *44*, 898-903.

Brouard, M. C., Saurat, J. H., Ghanem, G., and Siegenthaler, G. (2002). Urinary excretion of epidermal-type fatty acid-binding protein and S100A7 protein in patients with cutaneous melanoma. Melanoma Res *12*, 627-631.

Brown, T. A., Bouchard, T., St John, T., Wayner, E., and Carter, W. G. (1991). Human keratinocytes express a new CD44 core protein (CD44E) as a heparan-sulfate intrinsic membrane proteoglycan with additional exons. J Cell Biol *113*, 207-221.

Bryan, T. M., and Reddel, R. R. (1994). SV40-induced immortalization of human cells. Crit Rev Oncog *5*, 331-357.

Cabral, A., Voskamp, P., Cleton-Jansen, A. M., South, A., Nizetic, D., and Backendorf, C. (2001). Structural organization and regulation of the small proline-rich family of cornified envelope precursors suggest a role in adaptive barrier function. J Biol Chem *276*, 19231-19237.

Cangul, H., Salnikow, K., Yee, H., Zagzag, D., Commes, T., and Costa, M. (2002). Enhanced overexpression of an HIF-1/hypoxia-related protein in cancer cells. Environ Health Perspect *110 Suppl 5*, 783-788.

Casini, T., and Pelicci, P. G. (1999). A function of p21 during promyelocytic leukemia cell differentiation independent of CDK inhibition and cell cycle arrest. Oncogene *18*, 3235-3243.

Cheng, H., and Leblond, C. P. (1974). Origin, differentiation and renewal of the four main epithelial cell types in the mouse small intestine. V. Unitarian Theory of the origin of the four epithelial cell types. Am J Anat *141*, 537-561.

Clegg, C. H., Linkhart, T. A., Olwin, B. B., and Hauschka, S. D. (1987). Growth factor control of skeletal muscle differentiation: commitment to terminal differentiation occurs in G1 phase and is repressed by fibroblast growth factor. J Cell Biol *105*, 949-956.

Collins, A. T., Habib, F. K., Maitland, N. J., and Neal, D. E. (2001). Identification and isolation of human prostate epithelial stem cells based on alpha(2)beta(1)-integrin expression. J Cell Sci *114*, 3865-3872.

Cox, W. F., Jr., and Pierce, G. B. (1982). The endodermal origin of the endocrine cells of an adenocarcinoma of the colon of the rat. Cancer *50*, 1530-1538.

Cunha, G. R. (1994). Role of mesenchymal-epithelial interactions in normal and abnormal development of the mammary gland and prostate. Cancer *74*, 1030-1044.

Cunha, G. R., Fujii, H., Neubauer, B. L., Shannon, J. M., Sawyer, L., and Reese, B. A. (1983). Epithelial-mesenchymal interactions in prostatic development. I. morphological observations of prostatic induction by urogenital sinus mesenchyme in epithelium of the adult rodent urinary bladder. J Cell Biol *96*, 1662-1670.

Cunha, G. R., Reese, B. A., and Sekkingstad, M. (1980). Induction of nuclear androgen-binding sites in epithelium of the embryonic urinary bladder by mesenchyme of the urogenital sinus of embryonic mice. Endocrinology *107*, 1767-1770.

Cussenot, O., Berthon, P., Berger, R., Mowszowicz, I., Faille, A., Hojman, F., Teillac, P., Le Duc, A., and Calvo, F. (1991). Immortalization of human adult normal prostatic epithelial cells by liposomes containing large T-SV40 gene. J Urol *146*, 881-886.

Daniel, C. W., and Young, L. J. (1971). Influence of cell division on an aging process. Life span of mouse mammary epithelium during serial propagation in vivo. Exp Cell Res *65*, 27-32.

Davies, B. R., O'Donnell, M., Durkan, G. C., Rudland, P. S., Barraclough, R., Neal, D. E., and Mellon, J. K. (2002). Expression of S100A4 protein is associated with metastasis and reduced survival in human bladder cancer. J Pathol *196*, 292-299.

de Lange, T. (1994). Activation of telomerase in a human tumor. Proc Natl Acad Sci U S A *91*, 2882-2885.

Deloulme, J. C., Assard, N., Mbele, G. O., Mangin, C., Kuwano, R., and Baudier, J. (2000). S100A6 and S100A11 are specific targets of the calcium- and zinc-binding S100B protein in vivo. J Biol Chem *275*, 35302-35310.

Di Cunto, F., Topley, G., Calautti, E., Hsiao, J., Ong, L., Seth, P. K., and Dotto, G. P. (1998). Inhibitory function of p21Cip1/WAF1 in differentiation of primary mouse keratinocytes independent of cell cycle control. Science *280*, 1069-1072.

di Sant'Agnese, P. A. (1992). Neuroendocrine differentiation in human prostatic carcinoma. Hum Pathol *23*, 287-296.

Diederichs, S., Bulk, E., Steffen, B., Ji, P., Tickenbrock, L., Lang, K., Zanker, K. S., Metzger, R., Schneider, P. M., Gerke, V., *et al.* (2004). S100 family members and trypsinogens are predictors of distant metastasis and survival in early-stage non-small cell lung cancer. Cancer Res *64*, 5564-5569.

Donato, R. (2003). Intracellular and extracellular roles of S100 proteins. Microsc Res Tech *60*, 540-551.

Dontu, G., Abdallah, W. M., Foley, J. M., Jackson, K. W., Clarke, M. F., Kawamura, M. J., and Wicha, M. S. (2003a). In vitro propagation and transcriptional profiling of human mammary stem/progenitor cells. Genes Dev *17*, 1253-1270.

Dontu, G., Al-Hajj, M., Abdallah, W. M., Clarke, M. F., and Wicha, M. S. (2003b). Stem cells in normal breast development and breast cancer. Cell Prolif *36 Suppl 1*, 59-72.

Eckert, R. L., and Green, H. (1986). Structure and evolution of the human involucrin gene. Cell *46*, 583-589.

el-Deiry, W. S., Tokino, T., Velculescu, V. E., Levy, D. B., Parsons, R., Trent, J. M., Lin, D., Mercer, W. E., Kinzler, K. W., and Vogelstein, B. (1993). WAF1, a potential mediator of p53 tumor suppression. Cell *75*, 817-825.

el-Deiry, W. S., Tokino, T., Waldman, T., Oliner, J. D., Velculescu, V. E., Burrell, M., Hill, D. E., Healy, E., Rees, J. L., Hamilton, S. R., and et al. (1995). Topological control of p21WAF1/CIP1 expression in normal and neoplastic tissues. Cancer Res *55*, 2910-2919.

El-Rifai, W., Moskaluk, C. A., Abdrabbo, M. K., Harper, J., Yoshida, C., Riggins, G. J., Frierson, H. F., Jr., and Powell, S. M. (2002). Gastric cancers overexpress S100A calcium-binding proteins. Cancer Res *62*, 6823-6826.

Eltze, E., Wulfing, C., Von Struensee, D., Piechota, H., Buerger, H., and Hertle, L. (2005). Cox-2 and Her2/neu co-expression in invasive bladder cancer. Int J Oncol *26*, 1525-1531.

Enerback, C., Porter, D. A., Seth, P., Sgroi, D., Gaudet, J., Weremowicz, S., Morton, C. C., Schnitt, S., Pitts, R. L., Stampl, J., *et al.* (2002). Psoriasin expression in mammary epithelial cells in vitro and in vivo. Cancer Res *62*, 43-47.

English, H. F., Santen, R. J., and Isaacs, J. T. (1987). Response of glandular versus basal rat ventral prostatic epithelial cells to androgen withdrawal and replacement. Prostate *11*, 229-242.

Evans, G. S., and Chandler, J. A. (1987). Cell proliferation studies in the rat prostate: II. The effects of castration and androgen-induced regeneration upon basal and secretory cell proliferation. Prostate *11*, 339-351.

Feng, G., Xu, X., Youssef, E. M., and Lotan, R. (2001). Diminished expression of S100A2, a putative tumor suppressor, at early stage of human lung carcinogenesis. Cancer Res *61*, 7999-8004.

Fiala, S. (1968). The cancer cell as a stem cell unable to differentiate. A theory of carcinogenesis. Neoplasma *15*, 607-622.

Fietz, M. J., Rogers, G. E., Eyre, H. J., Baker, E., Callen, D. F., and Sutherland, G. R. (1992). Mapping of the trichohyalin gene: co-localization with the profilaggrin, involucrin, and loricrin genes. J Invest Dermatol *99*, 542-544.

Fonseca, I., Moura Nunes, J. F., and Soares, J. (2000). Expression of CD44 isoforms in normal salivary gland tissue: an immunohistochemical and ultrastructural study. Histochem Cell Biol *114*, 483-488.

Fuchs, E. (1988). Keratins as biochemical markers of epithelial differentiation. Trends Genet *4*, 277-281.

Fuchs, E., and Cleveland, D. W. (1998). A structural scaffolding of intermediate filaments in health and disease. Science *279*, 514-519.

Fuchs, E., and Green, H. (1980). Changes in keratin gene expression during terminal differentiation of the keratinocyte. Cell *19*, 1033-1042.

Galvin, S., Loomis, C., Manabe, M., Dhouailly, D., and Sun, T. T. (1989). The major pathways of keratinocyte differentiation as defined by keratin expression: an overview. Adv Dermatol *4*, 277-299; discussion 300.

Gartel, A. L., Serfas, M. S., Gartel, M., Goufman, E., Wu, G. S., el-Deiry, W. S., and Tyner, A. L. (1996). p21 (WAF1/CIP1) expression is induced in newly nondividing cells in diverse epithelia and during differentiation of the Caco-2 intestinal cell line. Exp Cell Res *227*, 171-181.

Gebhardt, C., Breitenbach, U., Tuckermann, J. P., Dittrich, B. T., Richter, K. H., and Angel, P. (2002). Calgranulins S100A8 and S100A9 are negatively regulated by glucocorticoids in a c-Fos-dependent manner and overexpressed throughout skin carcinogenesis. Oncogene *21*, 4266-4276.

Gibbs, S., Fijneman, R., Wiegant, J., van Kessel, A. G., van De Putte, P., and Backendorf, C. (1993). Molecular characterization and evolution of the SPRR family of keratinocyte differentiation markers encoding small proline-rich proteins. Genomics *16*, 630-637.

Gil, J., Kerai, P., Lleonart, M., Bernard, D., Cigudosa, J. C., Peters, G., Carnero, A., and Beach, D. (2005). Immortalization of primary human prostate epithelial cells by c-Myc. Cancer Res *65*, 2179-2185.

Goodell, M. A., Brose, K., Paradis, G., Conner, A. S., and Mulligan, R. C. (1996). Isolation and functional properties of murine hematopoietic stem cells that are replicating in vivo. J Exp Med *183*, 1797-1806.

Goodrich, D. W., Wang, N. P., Qian, Y. W., Lee, E. Y., and Lee, W. H. (1991). The retinoblastoma gene product regulates progression through the G1 phase of the cell cycle. Cell *67*, 293-302.

Googe, P. B., McGinley, K. M., and Fitzgibbon, J. F. (1997). Anticytokeratin antibody 34 beta E12 staining in prostate carcinoma. Am J Clin Pathol *107*, 219-223.

Gout, S. P., Jacquier-Sarlin, M. R., Rouard-Talbot, L., Rousselle, P., and Block, M. R. (2001). RhoA-dependent switch between alpha2beta1 and alpha3beta1 integrins is induced by laminin-5 during early stage of HT-29 cell differentiation. Mol Biol Cell *12*, 3268-3281.

Grigorian, M., Andresen, S., Tulchinsky, E., Kriajevska, M., Carlberg, C., Kruse, C., Cohn, M., Ambartsumian, N., Christensen, A., Selivanova, G., and Lukanidin, E. (2001). Tumor suppressor p53 protein is a new target for the metastasis-

associated Mts1/S100A4 protein: functional consequences of their interaction. J Biol Chem *276*, 22699-22708.

Gudjonsson, T., Villadsen, R., Nielsen, H. L., Ronnov-Jessen, L., Bissell, M. J., and Petersen, O. W. (2002). Isolation, immortalization, and characterization of a human breast epithelial cell line with stem cell properties. Genes Dev *16*, 693-706.

Gunsilius, E., Gastl, G., and Petzer, A. L. (2001). Hematopoietic stem cells. Biomed Pharmacother *55*, 186-194.

Gunthert, U., Hofmann, M., Rudy, W., Reber, S., Zoller, M., Haussmann, I., Matzku, S., Wenzel, A., Ponta, H., and Herrlich, P. (1991). A new variant of glycoprotein CD44 confers metastatic potential to rat carcinoma cells. Cell *65*, 13-24.

Gupta, S., Hussain, T., MacLennan, G. T., Fu, P., Patel, J., and Mukhtar, H. (2003). Differential expression of S100A2 and S100A4 during progression of human prostate adenocarcinoma. J Clin Oncol *21*, 106-112.

Hanukoglu, I., and Fuchs, E. (1982). The cDNA sequence of a human epidermal keratin: divergence of sequence but conservation of structure among intermediate filament proteins. Cell *31*, 243-252.

Harper, J. W., Adami, G. R., Wei, N., Keyomarsi, K., and Elledge, S. J. (1993). The p21 Cdk-interacting protein Cip1 is a potent inhibitor of G1 cyclin-dependent kinases. Cell *75*, 805-816.

Hayward, S. W., Dahiya, R., Cunha, G. R., Bartek, J., Deshpande, N., and Narayan, P. (1995). Establishment and characterization of an immortalized but non-transformed human prostate epithelial cell line: BPH-1. In Vitro Cell Dev Biol Anim *31*, 14-24.

Heider, K. H., Dammrich, J., Skroch-Angel, P., Muller-Hermelink, H. K., Vollmers, H. P., Herrlich, P., and Ponta, H. (1993a). Differential expression of CD44 splice variants in intestinal- and diffuse-type human gastric carcinomas and normal gastric mucosa. Cancer Res *53*, 4197-4203.

Heider, K. H., Hofmann, M., Hors, E., van den Berg, F., Ponta, H., Herrlich, P., and Pals, S. T. (1993b). A human homologue of the rat metastasis-associated variant of CD44 is expressed in colorectal carcinomas and adenomatous polyps. J Cell Biol *120*, 227-233.

Heider, K. H., Mulder, J. W., Ostermann, E., Susani, S., Patzelt, E., Pals, S. T., and Adolf, G. R. (1995). Splice variants of the cell surface glycoprotein CD44 associated with metastatic tumour cells are expressed in normal tissues of humans and cynomolgus monkeys. Eur J Cancer *31A*, 2385-2391.

Hermani, A., Hess, J., De Servi, B., Medunjanin, S., Grobholz, R., Trojan, L., Angel, P., and Mayer, D. (2005). Calcium-binding proteins S100A8 and S100A9

as novel diagnostic markers in human prostate cancer. Clin Cancer Res *11*, 5146-5152.

Hernan, R., Fasheh, R., Calabrese, C., Frank, A. J., Maclean, K. H., Allard, D., Barraclough, R., and Gilbertson, R. J. (2003). ERBB2 up-regulates S100A4 and several other prometastatic genes in medulloblastoma. Cancer Res *63*, 140-148.

Hertle, M. D., Jones, P. H., Groves, R. W., Hudson, D. L., and Watt, F. M. (1995). Integrin expression by human epidermal keratinocytes can be modulated by interferon-gamma, transforming growth factor-beta, tumor necrosis factor-alpha, and culture on a dermal equivalent. J Invest Dermatol *104*, 260-265.

Hoffmann, H. J., Olsen, E., Etzerodt, M., Madsen, P., Thogersen, H. C., Kruse, T., and Celis, J. E. (1994). Psoriasin binds calcium and is upregulated by calcium to levels that resemble those observed in normal skin. J Invest Dermatol *103*, 370-375.

Hoffmann, R., Baillie, G. S., MacKenzie, S. J., Yarwood, S. J., and Houslay, M. D. (1999). The MAP kinase ERK2 inhibits the cyclic AMP-specific phosphodiesterase HSPDE4D3 by phosphorylating it at Ser579. Embo J *18*, 893-903.

Horoszewicz, J. S., Leong, S. S., Chu, T. M., Wajsman, Z. L., Friedman, M., Papsidero, L., Kim, U., Chai, L. S., Kakati, S., Arya, S. K., and Sandberg, A. A. (1980). The LNCaP cell line--a new model for studies on human prostatic carcinoma. Prog Clin Biol Res *37*, 115-132.

Hsieh, H. L., Schafer, B. W., Sasaki, N., and Heizmann, C. W. (2003). Expression analysis of S100 proteins and RAGE in human tumors using tissue microarrays. Biochem Biophys Res Commun *307*, 375-381.

Hudson, D. L., Guy, A. T., Fry, P., O'Hare, M. J., Watt, F. M., and Masters, J. R. (2001). Epithelial cell differentiation pathways in the human prostate: identification of intermediate phenotypes by keratin expression. J Histochem Cytochem *49*, 271-278.

Hudson, D. L., O'Hare, M., Watt, F. M., and Masters, J. R. (2000). Proliferative heterogeneity in the human prostate: evidence for epithelial stem cells. Lab Invest *80*, 1243-1250.

Hudson, D. L., Sleeman, J., and Watt, F. M. (1995). CD44 is the major peanut lectin-binding glycoprotein of human epidermal keratinocytes and plays a role in intercellular adhesion. J Cell Sci *108 (Pt 5)*, 1959-1970.

Hudson, D. L., Speight, P. M., and Watt, F. M. (1996). Altered expression of CD44 isoforms in squamous-cell carcinomas and cell lines derived from them. Int J Cancer *66*, 457-463.

Hunter, M. J., and Chazin, W. J. (1998). High level expression and dimer characterization of the S100 EF-hand proteins, migration inhibitory factor-related proteins 8 and 14. J Biol Chem *273*, 12427-12435.

Huttunen, H. J., Kuja-Panula, J., Sorci, G., Agneletti, A. L., Donato, R., and Rauvala, H. (2000). Coregulation of neurite outgrowth and cell survival by amphoterin and S100 proteins through receptor for advanced glycation end products (RAGE) activation. J Biol Chem *275*, 40096-40105.

Iczkowski, K. A., Bai, S., and Pantazis, C. G. (2003). Prostate cancer overexpresses CD44 variants 7-9 at the messenger RNA and protein level. Anticancer Res *23*, 3129-3140.

Ide, T., Tsuji, Y., Ishibashi, S., Mitsui, Y., and Toba, M. (1984). Induction of host DNA synthesis in senescent human diploid fibroblasts by infection with human cytomegalovirus. Mech Ageing Dev *25*, 227-235.

Iizumi, T., Yazaki, T., Kanoh, S., Kondo, I., and Koiso, K. (1987). Establishment of a new prostatic carcinoma cell line (TSU-Pr1). J Urol *137*, 1304-1306.

Ilg, E. C., Schafer, B. W., and Heizmann, C. W. (1996). Expression pattern of S100 calcium-binding proteins in human tumors. Int J Cancer *68*, 325-332.

Isaacs, J. T., and Coffey, D. S. (1989). Etiology and disease process of benign prostatic hyperplasia. Prostate Suppl *2*, 33-50.

Isaacs, W. B. (1984). Structural and functional components in normal and hyperplastic canine prostates. Prog Clin Biol Res *145*, 307-331.

Isobe, T., Ishioka, N., and Okuyama, T. (1981). Structural relation of two S-100 proteins in bovine brain; subunit composition of S-100a protein. Eur J Biochem *115*, 469-474.

Iype, P. T., Iype, L. E., Verma, M., and Kaighn, M. E. (1998). Establishment and characterization of immortalized human cell lines from prostatic carcinoma and benign prostatic hyperplasia. Int J Oncol *12*, 257-263.

Jat, P. S., Noble, M. D., Ataliotis, P., Tanaka, Y., Yannoutsos, N., Larsen, L., and Kioussis, D. (1991). Direct derivation of conditionally immortal cell lines from an H-2Kb-tsA58 transgenic mouse. Proc Natl Acad Sci U S A *88*, 5096-5100.

Jat, P. S., and Sharp, P. A. (1989). Cell lines established by a temperature-sensitive simian virus 40 large-T-antigen gene are growth restricted at the nonpermissive temperature. Mol Cell Biol *9*, 1672-1681.

Kaighn, M. E. (1980). Human prostatic epithelial cell culture models. Invest Urol *17*, 382-385.

Kaighn, M. E., Lechner, J. F., Narayan, K. S., and Jones, L. W. (1978). Prostate carcinoma: tissue culture cell lines. Natl Cancer Inst Monogr, 17-21.

Kaighn, M. E., Reddel, R. R., Lechner, J. F., Peehl, D. M., Camalier, R. F., Brash, D. E., Saffiotti, U., and Harris, C. C. (1989). Transformation of human neonatal prostate epithelial cells by strontium phosphate transfection with a plasmid containing SV40 early region genes. Cancer Res *49*, 3050-3056.

Kallakury, B. V., Sheehan, C. E., Ambros, R. A., Fisher, H. A., Kaufman, R. P., Jr., Muraca, P. J., and Ross, J. S. (1998). Correlation of p34cdc2 cyclin-dependent kinase overexpression, CD44s downregulation, and HER-2/neu oncogene amplification with recurrence in prostatic adenocarcinomas. J Clin Oncol *16*, 1302-1309.

Kaneko, Y., Sakakibara, S., Imai, T., Suzuki, A., Nakamura, Y., Sawamoto, K., Ogawa, Y., Toyama, Y., Miyata, T., and Okano, H. (2000). Musashi1: an evolutionally conserved marker for CNS progenitor cells including neural stem cells. Dev Neurosci *22*, 139-153.

Kartasova, T., Roop, D. R., and Yuspa, S. H. (1992). Relationship between the expression of differentiation-specific keratins 1 and 10 and cell proliferation in epidermal tumors. Mol Carcinog *6*, 18-25.

Kartasova, T., van Muijen, G. N., van Pelt-Heerschap, H., and van de Putte, P. (1988). Novel protein in human epidermal keratinocytes: regulation of expression during differentiation. Mol Cell Biol *8*, 2204-2210.

Katz, A. B., and Taichman, L. B. (1999). A partial catalog of proteins secreted by epidermal keratinocytes in culture. J Invest Dermatol *112*, 818-821.

Kerkhoff, C., Klempt, M., Kaever, V., and Sorg, C. (1999). The two calcium-binding proteins, S100A8 and S100A9, are involved in the metabolism of arachidonic acid in human neutrophils. J Biol Chem *274*, 32672-32679.

Kerkhoff, C., Klempt, M., and Sorg, C. (1998). Novel insights into structure and function of MRP8 (S100A8) and MRP14 (S100A9). Biochim Biophys Acta *1448*, 200-211.

Kerr, M. K., Martin, M., and Churchill, G. A. (2000). Analysis of variance for gene expression microarray data. J Comput Biol *7*, 819-837.

Kim, N. W., Piatyszek, M. A., Prowse, K. R., Harley, C. B., West, M. D., Ho, P. L., Coviello, G. M., Wright, W. E., Weinrich, S. L., and Shay, J. W. (1994). Specific association of human telomerase activity with immortal cells and cancer. Science *266*, 2011-2015.

Kim, S. H., Banga, S., Jha, K. K., and Ozer, H. L. (1998). SV40-mediated transformation and immortalization of human cells. Dev Biol Stand *94*, 297-302.

Kim, T. E., Lee, H. S., Lee, Y. B., Hong, S. H., Lee, Y. S., Ichinose, H., Kim, S. U., and Lee, M. A. (2003). Sonic hedgehog and FGF8 collaborate to induce dopaminergic phenotypes in the Nurr1-overexpressing neural stem cell. Biochem Biophys Res Commun *305*, 1040-1048.

Kinbara, H., Cunha, G. R., Boutin, E., Hayashi, N., and Kawamura, J. (1996). Evidence of stem cells in the adult prostatic epithelium based upon responsiveness to mesenchymal inductors. Prostate *29*, 107-116.

Kligman, D., and Hilt, D. C. (1988). The S100 protein family. Trends Biochem Sci *13*, 437-443.

Koizumi, H., Kartasova, T., Tanaka, H., Ohkawara, A., and Kuroki, T. (1996). Differentiation-associated localization of small proline-rich protein in normal and diseased human skin. Br J Dermatol *134*, 686-692.

Kokame, K., Kato, H., and Miyata, T. (1996). Homocysteine-respondent genes in vascular endothelial cells identified by differential display analysis. GRP78/BiP and novel genes. J Biol Chem *271*, 29659-29665.

Kolquist, K. A., Ellisen, L. W., Counter, C. M., Meyerson, M., Tan, L. K., Weinberg, R. A., Haber, D. A., and Gerald, W. L. (1998). Expression of TERT in early premalignant lesions and a subset of cells in normal tissues. Nat Genet *19*, 182-186.

Kundu, N., Yang, Q., Dorsey, R., and Fulton, A. M. (2001). Increased cyclooxygenase-2 (cox-2) expression and activity in a murine model of metastatic breast cancer. Int J Cancer *93*, 681-686.

Kyprianou, N., and Isaacs, J. T. (1988). Activation of programmed cell death in the rat ventral prostate after castration. Endocrinology *122*, 552-562.

Lachat, P., Shaw, P., Gebhard, S., van Belzen, N., Chaubert, P., and Bosman, F. T. (2002). Expression of NDRG1, a differentiation-related gene, in human tissues. Histochem Cell Biol *118*, 399-408.

Laczko, I., Hudson, D. L., Freeman, A., Feneley, M. R., and Masters, J. R. (2005). Comparison of the zones of the human prostate with the seminal vesicle: morphology, immunohistochemistry, and cell kinetics. Prostate *62*, 260-266.

Lagasse, E., and Clerc, R. G. (1988). Cloning and expression of two human genes encoding calcium-binding proteins that are regulated during myeloid differentiation. Mol Cell Biol *8*, 2402-2410.

Lako, M., Lindsay, S., Lincoln, J., Cairns, P. M., Armstrong, L., and Hole, N. (2001). Characterisation of Wnt gene expression during the differentiation of murine embryonic stem cells in vitro: role of Wnt3 in enhancing haematopoietic differentiation. Mech Dev *103*, 49-59.

Lane, E. B., and Alexander, C. M. (1990). Use of keratin antibodies in tumor diagnosis. Semin Cancer Biol *1*, 165-179.

Lansdorp, P. M. (1995). Telomere length and proliferation potential of hematopoietic stem cells. J Cell Sci *108 (Pt 1)*, 1-6.

Lechner, J. F., Narayan, K. S., Ohnuki, Y., Babcock, M. S., Jones, L. W., and Kaighn, M. E. (1978). Replicative epithelial cell cultures from normal human prostate gland. J Natl Cancer Inst *60*, 797-801.

Lee, S. W., Tomasetto, C., Swisshelm, K., Keyomarsi, K., and Sager, R. (1992). Down-regulation of a member of the S100 gene family in mammary carcinoma cells and reexpression by azadeoxycytidine treatment. Proc Natl Acad Sci U S A *89*, 2504-2508.

Lesley, J., Hyman, R., and Kincade, P. W. (1993). CD44 and its interaction with extracellular matrix. Adv Immunol *54*, 271-335.

Levine, A. J. (1997). p53, the cellular gatekeeper for growth and division. Cell *88*, 323-331.

Leygue, E., Snell, L., Hiller, T., Dotzlaw, H., Hole, K., Murphy, L. C., and Watson, P. H. (1996). Differential expression of psoriasin messenger RNA between in situ and invasive human breast carcinoma. Cancer Res *56*, 4606-4609.

Li, F., Barnathan, E. S., and Kariko, K. (1994a). Rapid method for screening and cloning cDNAs generated in differential mRNA display: application of northern blot for affinity capturing of cDNAs. Nucleic Acids Res *22*, 1764-1765.

Li, R., Waga, S., Hannon, G. J., Beach, D., and Stillman, B. (1994b). Differential effects by the p21 CDK inhibitor on PCNA-dependent DNA replication and repair. Nature *371*, 534-537.

Liang, P., and Pardee, A. B. (1992). Differential display of eukaryotic messenger RNA by means of the polymerase chain reaction. Science *257*, 967-971.

Liu, A. Y., True, L. D., LaTray, L., Ellis, W. J., Vessella, R. L., Lange, P. H., Higano, C. S., Hood, L., and van den Engh, G. (1999). Analysis and sorting of prostate cancer cell types by flow cytometry. Prostate *40*, 192-199.

Liu, A. Y., True, L. D., LaTray, L., Nelson, P. S., Ellis, W. J., Vessella, R. L., Lange, P. H., Hood, L., and van den Engh, G. (1997). Cell-cell interaction in prostate gene regulation and cytodifferentiation. Proc Natl Acad Sci U S A *94*, 10705-10710.

Loop, S. M., Rozanski, T. A., and Ostenson, R. C. (1993). Human primary prostate tumor cell line, ALVA-31: a new model for studying the hormonal regulation of prostate tumor cell growth. Prostate *22*, 93-108.

Lowell, S., Jones, P., Le Roux, I., Dunne, J., and Watt, F. M. (2000). Stimulation of human epidermal differentiation by delta-notch signalling at the boundaries of stem-cell clusters. Curr Biol *10*, 491-500.

Lu, P. J., Lu, Q. L., Rughetti, A., and Taylor-Papadimitriou, J. (1995). bcl-2 overexpression inhibits cell death and promotes the morphogenesis, but not tumorigenesis of human mammary epithelial cells. J Cell Biol *129*, 1363-1378.

Ludlow, J. W., DeCaprio, J. A., Huang, C. M., Lee, W. H., Paucha, E., and Livingston, D. M. (1989). SV40 large T antigen binds preferentially to an underphosphorylated member of the retinoblastoma susceptibility gene product family. Cell *56*, 57-65.

Lyle, S., Christofidou-Solomidou, M., Liu, Y., Elder, D. E., Albelda, S., and Cotsarelis, G. (1998). The C8/144B monoclonal antibody recognizes cytokeratin 15 and defines the location of human hair follicle stem cells. J Cell Sci *111 (Pt 21)*, 3179-3188.

Mackay, C. R., Terpe, H. J., Stauder, R., Marston, W. L., Stark, H., and Gunthert, U. (1994). Expression and modulation of CD44 variant isoforms in humans. J Cell Biol *124*, 71-82.

Marenholz, I., Heizmann, C. W., and Fritz, G. (2004). S100 proteins in mouse and man: from evolution to function and pathology (including an update of the nomenclature). Biochem Biophys Res Commun *322*, 1111-1122.

Marenholz, I., Volz, A., Ziegler, A., Davies, A., Ragoussis, I., Korge, B. P., and Mischke, D. (1996). Genetic analysis of the epidermal differentiation complex (EDC) on human chromosome 1q21: chromosomal orientation, new markers, and a 6-Mb YAC contig. Genomics *37*, 295-302.

Matsumura, Y., and Tarin, D. (1992). Significance of CD44 gene products for cancer diagnosis and disease evaluation. Lancet *340*, 1053-1058.

McDonnell, T. J., Troncoso, P., Brisbay, S. M., Logothetis, C., Chung, L. W., Hsieh, J. T., Tu, S. M., and Campbell, M. L. (1992). Expression of the protooncogene bcl-2 in the prostate and its association with emergence of androgen-independent prostate cancer. Cancer Res *52*, 6940-6944.

McKinley-Grant, L. J., Idler, W. W., Bernstein, I. A., Parry, D. A., Cannizzaro, L., Croce, C. M., Huebner, K., Lessin, S. R., and Steinert, P. M. (1989). Characterization of a cDNA clone encoding human filaggrin and localization of the gene to chromosome region 1q21. Proc Natl Acad Sci U S A *86*, 4848-4852.

McLean, W. H., and Lane, E. B. (1995). Intermediate filaments in disease. Curr Opin Cell Biol *7*, 118-125.

McNeal, J. E. (1980). Anatomy of the prostate: an historical survey of divergent views. Prostate *1*, 3-13.

McNeal, J. E. (1981a). Normal and pathologic anatomy of prostate. Urology *17*, 11-16.

McNeal, J. E. (1981b). The zonal anatomy of the prostate. Prostate *2*, 35-49.

McNeal, J. E. (1984). Anatomy of the prostate and morphogenesis of BPH. Prog Clin Biol Res *145*, 27-53.

McNeal, J. E. (1988). Normal anatomy of the prostate and changes in benign prostatic hypertrophy and carcinoma. Semin Ultrasound CT MR *9*, 329-334.

Meeker, A. K., Sommerfeld, H. J., and Coffey, D. S. (1996). Telomerase is activated in the prostate and seminal vesicles of the castrated rat. Endocrinology *137*, 5743-5746.

Michel, M., Torok, N., Godbout, M. J., Lussier, M., Gaudreau, P., Royal, A., and Germain, L. (1996). Keratin 19 as a biochemical marker of skin stem cells in vivo and in vitro: keratin 19 expressing cells are differentially localized in function of anatomic sites, and their number varies with donor age and culture stage. J Cell Sci *109 (Pt 5)*, 1017-1028.

Mischke, D. (1998). The complexity of gene families involved in epithelial differentiation. Keratin genes and the epidermal differentiation complex. Subcell Biochem *31*, 71-104.

Mischke, D., Korge, B. P., Marenholz, I., Volz, A., and Ziegler, A. (1996). Genes encoding structural proteins of epidermal cornification and S100 calcium-binding proteins form a gene complex ("epidermal differentiation complex") on human chromosome 1q21. J Invest Dermatol *106*, 989-992.

Moll, R., Franke, W. W., Volc-Platzer, B., and Krepler, R. (1982). Different keratin polypeptides in epidermis and other epithelia of human skin: a specific cytokeratin of molecular weight 46,000 in epithelia of the pilosebaceous tract and basal cell epitheliomas. J Cell Biol *95*, 285-295.

Morrison, S. J., Uchida, N., and Weissman, I. L. (1995). The biology of hematopoietic stem cells. Annu Rev Cell Dev Biol *11*, 35-71.

Morrison, S. J., and Weissman, I. L. (1994). The long-term repopulating subset of hematopoietic stem cells is deterministic and isolatable by phenotype. Immunity *1*, 661-673.

Muraki, J., Addonizio, J. C., Choudhury, M. S., Fischer, J., Eshghi, M., Davidian, M. M., Shapiro, L. R., Wilmot, P. L., Nagamatsu, G. R., and Chiao, J. W. (1990). Establishment of new human prostatic cancer cell line (JCA-1). Urology *36*, 79-84.

Nagabhushan, M., Pretlow, T. G., Guo, Y. J., Amini, S. B., Pretlow, T. P., and Sy, M. S. (1996). Altered expression of CD44 in human prostate cancer during progression. Am J Clin Pathol *106*, 647-651.

Nagle, R. B., Brawer, M. K., Kittelson, J., and Clark, V. (1991). Phenotypic relationships of prostatic intraepithelial neoplasia to invasive prostatic carcinoma. Am J Pathol *138*, 119-128.

Nagy, N., Brenner, C., Markadieu, N., Chaboteaux, C., Camby, I., Schafer, B. W., Pochet, R., Heizmann, C. W., Salmon, I., Kiss, R., and Decaestecker, C. (2001). S100A2, a putative tumor suppressor gene, regulates in vitro squamous cell carcinoma migration. Lab Invest *81*, 599-612.

Nakhla, A. M., and Rosner, W. (1994). Characterization of ALVA-41 cells, a new human prostatic cancer cell line. Steroids *59*, 586-589.

Narayan, P., and Dahiya, R. (1992). Establishment and characterization of a human primary prostatic adenocarcinoma cell line (ND-1). J Urol *148*, 1600-1604.

Nevins, J. R. (1998). Toward an understanding of the functional complexity of the E2F and retinoblastoma families. Cell Growth Differ *9*, 585-593.

Newton, R. A., and Hogg, N. (1998). The human S100 protein MRP-14 is a novel activator of the beta 2 integrin Mac-1 on neutrophils. J Immunol *160*, 1427-1435.

Nikitenko, L. L., Lloyd, B. H., Rudland, P. S., Fear, S., and Barraclough, R. (2000). Localisation by in situ hybridisation of S100A4 (p9Ka) mRNA in primary human breast tumour specimens. Int J Cancer *86*, 219-228.

Noda, A., Ning, Y., Venable, S. F., Pereira-Smith, O. M., and Smith, J. R. (1994). Cloning of senescent cell-derived inhibitors of DNA synthesis using an expression screen. Exp Cell Res *211*, 90-98.

Noordzij, M. A., van Steenbrugge, G. J., Schroder, F. H., and Van der Kwast, T. H. (1999). Decreased expression of CD44 in metastatic prostate cancer. Int J Cancer *84*, 478-483.

Noordzij, M. A., van Steenbrugge, G. J., Verkaik, N. S., Schroder, F. H., and van der Kwast, T. H. (1997). The prognostic value of CD44 isoforms in prostate cancer patients treated by radical prostatectomy. Clin Cancer Res *3*, 805-815.

Oshima, H., Rochat, A., Kedzia, C., Kobayashi, K., and Barrandon, Y. (2001). Morphogenesis and renewal of hair follicles from adult multipotent stem cells. Cell *104*, 233-245.

Parkin, D. M., Pisani, P., and Ferlay, J. (1999). Global cancer statistics. CA Cancer J Clin *49*, 33-64, 31.

Passey, R. J., Williams, E., Lichanska, A. M., Wells, C., Hu, S., Geczy, C. L., Little, M. H., and Hume, D. A. (1999). A null mutation in the inflammation-associated S100 protein S100A8 causes early resorption of the mouse embryo. J Immunol *163*, 2209-2216.

Pedrocchi, M., Schafer, B. W., Mueller, H., Eppenberger, U., and Heizmann, C. W. (1994). Expression of Ca(2+)-binding proteins of the S100 family in malignant human breast-cancer cell lines and biopsy samples. Int J Cancer *57*, 684-690.

Peehl, D. M., Sellers, R. G., and McNeal, J. E. (1996). Keratin 19 in the adult human prostate: tissue and cell culture studies. Cell Tissue Res *285*, 171-176.

Peehl, D. M., and Stamey, T. A. (1986). Serum-free growth of adult human prostatic epithelial cells. In Vitro Cell Dev Biol *22*, 82-90.

Peehl, D. M., Wong, S. T., and Stamey, T. A. (1988). Clonal growth characteristics of adult human prostatic epithelial cells. In Vitro Cell Dev Biol *24*, 530-536.

Pellegrini, G., Dellambra, E., Golisano, O., Martinelli, E., Fantozzi, I., Bondanza, S., Ponzin, D., McKeon, F., and De Luca, M. (2001). p63 identifies keratinocyte stem cells. Proc Natl Acad Sci U S A *98*, 3156-3161.

Ponten, F., Berne, B., Ren, Z. P., Nister, M., and Ponten, J. (1995). Ultraviolet light induces expression of p53 and p21 in human skin: effect of sunscreen and constitutive p21 expression in skin appendages. J Invest Dermatol *105*, 402-406.

Postler, E., Lehr, A., Schluesener, H., and Meyermann, R. (1997). Expression of the S-100 proteins MRP-8 and -14 in ischemic brain lesions. Glia *19*, 27-34.

Potten, C. S. (1981). Cell replacement in epidermis (keratopoiesis) via discrete units of proliferation. Int Rev Cytol *69*, 271-318.

Potten, C. S., Schofield, R., and Lajtha, L. G. (1979). A comparison of cell replacement in bone marrow, testis and three regions of surface epithelium. Biochim Biophys Acta *560*, 281-299.

Propper, C., Huang, X., Roth, J., Sorg, C., and Nacken, W. (1999). Analysis of the MRP8-MRP14 protein-protein interaction by the two-hybrid system suggests a prominent role of the C-terminal domain of S100 proteins in dimer formation. J Biol Chem *274*, 183-188.

Purkis, P. E., Steel, J. B., Mackenzie, I. C., Nathrath, W. B., Leigh, I. M., and Lane, E. B. (1990). Antibody markers of basal cells in complex epithelia. J Cell Sci *97 (Pt 1)*, 39-50.

Quackenbush, J. (2001). Computational analysis of microarray data. Nat Rev Genet *2*, 418-427.

Quesenberry, P. J., and Becker, P. S. (1998). Stem cell homing: rolling, crawling, and nesting. Proc Natl Acad Sci U S A *95*, 15155-15157.

Radna, R. L., Caton, Y., Jha, K. K., Kaplan, P., Li, G., Traganos, F., and Ozer, H. L. (1989). Growth of immortal simian virus 40 tsA-transformed human fibroblasts is temperature dependent. Mol Cell Biol *9*, 3093-3096.

Reese, J. H., McNeal, J. E., Redwine, E. A., Samloff, I. M., and Stamey, T. A. (1986). Differential distribution of pepsinogen II between the zones of the human prostate and the seminal vesicle. J Urol *136*, 1148-1152.

Reiter, R. E., Gu, Z., Watabe, T., Thomas, G., Szigeti, K., Davis, E., Wahl, M., Nisitani, S., Yamashiro, J., Le Beau, M. M., *et al.* (1998). Prostate stem cell antigen: a cell surface marker overexpressed in prostate cancer. Proc Natl Acad Sci U S A *95*, 1735-1740.

Reya, T., Morrison, S. J., Clarke, M. F., and Weissman, I. L. (2001). Stem cells, cancer, and cancer stem cells. Nature *414*, 105-111.

Robinson, E. J., Neal, D. E., and Collins, A. T. (1998). Basal cells are progenitors of luminal cells in primary cultures of differentiating human prostatic epithelium. Prostate *37*, 149-160.

Roop, D. (1995). Defects in the barrier. Science *267*, 474-475.

Sack, G. H., Jr. (1981). Human cell transformation by simian virus 40--a review. In Vitro *17*, 1-19.

Saintigny, G., Schmidt, R., Shroot, B., Juhlin, L., Reichert, U., and Michel, S. (1992). Differential expression of calgranulin A and B in various epithelial cell lines and reconstructed epidermis. J Invest Dermatol *99*, 639-644.

Sato, N., Kokame, K., Shimokado, K., Kato, H., and Miyata, T. (1998). Changes of gene expression by lysophosphatidylcholine in vascular endothelial cells: 12 up-regulated distinct genes including 5 cell growth-related, 3 thrombosis-related, and 4 others. J Biochem (Tokyo) *123*, 1119-1126.

Schafer, B. W., and Heizmann, C. W. (1996). The S100 family of EF-hand calcium-binding proteins: functions and pathology. Trends Biochem Sci *21*, 134-140.

Schwab, T. S., Stewart, T., Lehr, J., Pienta, K. J., Rhim, J. S., and Macoska, J. A. (2000). Phenotypic characterization of immortalized normal and primary tumor-derived human prostate epithelial cell cultures. Prostate *44*, 164-171.

Screaton, G. R., Bell, M. V., Bell, J. I., and Jackson, D. G. (1993). The identification of a new alternative exon with highly restricted tissue expression in transcripts encoding the mouse Pgp-1 (CD44) homing receptor. Comparison of all 10 variable exons between mouse, human, and rat. J Biol Chem *268*, 12235-12238.

Screaton, G. R., Bell, M. V., Jackson, D. G., Cornelis, F. B., Gerth, U., and Bell, J. I. (1992). Genomic structure of DNA encoding the lymphocyte homing receptor CD44 reveals at least 12 alternatively spliced exons. Proc Natl Acad Sci U S A *89*, 12160-12164.

Sherwood, E. R., Berg, L. A., Mitchell, N. J., McNeal, J. E., Kozlowski, J. M., and Lee, C. (1990). Differential cytokeratin expression in normal, hyperplastic and malignant epithelial cells from human prostate. J Urol *143*, 167-171.

Siminovitch, L., McCulloch, E. A., and Till, J. E. (1963). The Distribution of Colony-Forming Cells among Spleen Colonies. J Cell Physiol *62*, 327-336.

Simon, G. A., Schmid, P., Reifenrath, W. G., van Ravenswaay, T., and Stuck, B. E. (1994). Wound healing after laser injury to skin--the effect of occlusion and vitamin E. J Pharm Sci *83*, 1101-1106.

Sinowatz, F., Chandler, J. A., and Pierrepoint, C. G. (1977). Ultrastructural studies on the effect of testosterone, 5alpha-dihydrotestosterone, and 5alpha-androstand-3alpha,17alpha-diol on the canine prostate cultured in vitro. J Ultrastruct Res *60*, 1-11.

Skelton, T. P., Zeng, C., Nocks, A., and Stamenkovic, I. (1998). Glycosylation provides both stimulatory and inhibitory effects on cell surface and soluble CD44 binding to hyaluronan. J Cell Biol *140*, 431-446.

Small, M. B., Gluzman, Y., and Ozer, H. L. (1982). Enhanced transformation of human fibroblasts by origin-defective simian virus 40. Nature *296*, 671-672.

Smith, G. H., and Boulanger, C. A. (2003). Mammary epithelial stem cells: transplantation and self-renewal analysis. Cell Prolif *36 Suppl 1*, 3-15.

Smith, G. H., and Chepko, G. (2001). Mammary epithelial stem cells. Microsc Res Tech *52*, 190-203.

Solomon, E., Borrow, J., and Goddard, A. D. (1991). Chromosome aberrations and cancer. Science *254*, 1153-1160.

Sorci, G., Riuzzi, F., Agneletti, A. L., Marchetti, C., and Donato, R. (2003). S100B inhibits myogenic differentiation and myotube formation in a RAGE-independent manner. Mol Cell Biol *23*, 4870-4881.

Spangrude, G. J., Heimfeld, S., and Weissman, I. L. (1988). Purification and characterization of mouse hematopoietic stem cells. Science *241*, 58-62.

Srinath, P., Rao, P. N., Knaus, E. E., and Suresh, M. R. (2003). Effect of cyclooxygenase-2 (COX-2) inhibitors on prostate cancer cell proliferation. Anticancer Res *23*, 3923-3928.

Stamps, A. C., Davies, S. C., Burman, J., and O'Hare, M. J. (1994). Analysis of proviral integration in human mammary epithelial cell lines immortalized by retroviral infection with a temperature-sensitive SV40 T-antigen construct. Int J Cancer *57*, 865-874.

Stasiak, P. C., Purkis, P. E., Leigh, I. M., and Lane, E. B. (1989). Keratin 19: predicted amino acid sequence and broad tissue distribution suggest it evolved from keratinocyte keratins. J Invest Dermatol *92*, 707-716.

Steinert, P. M. (1998). Structural-mechanical integration of keratin intermediate filaments with cell peripheral structures in the cornified epidermal keratinocyte. Biol Bull *194*, 367-368; discussion 369-370.

Steinert, P. M., and Bale, S. J. (1993). Genetic skin diseases caused by mutations in keratin intermediate filaments. Trends Genet *9*, 280-284.

Steinman, R. A., Hoffman, B., Iro, A., Guillouf, C., Liebermann, D. A., and el-Houseini, M. E. (1994). Induction of p21 (WAF-1/CIP1) during differentiation. Oncogene *9*, 3389-3396.

Streuli, C. (1999). Extracellular matrix remodelling and cellular differentiation. Curr Opin Cell Biol *11*, 634-640.

Stulik, J., Osterreicher, J., Koupilova, K., Knizek, Macela, A., Bures, J., Jandik, P., Langr, F., Dedic, K., and Jungblut, P. R. (1999). The analysis of S100A9 and S100A8 expression in matched sets of macroscopically normal colon mucosa and colorectal carcinoma: the S100A9 and S100A8 positive cells underlie and invade tumor mass. Electrophoresis *20*, 1047-1054.

Takenaga, K., Nakamura, Y., and Sakiyama, S. (1997). Expression of antisense RNA to S100A4 gene encoding an S100-related calcium-binding protein

suppresses metastatic potential of high-metastatic Lewis lung carcinoma cells. Oncogene *14*, 331-337.

Tarabykina, S., Kriajevska, M., Scott, D. J., Hill, T. J., Lafitte, D., Derrick, P. J., Dodson, G. G., Lukanidin, E., and Bronstein, I. (2000). Heterocomplex formation between metastasis-related protein S100A4 (Mts1) and S100A1 as revealed by the yeast two-hybrid system. FEBS Lett *475*, 187-191.

Tegtmeyer, P. (1975). Function of simian virus 40 gene A in transforming infection. J Virol *15*, 613-618.

Tesfaigzi, J., and Carlson, D. M. (1996). Cell cycle-specific expression of G(0)SPR1 in Chinese hamster ovary cells. Exp Cell Res *228*, 277-282.

Till, J. E., and Mc, C. E. (1961). A direct measurement of the radiation sensitivity of normal mouse bone marrow cells. Radiat Res *14*, 213-222.

Tolg, C., Hofmann, M., Herrlich, P., and Ponta, H. (1993). Splicing choice from ten variant exons establishes CD44 variability. Nucleic Acids Res *21*, 1225-1229.

Tran, C. P., Lin, C., Yamashiro, J., and Reiter, R. E. (2002). Prostate stem cell antigen is a marker of late intermediate prostate epithelial cells. Mol Cancer Res *1*, 113-121.

van Belzen, N., Dinjens, W. N., Diesveld, M. P., Groen, N. A., van der Made, A. C., Nozawa, Y., Vlietstra, R., Trapman, J., and Bosman, F. T. (1997). A novel gene which is up-regulated during colon epithelial cell differentiation and down-regulated in colorectal neoplasms. Lab Invest *77*, 85-92.

van Leenders, G., Dijkman, H., Hulsbergen-van de Kaa, C., Ruiter, D., and Schalken, J. (2000). Demonstration of intermediate cells during human prostate epithelial differentiation in situ and in vitro using triple-staining confocal scanning microscopy. Lab Invest *80*, 1251-1258.

van Leenders, G. J., and Schalken, J. A. (2001). Stem cell differentiation within the human prostate epithelium: implications for prostate carcinogenesis. BJU Int *88 Suppl 2*, 35-42; discussion 49-50.

Verhagen, A. P., Aalders, T. W., Ramaekers, F. C., Debruyne, F. M., and Schalken, J. A. (1988). Differential expression of keratins in the basal and luminal compartments of rat prostatic epithelium during degeneration and regeneration. Prostate *13*, 25-38.

Verhagen, A. P., Ramaekers, F. C., Aalders, T. W., Schaafsma, H. E., Debruyne, F. M., and Schalken, J. A. (1992). Colocalization of basal and luminal cell-type cytokeratins in human prostate cancer. Cancer Res *52*, 6182-6187.

Vogeli-Lange, R., Burckert, N., Boller, T., and Wiemken, A. (1996). Rapid selection and classification of positive clones generated by mRNA differential display. Nucleic Acids Res *24*, 1385-1386.

Wallach, D., Fellous, M., and Revel, M. (1982). Preferential effect of gamma interferon on the synthesis of HLA antigens and their mRNAs in human cells. Nature *299*, 833-836.

Wang, G., Rudland, P. S., White, M. R., and Barraclough, R. (2000). Interaction in vivo and in vitro of the metastasis-inducing S100 protein, S100A4 (p9Ka) with S100A1. J Biol Chem *275*, 11141-11146.

Wang, Y., Hayward, S., Cao, M., Thayer, K., and Cunha, G. (2001). Cell differentiation lineage in the prostate. Differentiation *68*, 270-279.

Webber, M. M., Bello, D., Kleinman, H. K., Wartinger, D. D., Williams, D. E., and Rhim, J. S. (1996a). Prostate specific antigen and androgen receptor induction and characterization of an immortalized adult human prostatic epithelial cell line. Carcinogenesis *17*, 1641-1646.

Webber, M. M., Bello, D., and Quader, S. (1996b). Immortalized and tumorigenic adult human prostatic epithelial cell lines: characteristics and applications. Part I. Cell markers and immortalized nontumorigenic cell lines. Prostate *29*, 386-394.

Weijerman, P. C., Romijn, H. C., and Peehl, D. M. (1994). Human papilloma virus type 18 DNA immortalized cell lines from the human prostate epithelium. Prog Clin Biol Res *386*, 67-69.

Welm, B. E., Tepera, S. B., Venezia, T., Graubert, T. A., Rosen, J. M., and Goodell, M. A. (2002). Sca-1(pos) cells in the mouse mammary gland represent an enriched progenitor cell population. Dev Biol *245*, 42-56.

Wernisch, L., Kendall, S. L., Soneji, S., Wietzorrek, A., Parish, T., Hinds, J., Butcher, P. D., and Stoker, N. G. (2003). Analysis of whole-genome microarray replicates using mixed models. Bioinformatics *19*, 53-61.

Whitehead, R. H., VanEeden, P. E., Noble, M. D., Ataliotis, P., and Jat, P. S. (1993). Establishment of conditionally immortalized epithelial cell lines from both colon and small intestine of adult H-2Kb-tsA58 transgenic mice. Proc Natl Acad Sci U S A *90*, 587-591.

Wicki, R., Franz, C., Scholl, F. A., Heizmann, C. W., and Schafer, B. W. (1997). Repression of the candidate tumor suppressor gene S100A2 in breast cancer is mediated by site-specific hypermethylation. Cell Calcium *22*, 243-254.

Wright, W. E., Brasiskyte, D., Piatyszek, M. A., and Shay, J. W. (1996). Experimental elongation of telomeres extends the lifespan of immortal x normal cell hybrids. Embo J *15*, 1734-1741.

Wright, W. E., Pereira-Smith, O. M., and Shay, J. W. (1989). Reversible cellular senescence: implications for immortalization of normal human diploid fibroblasts. Mol Cell Biol *9*, 3088-3092.

Wu, A. W., Gu, J., Li, Z. F., Ji, J. F., and Xu, G. W. (2004). COX-2 expression and tumor angiogenesis in colorectal cancer. World J Gastroenterol *10*, 2323-2326.

Wu, G., Burzon, D. T., di Sant'Agnese, P. A., Schoen, S., Deftos, L. J., Gershagen, S., and Cockett, A. T. (1996). Calcitonin receptor mRNA expression in the human prostate. Urology *47*, 376-381.

Wu, Y. J., Parker, L. M., Binder, N. E., Beckett, M. A., Sinard, J. H., Griffiths, C. T., and Rheinwald, J. G. (1982). The mesothelial keratins: a new family of cytoskeletal proteins identified in cultured mesothelial cells and nonkeratinizing epithelia. Cell *31*, 693-703.

Xue, Y., Smedts, F., Debruyne, F. M., de la Rosette, J. J., and Schalken, J. A. (1998a). Identification of intermediate cell types by keratin expression in the developing human prostate. Prostate *34*, 292-301.

Xue, Y., Smedts, F., Verhofstad, A., Debruyne, F., de la Rosette, J., and Schalken, J. (1998b). Cell kinetics of prostate exocrine and neuroendocrine epithelium and their differential interrelationship: new perspectives. Prostate Suppl *8*, 62-73.

Yang, Q., O'Hanlon, D., Heizmann, C. W., and Marks, A. (1999a). Demonstration of heterodimer formation between S100B and S100A6 in the yeast two-hybrid system and human melanoma. Exp Cell Res *246*, 501-509.

Yang, X. J., Lecksell, K., Gaudin, P., and Epstein, J. I. (1999b). Rare expression of high-molecular-weight cytokeratin in adenocarcinoma of the prostate gland: a study of 100 cases of metastatic and locally advanced prostate cancer. Am J Surg Pathol *23*, 147-152.

Yin, A. H., Miraglia, S., Zanjani, E. D., Almeida-Porada, G., Ogawa, M., Leary, A. G., Olweus, J., Kearney, J., and Buck, D. W. (1997). AC133, a novel marker for human hematopoietic stem and progenitor cells. Blood *90*, 5002-5012.

Yoneda, K., McBride, O. W., Korge, B. P., Kim, I. G., and Steinert, P. M. (1992). The cornified cell envelope: loricrin and transglutaminases. J Dermatol *19*, 761-764.

Yonemura, Y., Endou, Y., Kimura, K., Fushida, S., Bandou, E., Taniguchi, K., Kinoshita, K., Ninomiya, I., Sugiyama, K., Heizmann, C. W., *et al.* (2000). Inverse expression of S100A4 and E-cadherin is associated with metastatic potential in gastric cancer. Clin Cancer Res *6*, 4234-4242.

Zehner, Z. E. (1991). Regulation of intermediate filament gene expression. Curr Opin Cell Biol *3*, 67-74.

Zhao, X. P., and Elder, J. T. (1997). Positional cloning of novel skin-specific genes from the human epidermal differentiation complex. Genomics *45*, 250-258.

Zhou, S., Schuetz, J. D., Bunting, K. D., Colapietro, A. M., Sampath, J., Morris, J. J., Lagutina, I., Grosveld, G. C., Osawa, M., Nakauchi, H., and Sorrentino, B. P. (2001). The ABC transporter Bcrp1/ABCG2 is expressed in a wide variety of stem cells and is a molecular determinant of the side-population phenotype. Nat Med *7*, 1028-1034.

Zwadlo, G., Bruggen, J., Gerhards, G., Schlegel, R., and Sorg, C. (1988). Two calcium-binding proteins associated with specific stages of myeloid cell differentiation are expressed by subsets of macrophages in inflammatory tissues. Clin Exp Immunol *72*, 510-515.

Volume 52(8): 1083–1090, 2004
Journal of Histochemistry & Cytochemistry
http://www.jhc.org

ARTICLE

Differential Expression of CD44 During Human Prostate Epithelial Cell Differentiation

Tahirah N. Alam, Michael J. O'Hare, István Laczkó, Alex Freeman, Farah Al-Beidh, John R. Masters, and David L. Hudson

0022-1554/04/$3.30